MOLECULAR DISSECTION OF CELL DIVISION IN APICOMPLEXAN PARASITES

by

MARIA EUGENIA FRANCIA

(Under the Direction of Boris Striepen)

ABSTRACT

Apicomplexa are intracellular parasites that cause important human diseases including malaria and toxoplasmosis. Following invasion of a host cell, Apicomplexa undergo a fascinatingly complex process of division. Apicomplexa proliferate by a unique mechanism that combines closed mitosis of the nucleus with de-novo formation of daughter cells. Mitosis occurs in the presence of a nuclear envelope and with little appreciable chromatin condensation. Nuclear division is not always followed by cytokinesis. In some Apicomplexa, division results in a cytosol in which multiple nuclei and organelles are parceled into multiple daughter cells simultaneously. Budding is remarkably flexible in output and can produce two to thousands of progeny cells depending on the apicomplexan species. How genomes and daughters are counted and coordinated is unknown. Here, we use *Toxoplasma gondii* as a cell biological model to ask questions pertaining molecular aspects of apicomplexan division.  We had shown previously that all centromeres, the sites of kinetochore attachment on each chromosome, are constantly tethered to the centrosome positioned in a specific region of the nuclear periphery. Centromeres are clustered throughout the cell cycle. We show that centromere clustering is mediated by elements of the nuclear envelope. In particular, components of the nuclear pore complex appear to be important for maintenance of centromere tethered to the nuclear

envelope. We also show that nuclear events are coordinated with assembly of daughter cells through structures associated to the centrosome during division. A fiber-like structure, derived from the algal past of apicomplexan parasites, assembles on the centrosome during mitosis and initiates daughter cell assembly. This fiber is made of striated fiber assemblin proteins which in algae participate in the positioning and organization of the flagellar basal body. These findings have broad evolutionary implications. We propose that Apicomplexa retained the organizing principle of the flagellar microtubule organizing center. Instead of ensuring appropriate numbers of flagella, the system now positions the microtubule organizing center of the daughter cell.  Finally, the results herein presented derive a novel model of regulation of division in which individual elements of the cell are linked through physical tethers to the centrosome providing both spatial organization and temporal control.

INDEX WORDS:        *Toxoplasma,* Apicomplexa, division, replication, mitosis, centromere, centrosome, striated fiber, histone, nuclear pore complex, microtubule organizing center.

MOLECULAR DISSECTION OF CELL DIVISION IN APICOMPLEXAN PARASITES

by

MARIA EUGENIA FRANCIA

B.S., University of Idaho, 2007

M.Sc., University of Idaho, 2009

A Dissertation Submitted to the Graduate Faculty of The University of Georgia in Partial

Fulfillment of the Requirements for the Degree

DOCTOR OF PHILOSOPHY

ATHENS, GEORGIA

2013

MOLECULAR DISSECTION OF CELL DIVISION IN APLICOMPLEXAN PARASITES

by

MARIA EUGENIA FRANCIA

Major Professor:     Boris Striepen

Committee:     Jacek Gaertig

Stephen Hajduk

Kelly Dawe

Electronic Version Approved:

Maureen Grasso

Dean of the Graduate School

The University of Georgia

August 2013

DEDICATION

A Mama, Papa, Vale, Nico, Vero y Maxi.

And

To George Simmons, for you will never know how much meeting you changed and
defined my life.

Thank you to my Coco pup for giving me a reason to come back home from the lab, and to go outside.  Thank you for your unconditional love and company.

Thank you to all my Striepenites; Lilach, Swati, Sri, Melissa, Carrie, Sumiti, Justin, Sheila, Jessica, Katherine and Zach. I wouldn't have enjoyed these four years as much as I did if it weren't for all of you. Very special thanks to Carrie Brooks. Thanks for always dropping anything you were doing to help me. Thank you for your support and encouragement. Thank you for your friendship. Thanks to Lilach for our many work-related conversations which undoubtedly have made me a better thinker and scientist. I admire your motivation and dedication. Thank you for your encouragement in all aspects of life and for your friendship. Thanks to Sheila Bhavsar for being such a great learner, responsible and reliable, and for all of the work you helped me with through the past two years. This thesis wouldn't have happened without you all.

Thanks to Jean-Francois Dubremetz for teaching me to be patient and to love EM, and for your willingness to always address my questions. Thanks to Maryse Lebrun for receiving me in her lab and her home, and for treating me like family while I was in France. Thanks to everyone in the Dubremetz-Lebrun labs for making me feel welcome and like home while in France. Thanks to Gustavo Arrizabalaga, for always supporting me, and for taking an interest on my work and my well being. Thanks to my friend Greg for always taking time to email me and for reminding me that continuing on was worth it. Thanks to Carrie Harden, for being so efficient and reliable, without whom I wouldn't have been able to keep up with paperwork. Thanks to my thesis committee for your support and guidance. Special thanks to Steve Hajduk for your encouragement and support throughout my PhD.

Most importantly, thanks to my mentor, Boris. Thanks for taking me on and helping me grow and become a better scientist. Thanks for your mentoring, advice and patience. Thanks for

listening to and considering my ideas. Thank you for motivating me to be better and to work

harder by being a truly passionate scientist yourself.  Thank you for including me in discussion to

decide the direction of a number of projects, promoting my work and providing me with

countless opportunities to grow professionally. Thank you for your support every time I pursued

something that was important to me.

TABLE OF CONTENTS

LIST OF TABLES

LIST OF FIGURES

CHAPTER 1

INTRODUCTION AND LITERATURE REVIEW

**<u>INTRODUCTION</u>**

The phylum Apicomplexa encompasses numerous important human and veterinary

disease-causing parasites including the causative agents of malaria, toxoplasmosis,

cryptosporidiosis, Texas and East Coast fever, and coccidiosis. Apicomplexans are all obligate

intracellular pathogens. The ability of parasites to effectively replicate within different host cell

niches is crucial to the infection, and the severity and outcome of the disease. Tremendous

progress has been made in understanding the molecular mechanisms used by these parasites to

invade cells; however, the cell biology of the intracellular development traditionally received

modest attention from the field. The fundamental structural aspects of apicomplexan division

were first established with the advent of transmission electron microscopy in the early sixties.

However, studies describing apicomplexan division at the molecular level only began to emerge

recently.

Parasites in the phylum Apicomplexa divide by closed mitosis of the nucleus and internal

assembly of daughter cells. The work presented here ties emerging molecular insights and

classic ultrastructural work into a consolidated view of two complex processes; the organization

of chromatin elements important for division of the nucleus and the regulation of daughter cell

assembly. The peculiar aspects of apicomplexan division can only be understood on the

drawback of their evolutionary history and a thorough understanding of their structural

complexity. Therefore, chapter 1 of this thesis reviews the literature describing the evolutionary

origin of Apicomplexan parasites and their mechanisms of pathogenesis. It describes the cell biology of the cytoskeletal and membranous elements important for division, and discusses, in general terms, the division mechanism of *Toxoplasma gondii*. Chapter 1 aims to provide the context and rationale for understanding the questions I set out to answer during my doctoral studies.  It also provides the reader with the theoretical foundation, required to interpret the experimental results outlined in chapters 2 and 3.

Chapter 2 describes findings on the mechanisms used by *Toxoplasma gondii* parasites to maintain its chromosomes organized at a defined nuclear territory. My data suggests a novel role for nuclear pore components in maintaining nuclear organization, and tethering centromeres to the nuclear envelope in *T. gondii*.  Chapter 3 describes a novel cell-cycle control mechanism used by *Toxoplasma gondii* parasites to coordinate daughter cell assembly with nuclear events during division.  In this chapter, I describe the role of a cytoskeletal element, a fiber-like structure of algal origin, which is required for initiating assembly of daughter cells. This fiber physically connects the daughter cell to the centrosome properly positioning the site of budding.

Chapter 4 integrates our findings in *Toxoplasma gondii* with the most recent literature on the mechanisms of division of other parasites in the phylum Apicomplexa. It proposes three novel levels of regulation of the division process and contrasts them with canonical cytosolic cell cycle regulation (i.e. kinases, cyclins/CDKs, etc). These mechanisms for regulation of cell cycle progression are; temporal control of expression of different elements required for daughter cell assembly, organization of the nucleus into defined nuclear territories and chromatin sub-domains, and physical tethering /constraint to the centrosome. Beyond reviewing the literature this chapter serves as a "conclusion" chapter providing a unified model for the control of

progression of the apicomplexan cell cycle, and highlighting open questions for the future not only pertinent to the biology of *Toxoplasma gondii* but also to that of other parasites in the phylum, including the major pathogen and causative agent of human malaria, *Plasmodium falciparum*.

**LITERATURE REVIEW**

**Apicomplexan Parasites are Important Human and Veterinary Pathogens**

The phylum Apicomplexa comprises many unicellular protozoa, all of which are obligate intracellular pathogens. The most notable of these, and the most heavily studied, are the human malaria causing *Plasmodium* species [1]. The phylum also includes important veterinary pathogens. *Sarcocystis neurona* parasitizes the nervous system of horses, among other animals, causing myeloencephalitis [2]. *Eimeria tenella* infects the intestinal epithelia of poultry causing avian coccidiosis[3], and *Theileria parva* infects the bovine lymphocytes, causing East Coast fever [4, 5]. *Toxoplasma gondii*, the focus of this thesis, is able to infect all warm blooded animal including humans. Within its host, *T. gondii* can infect any nucleated cell, causing Toxoplasmosis [6].

*Toxoplasma* is found worldwide. Recent surveys demonstrate that 11 to 25% of native-born US residents are infected with *T. gondii*. The percentage of infected individuals rises up to 85% of the population in countries such as France, El Salvador and Brazil where cultural practices associated with consumption of undercooked meat facilitate the parasite's transmission[6]. On average, around one third of the world's population is sero-positive for *T. gondii.*

T. gondii Infections can be acquired by ingestion of food or water contaminated with environmentally resistant oocyst or by congenital transmission. Toxoplasmosis is usually asymptomatic in healthy hosts. Symptoms of the acute infection phase appear as flu-like and include fever, headaches, muscle pain and lymph node inflammation. In immuno-competent individuals the infection is normally controlled through production of high levels of IFN-γ by natural killer and T-cells [7]. However, in immuno-naïve infants, congenitally infected, and immunocompromised individuals, life-threatening disease can occur. Toxoplasma infection is one of the leading causes of death among AIDS patients. Reactivation of latent tissue cysts in the brain leads to encephalitis in up to 40% of individuals with AIDS, which if left untreated can be lethal [8]. In addition, the infective form of the parasite readily crosses the placenta so women infected during pregnancy can transmit the parasite to the fetus. Congenital toxoplasmosis occurs at an annual rate of 1-10 cases every 10,000 live births in the US [9]. Congenitally acquired T. gondii may result in abortion or severe congenital defects such as hydrocephalus, brain calcification and blindness, among others. Children born asymptomatic may develop neurological symptoms later on in life, which can lead to mental retardation and even death [9].

**Phylogeny of Apicomplexa**

Apicomplexa are eukaryotic cells and belong to the kingdom of the Chromalveolata and infrakingdom (super-phylum) Alveolata. The Chromalveolates descended from a heterotrophic bikont (bi-flagellated eukaryote), in which a secondary endosymbiotic event, between an alga and a flagellated ancestor, gave rise to a plastid-like organelle [10, 11]. Members of the Alveolata are characterized by the presence of cortical alveolae, and a cilliary pit or micropore [12]. The Alveolates are further divided into the phyla ciliates, dinoflagellates and Apicomplexa, which differ mainly in their motility machinery [13-15]. While Ciliates and dinoflagellates move

by means of cilia or flagella respectively, apicomplexans move by gliding motility and lack a visible locomotive structure for most of their life cycle (with the exception of the sexual stages). Additionally, many ciliates and dinoflagellates are free-living, while Apicomplexa are obligate intracellular parasites. Ciliates diverged 1400 million years ago from the common Alveolate ancestor, while Dinoflagellates and Apicomplexa diverged from each other 800-900 million years ago and are more closely related to each other [16, 17].

**The Lytic Cycle**

Apicomplexa are characterized by the presence of a complex apparatus of secretory organelles known as the rhoptries, dense granules and micronemes, which localize to the anterior end of the parasite (Figure 1.2A). In fact, the phylum name "Apicomplexa" is owed to the apical localization of this complex. Parasites discharge adhesins from micronemes, which allow them to engage the host's plasma membrane and invade to initiate an infection. In addition, rhoptry secreted kinases modify the host enabling the infection [18-20]. In most cases apicomplexans develop within a parasitophorous vacuole once inside their host cell, although exceptions exist and some apicomplexans live free in the host's cytosol. Once invaded, apicomplexans continue to secrete their rhoptries and dense granules to modify their host cell even further. Gene expression pathways associated with clearing the infection are altered in the host cell [19, 21]. Establishment of infection is followed by cell division and parasite replication (Figure 1.1).

Parasite replication results in a single apicomplexan cell scaling up to thousands within a single host cell. Replication is followed by lysis of the host cell, release of infection-competent parasites, and re-infection of healthy neighboring cells. The cycle, involving invasion of a host cell, intracellular replication, egress/host cell lysis and re-invasion is known as the "lytic cycle."

This is a proliferation scheme followed by all parasites in the phylum (Figure 1.1)[22]. Some parasites in the phylum can only undergo the lytic cycle for a limited number of times until they differentiate into sexual stages, thus infections are self-limiting within definitive hosts. *T. gondii*, however, can perpetuate asexual growth limitless in the absence of an immune response. Modulation of the host cell response by rhoptry secreted kinases, and the rate of apicomplexan cell division contribute to pathogenicity [19]. In particular, slow growing strains tend to be less virulent than faster replicating ones [23, 24]. Thus, Apicomplexa intracellular replication is a major source of pathogenicity.

Once intracellular, apicomplexan parasites replicate by modes of division that differ from those used by their hosts. The most notable distinction between mammalian cell division and Apicomplexa cell division is that the first occurs by open nuclear mitosis immediately followed by cytokinesis (with a few exceptions). The second occurs by closed nuclear mitosis, and only in a small number of species is followed by cytokinesis [25]. Additionally, daughter cells do not derive from fission of the mother cytosol and equal partitioning of cellular components, but instead are formed by budding. Budding encompasses de-novo assembly of new cells and major disassembly of the mother cell (Figure 1.3 and 4.2) [25].

**Structural Overview: What does it take to put together a *Toxoplasma gondii* Cell?**

*Toxoplasma gondii* tachyzoites are oval-shaped cells of approximately 2 x 7 µm in size. From a research standpoint, it presents the advantage of being highly polarized. The cell poles are readily identifiable, and the position of organelles is well known and easily recognizable by microscopy. The anterior pole of the cell is termed the apical end, and the posterior pole is called the basal end. Many protein markers have been identified which allows ready

identification of the cell's orientation and its progression through the cell cycle, making *T. gondii* an excellent model to study apicomplexan division.

A *T. gondii* cell has relatively simple organellar architecture; it contains a single mitochondrion, a single plastid-like organelle, a single interconnected ER network and a single Golgi apparatus (Figure 1.2B). The apical end of the cell contains membranous organelles and cytoskeletal structures. Cytoskeletal elements found at the apical end of a *T. gondii* cell include the conoid, the pre-conoidal and the apical polar ring (APR) (Figure 1.2A). The APR is regarded as the microtubule organizing center of the cell cytoskeleton[26]. This structure is composed of two rings apparently attached to each other. From it, 22 sub-pellicular microtubules of about 5 µm in length emerge and run down two thirds of the cell's length [27-29]. This microtubule arrangement confers the cell with its characteristic shape and polarity, and remarkable flexibility, allowing it to squeeze through the tight junction formed with the host cell's plasma membrane upon invasion. The APR is the first cytoskeletal element positioned during daughter cell formation [26, 27, 30]. How it is positioned in the correct place and number was unknown prior to my dissertation studies. The mechanism of APR positioning during daughter cell formation is the subject matter addressed in Chapter 3.

The conoid is a basket-shaped structure located posterior to the pre-conoidal rings and anterior to the APR (Figure 1.2A). The conoid is only found among the coccidian species within the phylum which include *Toxoplasma, Sarcocystis* and *Eimeria*. The conoid is composed of fourteen tightly apposed filamentous subunits that spiral counterclockwise toward the pre-conoidal rings [31]. The subunits are composed of a unique tubulin polymer formed from a curved sheet of nine protofilaments. It is a highly motile structure, able to extend and retract from its position in the apical end of the parasite in a calcium-dependent manner. When

retracted, the conoid rests within the APR. Though no direct evidence for its function has been

demonstrated, a role in invasion has been frequently ascribed to this structure, as it extrudes

prior to and during host cell invasion[32].

Two microtubules are present within the conoid itself, known as the intra-conoidal

microtubules. These are nucleated from the anterior pre-conoidal ring and they extend down

through the conoid (Figure 1.2A) [32]. They are approximately 400 nm in length. Micronemes

and rhoptries (briefly mentioned above) are positioned at the apical end by de-novo synthesis

during daughter cell assembly (Figure 1.2B). Micronemes seem to align with the sub-pellicular

microtubules which suggest that they are positioned and transported by kinesins[33]. Rhoptries

are tethered to the cell pellicle by protein acylation[34], and their necks are contained within

the conoid (Figure 1.2B).

*Toxoplasma gondii* contains two distinct populations of microtubules, each nucleated

from a different microtubule organizing center. As mentioned above, the subpellicular

microtubules are nucleated from the apical polar ring and are a stable population until the end

of division at which point they undergo major disassembly to allow daughter cells to emerge.

The second population of microtubules nucleates to form the mitotic spindle.  Spindle

microtubules are anchored at the centrosome, the MTOC for this microtubule subset. The

centrosome contains 2 parallel centrioles composed of an atypical microtubule arrangement of

9+1 singlets. Further structural details on the Apicomplexa centrosome and its role in division

can be found in Chapter 4.

Spindle microtubules are a dynamic population mediating chromosome segregation

during mitosis. In coccidian Apicomplexa, the mitotic spindle is housed within an elaboration of

the nuclear envelope which consists of a conical protrusion named the centrocone (Figure 1.3A)

[35-37]. Immunofluorescence assays using anti-TgMORN1 (membrane occupation and recognition nexus), a molecular marker for the *T. gondii* centrocone, show that the molecular marker of the structure persists throughout the cell cycle in these parasites. Prior to my dissertation work it was not clear whether the spindle itself was also maintained. This is one of the questions addressed in Chapter 2.

In addition to microtubules, the pellicle of apicomplexan parasites is composed of the plasma membrane and cortical alveoli. Alveoli consist of flattened vesicles located between the plasma membrane and the subpellicular microtubules. This specialized membranous system is characteristic of all members of the super-phylum Alveolata, and in Apicomplexa is known as the inner membrane complex (IMC) (Figure 1.2A). The apicomplexan IMC plays a critical role in motility, as it anchors the gliding machinery [38-40]. It also tethers organelles to the pellicle[41].

The IMC is organized into a network of 10 nm filaments which span the entire length of the *T. gondii* parasite, except for the very apical tip. Freeze-fracture studies of *T. gondii* tachyzoites showed that the IMC is composed of multiple parallel rectangular plates along the body of the parasite, and a single cone-shaped plate at the apex, called the apical cap [42]. More recent studies identified four proteins with specific sub-localization to three sub-compartments of the IMC plates, thus named IMC Sub-compartment Proteins or ISPs[43, 44]. In *T. gondii*, ISP1 is localized at the apical cap, ISP2 and 4 cover a central section of the IMC, and ISP3 is found in both the central and basal regions. ISPs are believed to be recruited to different sections of the IMC plates by specific acyl-transferases [43, 44]. A recent study describing the localization of the majority of predicted palmytoyl transferases in the genomes showed that both *in T. gondii* and *P. falciparum* these proteins are localized at specific areas of the IMC, further supporting this hypothesis [45].

In addition to ISPs, the IMC is lined with intermediate filament-like proteins known as IMC proteins [42, 46, 47]. Recently it was determined that as many as 14 distinct IMC proteins in *T. gondii* are differentially expressed and targeted, throughout the intracellular development of the parasite [48]. IMC proteins expression is up-regulated during division. Newly- made IMC proteins serve to from the emerging daughter cells.  Many IMC proteins appear very early during division and are first detectable in the vicinity of the centrosome, where daughter cell formation initiates. A few IMC proteins, however, display mother-cell only localization. These IMC have been proposed as molecular markers that distinguish the pellicle of the mature mother cell from that of the emerging new cells, for the purposes of organellar partitioning and disassembly, during division [46, 48].

**Overview of the Mechanism of Cell Division of *Toxoplasma gondii***

*Toxoplasma gondii* divides by two different modes.  In felines, *T. gondii*'s definitive hosts, the parasite can complete its sexual cycle, differentiating into gametes which can mate, resulting in formation of oocyst which are shed in the cat's feces [49, 50]. Oocysts are highly stable in the environment, and constitute the main route of parasite transmission [51, 52]. Oocysts passed in feline feces will form eight infective sporozoites following sporulation. Ingestion of infective sporozoites in oocysts initiates infection in the intestinal epithelium of the intermediate host. Within the intestinal epithelial *T. gondii* sporozoites divide by schizogony. In this mode of division multiple rounds of nuclear division precede a single round of cytokinesis. This results in an intermediate multi-nucleated syncytium. Nuclei are ultimately parceled out into multiple daughter cells which form prior to cytokinesis. The sporozoite stage is short lived, as parasites convert to the tachyzoite stage just twelve hours after invading a host cell. The tachyzoite is the major proliferative stage of the parasite. This phase of infection is known as the

acute form, and it is limited by the immune system in a healthy host. Immune stressors induce the conversion from tachyzoite to the slow growing bradyzoites, which persist in the healthy host turning the infection into its chronic stage [53].

During the acute phase of infection, parasites rapidly divide by a mechanism known as endodyogeny. This consists of a single round of mitosis and assembly of two internal daughter cells (Figure 1.3) [25, 28, 54, 55]. This is the simplest mode of division within the apicomplexan phylum. This is in contrast with more complex – hence more difficult to study- modes of division such as schizogony, briefly described above, or endopolygeny in which a massive polyploid nucleus undergoes parceling while assembly of hundreds of daughter cells occurs simultaneously (Figure 4.2)[56]. Also, the study of division in other apicomplexans is limited due to the lack of molecular markers for structural and regulatory elements, which abound for the study of division in *T. gondii*. Interestingly, apicomplexan cell division is based on the same fundamental principles regardless of the specific division scheme used by individual species [25]. Thus, mechanistic insights obtained from the study of *T. gondii* can typically be extrapolated to most other species in the phylum. For these reasons, *T. gondii* represents an excellent model organism to investigate the mechanistic underpinnings of cell division in apicomplexans. [For a detailed mechanistic description of the various modes of division used by apicomplexans see Chapter 4 and Figure 4.2]

In short, the cell cycle of *T. gondii* is composed of three phases; G1, S and M, with G2 being absent or very short [25, 57, 58]. The start of S phase is marked by duplication of the centrosome (Figure 1.3 G). Mitosis occurs with no appreciable changes in the nuclear envelope (closed mitosis) and without appreciable DNA condensation (Figure 1.3 F-I). The mitotic spindle assembles within the nuclear envelope in a specialized structure known as the centrocone

(Figure 1.3A) [37, 59]. Daughter cell assembly initiates in physical proximity to the centrosome. Commonly, *T. gondii* assembles two daughter cells for every round of replication. Progression of nuclear division events occurs at the same time as assembly of daughter cells. The nucleus and other organelles are packed into the developing daughter cell as division progresses (Figure 1.3). Upon completion, the mother cell cytoskeleton disassembles and invasion-competent daughter cells emerge from it, acquiring its plasma membrane as cytokinesis resumes.

## SPECIFIC AIMS

A problem unique to the biology of Apicomplexa is that multiple nuclei and multiple copies of the genome need to be segregated simultaneously. How do Apicomplexa count out, and segregate chromosomes into multiple nuclei and multiple daughters in the context of a shared cytosol, without condensing the DNA or breaking down the nuclear envelope?

Until recently, how mitosis progressed in apicomplexan parasites was not understood due to our inability to visualize chromosomes. Direct visualization of chromosomes is impaired by lack of chromatin condensation. Centromeres are typically a single location on a chromosome where the kinetochore assembles during mitosis. The kinetochore is the point of attachment for microtubules of the mitotic spindle. Centromeres are marked by the presence of a variant histone H3, known as CenH3 or CenPA. To visualize individual chromosomes, our laboratory generated recently a strain in which a histone H3 allows visualization of the centromere-associated nucleosomes in *T. gondii* [60]. To our surprise, immunofluorescence assays revealed that in *T. gondii* CenH3 and its associated DNA cluster at the periphery of the nucleus at a location intimately related to the position of the centrosome [60]. Moreover, the clustering of all centromeres and their proximity to the centrosome is maintained throughout the cell cycle,

even outside of division (Figure 1.3 F). We hypothesize that centromere clustering is important for maintenance of genome integrity in *T. gondii* both during division and interphase.

**Aim 1:**

**To determine the mechanism of centromere sequestration at the periphery of the nucleus in *Toxoplasma gondii,* and its role in parasite survival**

Nuclear mitosis occurs simultaneously with daughter cell assembly in *T. gondii*. The number of daughters assembled must match the number of genomes and nuclei to ensure that each daughter is endowed with a single, not less, not more, complete chromosome complement. Budding occurs with concomitant segregation of all other organelles. Organelles such as the Golgi, the ER, the mitochondria and the apicoplast must be replicated in a timely manner and in the correct number. Organelles must be parceled out into each individual daughter cell, simultaneously and in the context of a shared cytosol. How nuclear events are coordinated with daughter cell assembly is not understood. Data generated by Lechtreck and colleagues suggested that homologs of the algal SFA protein were expressed in Apicomplexa [61, 62]. The dissertation work of a previous graduate student in our laboratory, Dr. Carly Jordan, established that at least two homologs of the algal SFA protein are expressed in *Toxoplasma gondii* during division. The structure formed by these proteins appears to connect the centrosomes of dividing nuclei with daughter cells. This suggests that SFA proteins, and the structure they form during division could be involved in daughter cell assembly.

**Aim 2:**

**To determine the role of SFA homolog proteins in daughter cell assembly during *Toxoplasma gondii's* division.**
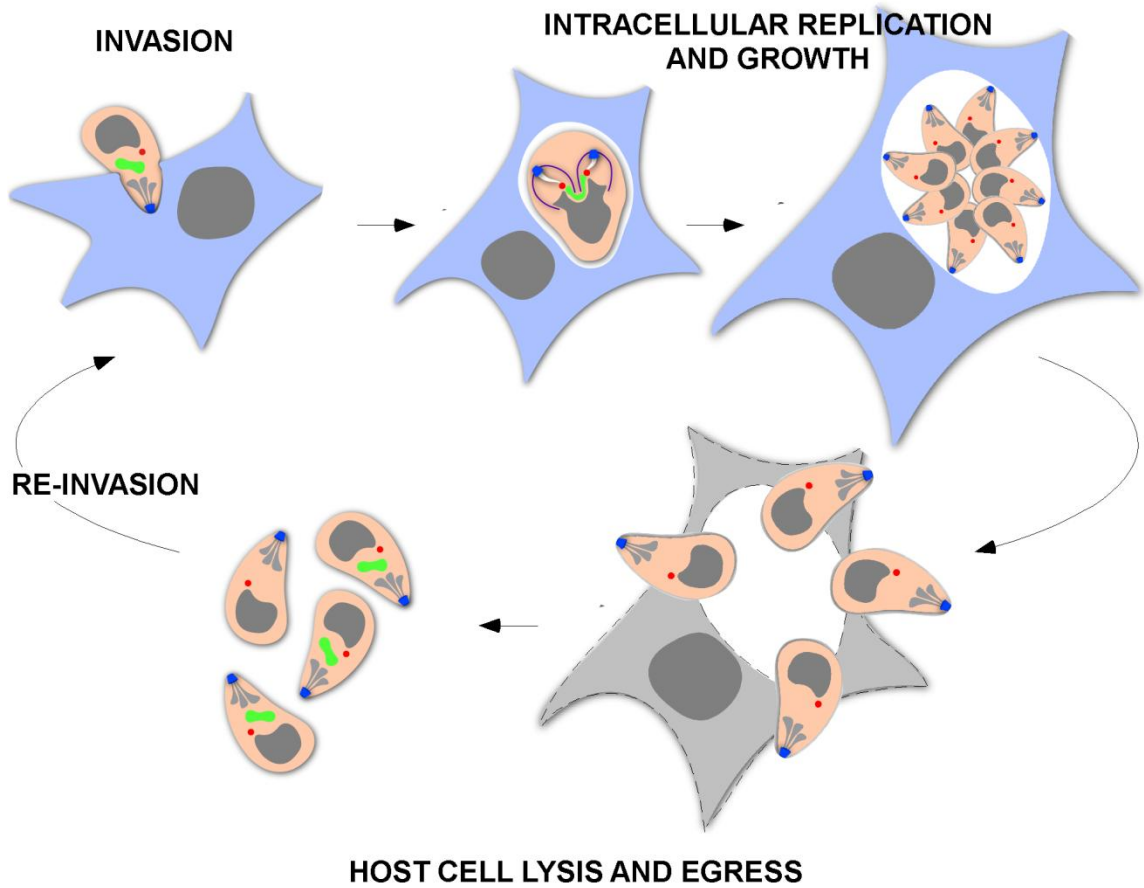
**Figure 1.1. The Lytic Cycle**.  Apicomplexa are all obligate intracellular parasites.  Active

penetration of the host cell, powered by the parasite's gliding motility results in invasion. Once

inside the host cell most apicomplexan parasites establish a parasitophorous vacuole where

they replicate and grow, scaling up their numbers. Following completion of their intracellular

development, parasites lyse their host cells, egress and rapidly re-invade a neighboring healthy

cell.  The host cell cytoplasm is represented in blue or grey. Parasites' cytosol is represented in

pink. Parasites and host cell nuclei are represented in grey. The apical end of the parasite is

marked in blue, the apicoplast is represented in green, and the centrosome is represented as a

red dot.
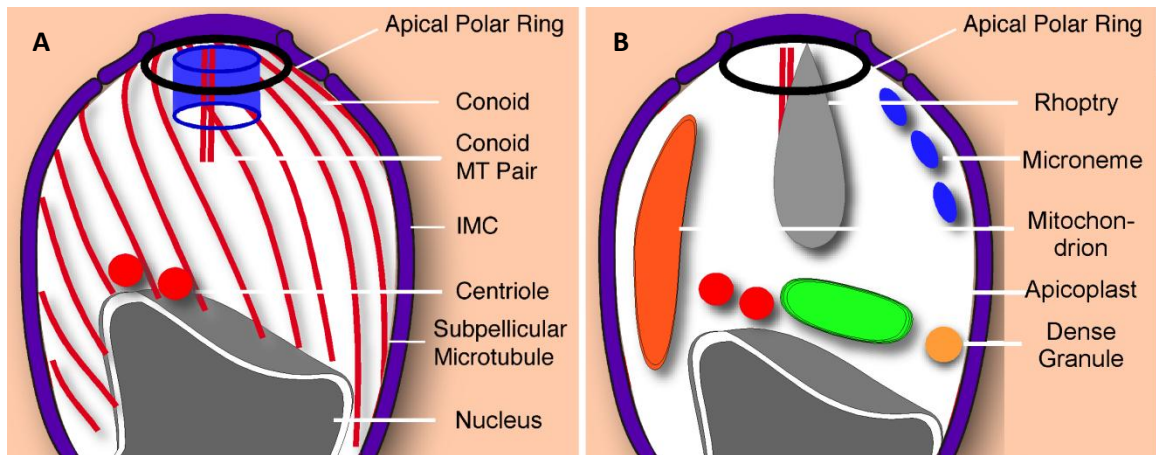
**Figure 1.2. Structural Overview of a *T. gondii* Cell**. **A.** Schematic representation of the

cytoskeletal elements of a *T. gondii* cell. Cytoskeletal organization determines the cell's

characteristic shape and polarity. The two main microtubule organizing centers in the cell are

shown. The apical polar ring organizes the subpellicular microtubules (red), houses the conoid

(blue) and the intra-conoidal microtubule pair (red). The centrosome, composed by two

centrioles (red) organizes the mitotic spindle (not shown) during nuclear division. The inner

membrane complex (IMC, purple) associates with the sub-pellicular microtubules and serves to

anchor the motility machinery (not shown) and organelles**. B.** Schematic representation of *T.*

*gondii* – specific organelles. Apicomplexan cells are polarized and organellar

location/organization is conserved within and between species. Their approximate position

within the cell and their relationship to other cellular structures are shown. Rhoptries and

micronemes are apical secretory organelles important for invasion and host cell modification

(Note that each *T. gondii* cell contains multiple rhoptries and micronemes, few are shown for

simplicity). Dense granules are secretory organelles more randomly distributed in the cytosol. *T.*

*gondii* contains two endosymbiotic organelles; a single tubular mitochondrion and a secondary

plastid known as the apicoplast. Adapted from Figure 10 in [30].
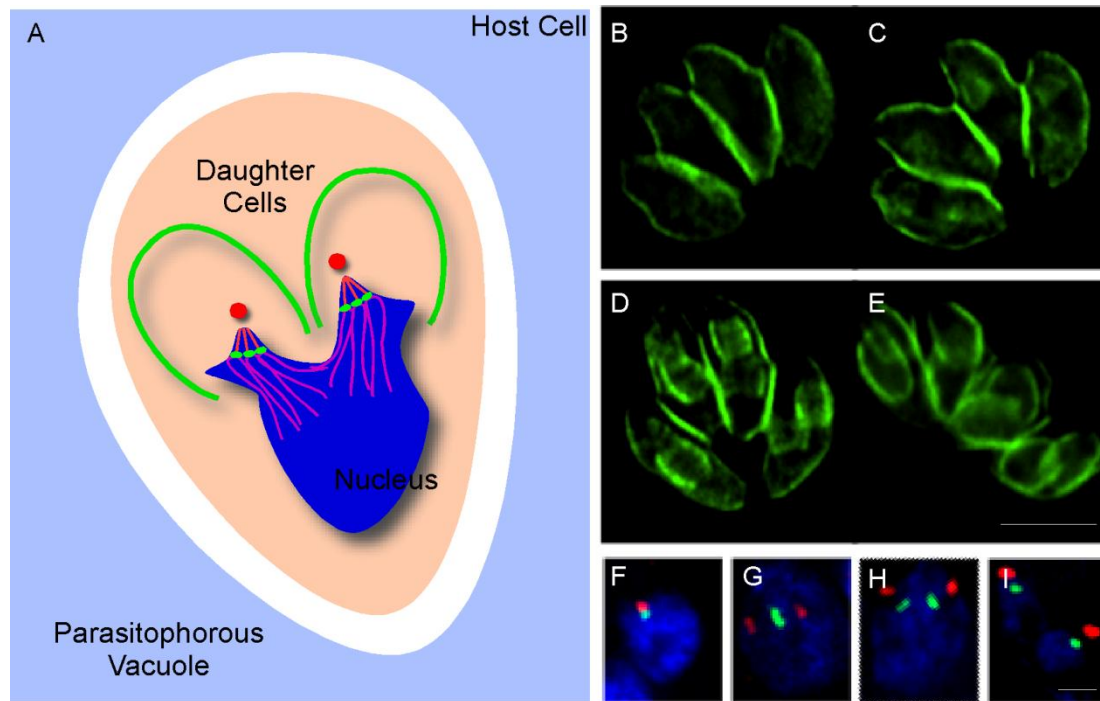
**Figure 1.3. *Toxoplasma gondii* divides by endodyogeny**. *Toxoplasma* divides by closed mitosis of the nucleus and assembly of two internal daughter cells. **A.** Two daughter cells are assembled within the mother cell. The inner membrane complex (IMC) of the daughter cells is shown in green. Centrosomes are shown in red. The mitotic spindle forms within an elaboration of the nucleus known as the centrocone. Microtubules of the mitotic spindle are shown in orange. Centromeres, represented in green, cluster at the base of the centrocone where the kinetochores interact with the spindle microtubules through pores in the nuclear envelope. Adapted from Figure 3.1 and [30]. **B-E**. Immunofluorescence assay of vacuoles containing four parasites stained with anti-IMC1 which labels the parasite's pellicle. **B.** Interphase. **C.** Two small daughter cells begin to assemble within the mother cell early in division. **D.** Daughter cells grow as the cell cycle progresses. **E.** Two daughter cells emerge from the mother cell upon cytokinesis. Scale bar = 5 μm. **F-I**. Dynamics of the nucleus throughout the cell cycle. Centrosomes are labeled with anti-Centrin1 (red), centromeres with anti-CenH3 (green) and

DNA stained with DAPI (blue). Scale bar = 1 μm. **F**. Nucleus in Interphase/G1. Centromeres remain clustered at the periphery of the nucleus, in proximity to the centrosome. **G.** Nucleus in metaphase. Chromosomes align in the metaphase plate, equidistant to the duplicated centrosomes. **H**. Nucleus in anaphase. Chromosomes begin to separate. **I**. Telophase. The nucleus has undergone fission and two individual nuclei are distinguishable.

CHAPTER 2

CENTROMERE CLUSTERING IN *Toxoplasma gondii* IS MEDIATED BY COMPONENTS OF THE

NUCLEAR PORE COMPLEX[1]

## ABSTRACT

Apicomplexa proliferate by a unique mechanism that combines closed mitosis of the nucleus and assembly of daughter cells by budding. Mitosis occurs in the presence of a nuclear envelope and with little appreciable chromatin condensation. In past work we demonstrated that the centromeres of *T. gondii* remain clustered at a defined region of the nuclear periphery proximal to the centrosome. We hypothesize that this is required for proper chromosome segregation during division and to keep count of chromosomes throughout the parasite's development. Here we show that centromere clustering is not mediated by microtubules of the mitotic spindle. We define factors with roles in chromatin organization that physically interact with centromeres. Through co-immunoprecipitation and mass spectrometry we identify additional proteins with broader nuclear distribution that interact with centromeres. One of them, TgExportin1, interacts with centromere-binding proteins. Exportin1 homologs localize to the nuclear pore complex (NPC). Super-resolution microscopy revealed that TgExportin1 localizes to discrete foci on the nuclear envelope and a network that penetrates the nucleoplasm. Pharmacologically-induced TgExportin1 mislocalization to the cytosol results in changes on overall chromatin organization, and causes centromeres to disperse with concomitant parasite death. Our results suggest that the nuclear pore complex plays a role in positioning centromeres to the nuclear periphery and that centromere clustering is crucial for parasite viability.

## INTRODUCTION

Apicomplexa are obligate intracellular parasites which cause various animal and human diseases including malaria, toxoplasmosis and cryptosporidiosis. All apicomplexan parasites invade and replicate within cells. After intracellular replication, parasites lyse their host to

reinvade a neighboring healthy cell thus perpetuating the infection. While intracellular, apicomplexan parasites replicate by modes of division that differ from those used by their hosts. The most notable distinction between mammalian and Apicomplexa cell division is that the former occurs by open nuclear mitosis immediately followed by cytokinesis (with a few exceptions) while the latter occurs by closed nuclear mitosis, and only in a small number of species is immediately followed by cytokinesis. Additionally, daughter cells do not derive from fission of the mother cytosol and equal partitioning of cellular components, but instead are formed by budding. Budding encompasses de-novo assembly of new cells and major disassembly of the mother cell. The fundamental differences between the modes of cell division used by mammalian cells and parasites suggest that cell division could be a rich source of drugable targets to treat apicomplexan-caused diseases. However, many structural and regulatory aspects of apicomplexan cell division are not well understood.

Until recently, how mitosis progressed in apicomplexan parasites was not understood due to our inability to visualize chromosomes. Direct visualization of chromosomes is impaired by the apparent lack of chromatin condensation throughout the cell cycle in the parasites' nuclei. In past work, however, our laboratory generated a strain in which a histone H3 allows visualization of the centromere-associated nucleosomes [60]. Centromeres are typically a single location on a chromosome where the kinetochore assembles during mitosis. The kinetochore is the point of attachment for microtubules of the mitotic spindle. Centromeres are marked by the presence of a variant histone H3, known as CenH3 or CenPA. With this strain, not only did we map the *T. gondii* centromeres in the genome, but we also observed a particularly puzzling arrangement of centromere in the nucleus. *Toxoplasma gondii*'s 65 MB haploid genome is distributed in 14 chromosomes. Surprisingly, we observed by immunofluorescence assays that all 14 centromeres cluster in the proximity of the centrosome into a single spot [60].

Centromeres move, organize and cluster by interacting with the mitotic spindle through kinetochore components. By visualizing the dynamics of TgCenH3 we identified that mitosis in *T. gondii* includes all stages observed in eukaryotic mitoses. We observed that chromosomes align establishing a metaphase plate following entry into S phase, upon centrosome duplication. Next, chromosomes go through anaphase and telophase, after which mitosis completes. Following mitosis, the nucleus undergoes fission and is parceled into each one of two daughter cells. Based on ultrastructural work describing the presence of intranuclear microtubules during apicomplexan mitosis, we hypothesize that the dynamics of the *T. gondii* centromeres during division are most likely controlled by the mitotic spindle and the centrosome. Moreover, parasites treated with microtubule-disrupting agents fail to segregate their nuclei properly [63].

Normally, upon entry into interphase or G1 centromeres of most cell types dissociate from the mitotic spindle and redistribute throughout the nucleus; in *T. gondii* this is not the case. Following mitosis its centromeres remain clustered at the periphery of the nucleus, at a location intimately associated with the position of the centrosome. Recently, centromeres of *Plasmodium falciparum* were shown to cluster in the proximity of its centrosome equivalents outside of mitosis [64]. We have observed a similar phenomenon in *Sarcocystis neurona* (Figure S2.4). Thus, centromere clustering appears to be a wide spread phenomenon among apicomplexans. We hypothesize that centromere clustering is a mechanism used by parasites to keep track of their chromosomes throughout their intracellular development in the absence of chromatin condensation, and that this is essential for maintenance of genome integrity.

The molecular mechanisms mediating chromatin sequestration to defined nuclear territories and specialized sub-compartments are unknown in Apicomplexa. Cytoskeletal elements of the nuclear envelope, DNA and membrane-binding proteins are likely involved.

21

Here, we set out to determine the mechanism of centromere clustering using *T. gondii* as a model for the phylum. We show that centromere clustering is not mediated by microtubules or the actin cytoskeleton. We identify TgSMC1, a novel centromeric factor with roles in chromatin organization. Through co-immunoprecipitation and mass spectrometry analysis of TgSMC1's interactors, we identify additional proteins with broader nuclear distribution that interact with centromeres. One of them, TgExportin1, interacts with both TgCenH3 and TgSMC1. Exportin1 homologs in yeast and mammalian cells localize to the nuclear pore complex (NPC). Super-resolution microscopy revealed that TgExportin1 localizes to discrete foci on the nuclear envelope and flanks the centromeres. Pharmacologically-induced mislocalization of TgExportin1 to the cytosol results in changes on overall chromatin organization, and causes centromeres to disperse with concomitant parasite death. Our results suggest that the NPC plays a role in positioning centromeres to the nuclear periphery and that centromere clustering is key for parasite viability.

**RESULTS**

To explain centromere clustering in *T. gondii* during interphase we set out to test two alternative hypotheses (Figure 2.1C). Our first model predicts that persistent spindle microtubules are constitutively interacting with centromeres, thus maintaining their position, and ascribing the centrosome (MTOC) direct involvement in the process. The second model proposes that proteins present at the nuclear envelope, and interacting with centromeric chromatin, are responsible for centromere clustering (Figure 2.1C).

To test our first model we used pharmacological treatment to disrupt microtubules of the mitotic spindle. Oryzalin is a tubulin-binding drug which prevents tubulin polymerization [65]. At concentrations of 2.5 μM oryzalin prevents polymerization of microtubules into

daughter cell structures, as well as formation of the mitotic spindle [63]. Parasites expressing an

triple HA tagged version of a centromeric marker, TgCenH3 [60], were subjected to treatment

with 2.5 μM oryzalin for 24 hours, fixed and observed by immunofluorescence assay staining for

anti-HA and anti-IMC1.  IMC1 (Inner membrane complex protein 1) labels the parasite pellicle,

and marks of the outline of dividing and non-dividing parasites. In dividing parasites, IMC1 labels

the emerging daughter cell structures (Figure 1.3A).  Upon drug treatment, dividing parasites do

not assemble distinguishable daughter cell structures and fail to segregate their genome

properly (Figure 2.2). This is consistent with previous reports that oryzalin disrupts nuclear

division [63]. Improper nuclear division can be denoted by the presence of 3 centromere

clusters within a single parasite (Figure 2.2D). Interestingly, interphase as well as dividing

parasites treated with oryzalin exhibit a single spot-like localization for TgCenH3, suggesting that

oryzalin treatment does not cause centromeres to disperse in interphase, or division. These

results suggested to us that a mitotic spindle was likely not responsible for centromere

clustering during interphase. However, markers to directly observe the mitotic spindle upon

oryzalin treatment are not available, thus we cannot rule out partial or insufficient spindle

disruption upon drug treatment.

To unequivocally show that a mitotic spindle is not present during interphase in *T.*

*gondii,* we serially sectioned parasite nuclei and observed them by transmission electron

microscopy. Parasites were categorized as "interphase" when a single, unduplicated centrosome

could be seen, and by the absence of signs of division (such as daughter cell structures). In all

cases, sections spanning the entire nucleus were obtained. In the vast majority of cases, sections

spanned the entire parasite, thus ruling out presence of additional centrosomes in parasites

considered to be in interphase. Upon three dimensional reconstructions, we observed that

while mitotic spindle microtubules are readily observable in dividing parasites (duplicated

centrosomes) (Figure 2.3A) they cannot be detected in interphase parasites (Figure 2.3B and Movie S2.1). In fact, we detect microtubules in 98% of the dividing parasites (n=13), while microtubules are seen in only 4% of parasites considered to be in interphase (n=60). The latter could represent parasites just emerged from a division cycle.  This structural work supports our results obtained by pharmacological treatment. Taken together these results strongly suggest that microtubules are not responsible for mediating centromere clustering in *T. gondii*.

Local actin polymerization was recently reported to affect telomere positioning in *the P. falciparum* nucleus [66]. To assess the role of actin in centromere clustering, parasites were treated with Cytochalasin D, an actin de-polymerizing agent. Treated parasites did not exhibit centromere un-clustering (Figure S2.1).  Additionally, a *T. gondii* temperature sensitive mutant of the nuclear actin ARP4 exhibits normal centromere clustering [67]. Taken together, these results suggest that elements of the nuclear actin or microtubules are not involved in maintaining centromere clustering during interphase.

We then set out to test our second hypothesis, which proposed that chromatin-binding factors mediate centromere clustering. We set out to identify centromere binding factors which could be involved in the process. First we attempted to determine the protein partners and interactors of TgCenH3 by co-immunoprecipitation. However, we repeatedly failed to precipitate TgCenH3. Most likely this was due to technical limitations owed to the low abundance and high insolubility of this protein.  Therefore we set out to identify additional centromeric proteins which would serve our purposes better.

Structural Maintenance of Chromosome proteins, SMCs, are ATPases which play multiple roles in chromatin organization. They can be functionally divided into three categories. SMC1 and SMC3 homologs dimerize to form the "cohesin" complex, which is responsible for

maintaining sister chromatid cohesion up until chromosome segregation onset during late

metaphase/anaphase. SMC2 and SMC4 homologs dimerize to form the "condensin" complex

which aids in chromosome condensation throughout the cell cycle and especially during mitosis.

SMC5 and SMC6 form a distinct complex with not well characterized functions in meiosis. In

addition to their canonical functions in the cohesin complex, SMC1 homologs have been

implicated in processes ranging from control of gene expression to membrane anchoring of

heterochromatin to DNA damage repair and recombination, to cross linking of mitotic spindle

microtubules [68, 69]. Importantly, SMC1 homologs have been shown to directly associate with

the centromeric histone H3 both in yeast and in drosophila [68, 69].

We identified four genes with sequence similarity to SMC proteins in the *T. gondii* genome

by searching for homologs of the budding yeast *Saccharomyces cerevisiae* SMCs (Figure S2.1).

Phylogenetic analysis showed that each of *T. gondii*'s predicted SMC protein coding genes

clustered with a given subset of SMCs.TgME49_288700 clusters with SMC1-like SMCs;

TgME49_297800 is more closely related to SMC2 from yeast and plants, while TgME49_106310

and TgME49_231170 are homologous to SMC3 and SMC4 respectively (Figure S2.1A).  To

further investigate the predicted SMC1 homolog in *T. gondii* we generated epitope tagged

strains by inserting the 3' end of the TgME49_288700 gene (from here on referred to as

TgSMC1), with a triple hemagglutinin (HA) epitope tag or a yellow fluorescent protein (YFP)

(Figure S2.1B).  In addition, we raised mouse and rabbit anti-sera against a recombinant C-

terminal fragment of TgSMC1 consisting of the last 400 amino-acids of the protein. Specific

antibodies raised against TgSMC1 recognize a protein of the predicted size of 183 KD (or the

expected molecular weight shift in the C-terminal YFP labeled strain) by western blot (Figure

S2.1C).

Using these reagents we investigated TgSMC1's localization by immunofluorescence assays

(IFA). Co-staining with the pellicle marker IMC1 revealed that TgSMC1 localizes to a single spot

in the nuclear periphery in non-dividing parasites. In dividing parasites, denoted by the presence

of daughter cell IMC structures, TgSMC1 spot duplicates, and two dots per nucleus can be seen

(Figure 2.4A). To better characterize TgSMC1's localization within the nucleus we co-stained our

tagged cell lines with antibodies which label specific sub-compartments of the nuclear

periphery. Anti-Morn1 labels the basal complex of the IMC, as well as, a nuclear structure in

immediate proximity of the centrosome know as the centrocone [37, 70]. The centrocone is a

conical structure in the nuclear envelope which houses the mitotic spindle during division.

TgChromo1 is a DNA-binding protein with affinity for heterochromatin localized at peri-

centromeric and telomeric regions of the *T. gondii* genome.  While TgSMC1 largely co-localizes

with TgMorn1 (Figure 2.4A), TgChromo1 appears to flank TgSMC1's localization (Figure 2.4B).

Taken together, these observations suggest that TgSMC1 may localize to the centromeres.

To unequivocally determine whether TgSMC1 localizes to the centromeres, we performed

immuno-fluorescence assays co-staining with the marker of centromeres, TgCENH3. Using a

monoclonal antibody raised against TgCenH3 [30], we observed that indeed TgSMC1's nuclear

punctuate localization coincides with that of the centromeric marker TgCENH3 (Fig 2.5A-B). To

investigate this further, we performed immunoprecipitation of TgSMC1-HA associated

chromatin, followed by hybridization to a microarray chip covering the majority of *T. gondii*'s

genome (ChIP-CHIP). Significant hybridization was obtained for 10 out of the 14 chromosomes in

the genome. We failed to detect a signal for chromosomes Ia, Ib, VIIa and VIIb. The hybridization

peaks for chromosomes II, III, V, VI, and VIII-XI coincide with the position of centromeres in

these chromosomes mapped by ChIP-CHIP of TgCenH3 [60]. Moreover, TgSMC1 ChIP-CHIP

hybridization signal shows almost perfect overlap with the chromatin regions bound by

TgCENH3 (Figure 2.5C). The only exception is Chromosome XII, in which SMC1 hybridization appears to be at the 3' end of the chromosome while TgCenH3 associated chromatin mapped to the 5' end of the chromosome. This suggests that TgSMC1 physically interacts with centromeric chromatin of chromosomes. Consistent with this assignment, co-staining with anti-Centrin1, a marker for the centrosome revealed that TgSMC1 localizes in its proximity (Figure 2.6A). We had previously established that TgCenH3 localizes in the proximity of the centrosome throughout the cell cycle. TgSMC1's localization appears intimately related to that of the centrosome as well.

SMC1 homologs are most commonly found as part of the cohesin complex. This complex maintains sister chromatids cohesion following DNA replication up to the onset of anaphase. In mammalian cells, SMC1 enters the nucleus in S phase, but is translocated back to the cytosol at the mid of mitosis. Therefore, homologs of SMC1 normally exhibit cell-cycle dependent changes in their localization. Surprisingly, when we examined TgSMC1's dynamics throughout the cell cycle, we noticed that it appears to persist in the nucleus, and in the proximity of the centrosome (Figure 2.6B). By IFA, co-staining with anti-Centrin1, we observe that TgSMC1 follows the same dynamics as those previously described for the centromeric marker TgCenH3. TgSMC1 can be first detected in interphase parasites at the periphery of the nucleus, in close proximity to the centrosome (Figure 2.6B, panel 1). Following centrosome duplication, which marks entry into S phase, TgSMC1 can be detected within the nucleus, and arranged in a cluster that is more or less equidistant from each centrosome (Figure 2.6B, panel 2). This likely represents metaphase. As mitosis progresses the single focus of TgSMC1 separates into two distinct dots, each associated with a different centrosome (Figure 2.6B, panels 3 and 4). Upon completion of mitosis and re-entry into G1, TgSMC1 localizes at the periphery of the nucleus (Figure 2.6B, panel 5). Similar cell-cycle dependent localization dynamics can be detected in

Cryo-immuno gold labeled TgSMC1-HA parasites when observed by TEM. In non-dividing

parasites, gold particles can be detected proximal to the nuclear envelope (Figure 2.6C).

Interestingly, a cleft in the nuclear envelope can be observed where gold particles seem to

accumulate (Figure 2.6C, inset). During division, TgSMC1 can be detected almost equidistant to

the two centrocone structures of the dividing nucleus (Figure 2.6D). This might represent a

metaphase plate. Gold particles can be detected at the base of the centrocone during the

remaining stages of mitosis (Figure 2.6E). Taken together, our results suggest that TgSMC1 is a

centromere-binding protein which persists at this location throughout the cell cycle.

Next, we set out identify the interactors of TgSMC1. Parasites were subjected to lysis under

mild conditions, incubated with appropriate anti-sera, and TgSMC1 was precipitated. Proteins

co-immuno-precipitated with TgSMC1 were separated by gel electrophoresis, excised from the

gel, subjected to trypsin digestion, and identified by LC-MS. Four independently obtained

samples were analyzed. Sample 1 consisted of proteins obtained from a wild type RH strain

using rabbit anti-TgSMC1 to immunoprecipitate TgSMC1. Sample 2 was obtained similarly; with

the only difference being that the anti-TgSMC1 antibody was subjected to affinity purification

prior to the experiment. Sample 3 consisted of proteins obtained from the TgSMC1-YFP strain

using anti-GFP to immunoprecipitate TgSMC1. Sample 4 was obtained from a wild type RH strain

using anti-GFP for immunoprecipitation and served as a negative control. Figure 2.7 A shows

sample 3 as a representative example of the immunoprecipitation scheme followed in this

experiment for all samples. Western blot reveals that TgSMC1 is quantitatively recovered in the

elution fraction (Figure 2.7A). Fractions visualized in a silver-stained acrylamide gel reveal

minimal loss of TgSMC1 in the flow through or washes fractions (Figure 2.7A). The elution

fraction contains a limited number of bands corresponding to proteins which co-precipitate with

TgSMC1. Figure 2.7 B shows a western blot of the elution fractions for all the samples.

Immunoprecipitation experiments in the absence of a primary antibody or using pre-immune

rabbit sera fail to pull down TgSMC1. Elution fractions analyzed by western blot show that

minimal amount of tubulin co-precipitate with TgSMC1 (Figure 2.7C). TgSMC1's elution fraction

contains TgCenH3, suggesting that there is physical interaction between these two proteins

(Figure 2.7C). Importantly, TgChromo1 which binds chromatin immediately adjacent to the

centromeres does not co-precipitate with TgSMC1 (Figure 2.7C).

The results of the mass spectrometry analysis of proteins contained in the elution fractions

of all four samples are shown in Table 2.1 by ascending order of accession number in the *T.

gondii* genome database. Hits exhibiting the highest number of peptides per sample are

highlighted in grey.  In order to further study these proteins and their potential interaction with

centromeres, we generated reporter strains by replacing the genes' 3' end with a 3-HA tag of

two of them; TgImportin1 and TgExportin1 (TgME49_253730 and TgME49_249530 respectively)

(Figure 2.8 A and B). To investigate whether the interactions between TgSMC1 and TgImportin1,

and TgSMC1 and TgExportin1 were real, we performed reciprocal co-immunoprecipitation

assays. First, we pulled down either TgImportin1 or TgExportin1 with anti-HA antibodies, and

probed the elution fraction with anti-TgSMC1 (Figure 2.8 C and D). Conversely, we

immunoprecipitated TgSMC1 using anti-TgSMC1 in the TgImportin1-HA and TgExportin1-HA cell

lines, and probed the elution fraction with anti-HA (Figure 2.8 E and F). In both cases, TgSMC1

co-precipitated with TgImportin1 and TgExportin1, consistent with the mass spectrometry

analysis results. Interestingly, we were able to detect TgCenH3 in TgExportin1's elution fraction

(Figure 2.8G).

Next, we investigated the localization of TgImportin1 and TgExportin1 by immuno-

fluorescence assays using anti-HA antibodies and anti-IMC1 to label the parasites' outlines.

TgImportin1 and TgExportin1 localize to the nucleus both in interphase and in dividing parasites (Figure 2.8 H). IFAs co-staining with anti-HA to label TgImportin1 and TgExportin1 and anti-TgSMC1 revealed that while these proteins co-localize with TgSMC1, they do not exclusively localize to the centromeric foci but appear homogenously distributed throughout the nucleus (Figure 2.8 I).

To our surprise, the potential interactors of TgSMC1 best represented in all samples, are annotated as homologs of the Exportin and Importin family of proteins. Exportins and Importins are nuclear proteins which interact with transmembrane components of the nuclear pore complex (NPC). Nuclear pores are readily observable in sections through the nucleus by TEM. They can be seen as interruptions in the nuclear envelope if sectioned perpendicularly (Figure 2.9 A), or appearing as an orthogonal-shaped structure on the surface of the nucleus (Figure 2.9A). We reasoned that if an NPC is involved in centromere clustering, it should be observable in serial sections of interphase nuclei in the region where centromeres cluster. Indeed, we observed that in the proximity of the centrosome regions of the nuclear envelope appear to be discontinue (Figure 2.9B). This is clearly observable in 84% of the interphase parasites nuclei we observed by TEM (n=60) (Figure 2.9H). Structured Illumination super resolution microscopy (SIM-SR) revealed that TgExportin1 localizes to discrete foci on the nucleus, consistent with its predicted NPC localization (Figure 2.9C). Some of the TgExportin1 foci co-localize with TgCenH3 (Figure 2.9D-E). When observed by SIM-SR microscopy, the localization of TgSMC1 is better defined as a semi-circle arranged around an empty spot, which is filled by the centromeres marked by TgCenH3 (Figure 2.9 F and G).

TgExporin1 is a well conserved homolog of the fission yeast SpCRM1. Leptomycin B (LMB), an anti-fungal drug produced by the *Streptomyces* species inhibits the nuclear transport

functions of SpCRM1 by glycosylating its cysteine 529 and causing it to localize to the cytosol

[71]. *Saccharomyces cerevisiae* CRM1, on the other hand, is not sensitive to Leptomycin B due

to a single amino-acid change to Threonine at position 539. The Leptomycin-B targeted cysteine

residue and its amino-acidic context are highly conserved between TgExportin1 and SpCRM1

(Figure S2.3 A). Immunoprecipitated TgExportin1 upon LMB treatment exhibits motility shifts

appreciable by western blot (Figure S2.3B).  Moreover, Leptomycin B treatment of *T. gondii*

parasites, at low concentrations, causes TgExportin1 to change its localization from the nucleus

to the cytosol (Figure S2.3C). This effect is akin to what is observed for ScCRM1's localization

upon LMB treatment [71, 72]. Prolonged exposure of *T. gondii* parasites to LMB results in

parasite loss of viability (Figure 2.10E).

We took advantage of TgExportin1's sensitivity to LMB to analyze its role in centromere

clustering. We treated parasites with LMB and observed the localization of TgCenH3 by IFA

following treatment. In treated samples, the majority of the parasites exhibited re-localization of

TgExportin1 to the cytosol. However, a few parasites conserved a tight nuclear localization. In

those parasites TgCenH3's localization was not affected (Figure 2.10A). However, parasites

exhibiting cytosolic TgExportin1 showed altered TgCenH3 localization. In particular, multiple foci

per nucleus could be detected (Figure 2.10A). Moreover, when we co-stained with anti-centrin1

to label the centrosome, we noticed multiple TgCenH3 foci could be seen in the presence of a

single centrosome (Figure 2.10B). Up to 5, and an average of 1.7 TgCenH3 "spots" were

detectable in nuclei associated with a single centrosome following LMB treatment (Figure

2.10C). We believe this to be a consequence of loss of centromere clustering. However, the

most striking effect of LMB treatment was that TgCenH3 was not at all detectable in 30% of the

nuclei (Figure 2.10D). We hypothesized that in LMB treated parasites dispersion of centromeres

may lower our ability to detect them.

To overcome the sensitivity limitations of IFAs, and further investigate the effect of Leptomycin B on centromere clustering, we resorted to fluorescence in situ hybridization experiments. We used fluorescently labeled probes that would allow us to directly observe the localization of individual centromeres independently of TgCenH3. Two probes which hybridize to DNA immediately adjacent to the centromeres of Chromosomes IX and IV were labeled with Alexa-488 and -594 respectively [73]. Consistent with our previous results, we observed that in control parasites these two centromeres co-localize (Figure 2.11 A). However, in LMB treated parasites, we note that the two centromeres localize to apparently distinct regions of the nucleus (Figure 2.11A). In LMB treated nuclei in which signal for both chromosomes could be detected, 56% of the time the centromeres of Chromosomes IX and IV did not co-localize (n=20) (Figure 2.11C). By FISH-IFA we were able to observe simultaneously the localization of Chromosome IX's centromere with respect to that of the centrosome (marked by anti-centrin staining). We established that in control treated parasites, the signal of chromosome IX's centromeres is adjacent to the centrosome (Figure 2.11B). However, in LMB treated nuclei, Chromosome IX centromeres appeared distant from the centrosome (Figure 2.11B). Taken together, our results suggest that mis-localization of TgExportin1 to the cytosol caused by LMB treatment, causes a loss of centromere clustering in the vicinity of the centrosome.

**DISCUSSION**

We set out to identify the mechanism mediating centromere clustering in *T. gondii*. Our first set of experiments demonstrated that microtubules of the mitotic spindle do not mediate the process. We proposed that chromatin binding factors at the centromeres could be mediating the maintenance of their localization at the periphery of the nucleus. We identified a novel component of the *Toxoplasma gondii* with homology to structural maintenance of

chromosomes (SMC). SMCs are a family of proteins containing two ATPase globular domains at the C and N-terminal portions of the protein, and a hinge domain which establishes interactions with chromatin and other SMC and non-SMC proteins. SMCs have multiple roles in higher order chromatin organization and dynamics, powered by ATP hydrolysis [74, 75]. We determined that TgSMC1 is a centromere-associated protein in *T. gondii* which possibly interacts with the centromeric histone variant H3, TgCenH3, and centromeric chromatin. SMC1 interactions with CenH3 homologs have been previously reported in yeast and drosophila, and our data suggests that this might also be the case in *T. gondii* [76, 77].

SMC1 homologs have a role in chromosome segregation during mitosis [78]. Typically, SMC1 localizes to sister chromatids, in the proximities of or at the centromeres, during mitosis and up until late metaphase/early anaphase. The cohesion function of the complex, formed by SMC1 and its partners, is well established. Two models have been proposed to explain cohesion established by SMC proteins. One proposes that cohesin embraces the replicated DNA as a ring. The second model proposes that two cohesin complexes could form a symmetric dimer that handcuffs chromatids to each other [79-81]. During interphase, SMC1 homologs are translocated to the cytosol or associate with non-centromeric chromatin [77, 82].

In *Toxoplasma gondii*, however, we observed that TgSMC1 persists at the centromeres throughout the cell cycle. This argues against an exclusive function in chromatid sister cohesion. It has been proposed that the complex could have alternative functions, which are less well understood. Cohesin appears to contribute to gene regulation, DNA damage repair, transcriptional control, and maintenance of higher order chromatin structure[79]. In human cells, SMC1 has been shown to mediate transcriptional insulation by binding chromatin boundaries in post-mitotic cells [83-85]. Interestingly, in the closely related Apicomplexa *Eimeria*

33

*tenella,* SMC1 is part of a plaque formed at the nuclear envelope in which telomeres attach during meiotic division of the parasite [86]. Our results suggest that TgSMC1 could fulfill a similar role in mediating the attachment of centromeres to the nuclear envelope.

We used TgSMC1 to identify further interactors of the centromeres. In particular, we were interested in determining the nature of components that could mediate the interactions between the centromeres and the nuclear envelope. TgSMC1 co-precipitated with components of the nuclear pore complex, TgExportin7, TgExportin1 and TgImportin1. These results suggest that components of the nuclear pore complex could be a structural landmark at the nuclear envelope required for organization of a chromatin domain, the centromeres, within the nucleus.

Nuclear pores consist of a central scaffold which spans the nuclear envelope. Their octagonal shape is imparted by 8 filaments, each formed by more than 30 different proteins, which extend into the nucleoplasm and are conjoined at the end by 8 other filaments, resulting in a basket-like structure [87]. Proteins of the nuclear pore are collectively known as nucleoporins (NUPs), and can add up to several hundred per nuclear pore complex. At least three transmembrane domains containing NUPs, anchor the NPC to the nuclear envelope. FG NUPs line the central channel of the pore. These NUPs contain hydrophilic amino-acids with hydrophobic stretches of phenylalanine and glycine (FG repeats). FG repeats in the central channel associate with each other forming a molecular sieve which prevents the diffusion of molecules larger than 40 KDa or 5 nm through the pore. For larger molecules to travel through the pore, they must reversibly associate with FG nucleoporins[87]. Translocation of molecules through the nuclear pore depends on importins, exportins and transportins, collectively known as nuclear transport receptors (NTRs) [88]. NTRs bind nuclear localization signals or nuclear export signals on molecules, and facilitate their unidirectional translocation through the pore by

interacting the FG repeats within the pore. Translocation, facilitated by NTRs, occurs at the impressive rate of 1500 molecules per second per nuclear pore complex [87].

Of the TgSMC1 interactors identified, TgExportin7, TgExportin1 and TgImportin1, we were able to determine the localization of the latter two. Consistent with their predicted functions and annotation as components of the nuclear pore complex, they localize to the nucleus. By super-resolution microscopy we showed that TgExportin1 and TgImportin1 localize to discrete foci in the nucleus, which co-localize or flank the location of centromeres in the nuclear periphery. Interestingly by super-resolution microscopy we observed that TgSMC1 organizes in to a donut-like localization which surrounds a void oval.  By EM, we observed that gold particles labeling TgSMC1 in cryo-sections seem to accumulate in a cleft of the nuclear envelope. Taken together, our structural work strongly suggests that centromeres arrange around a pore-like structure. Consistently, when TgExportin1's localization is disrupted, centromeres disperse in the nucleoplasm and lose their connection with the nuclear envelope and their centrosome-dependent localization.

Proteins associated peripherally with the NPC, such as NTRs, have been shown to fulfill additional roles other than their transport function. A genetic screen for chromatin boundary activities (i.e. transcriptional insulation) in *S. cerevisiae* identified various proteins involved in nuclear-cytoplasmic traffic which also exhibit chromatin insulating activity [89]. Several transportins showed strong boundary activity, and intriguingly, like TgExportin1 and TgImportin1, they all belong to the Importin-β superfamily.  Boundary activity of transportins is exerted by association with components of the nuclear pore. In particular Nup2, a peripheral NUP associated with the nuclear pore basket, is essential for boundary activity of transportins in yeast [89, 90].

NUPs have been shown to interact with chromatin, and to regulate chromatin

organization and activity. Interestingly, Nup98 co-precipitates with SMC1 and the cohesin

complex in Drosophila [91]. ChIP-CHIP of Nup93 demonstrated direct chromatin association with

the nuclear pore complex in human cells. This association is dependent on the state of

chromatin condensation. Changes in chromatin condensation correlate with chromatin re-

organization with respect to the nuclear pore complex in mammalian cells [92].  Dynamic

changes in the localization of nuclear pores were extensively characterized by elegant

microscopy techniques during the intracellular development of *Plasmodium falciparum*. These

changes in localization correlate with changes in the state of chromatin condensation,

observable by EM. During schizogony, nuclear pore biogenesis seems to stall. As a consequence,

the number of nuclear pore complexes per nucleus decreases as mitosis advances. Late

schizonts are left with 2-6 nuclear pores per nucleus, which cluster together and invariably are

surrounded by heterochromatin [93].  These findings suggest that nuclear pores associate with

specific states of chromatin condensation, and in particular heterochromatin, in the *P.

falciparum* nuclei.  In this context, it is worth noting that epigenetic marks associated with

heterochromatic state flank the centromeres of *T. gondii* [73, 94].

Much like Apicomplexa, the fission yeast *Schizosaccharomyces pombe* divides by closed

mitosis of the nucleus. The centromeres of its three chromosomes are clustered during

interphase, adjacent to the spindle pole body – the microtubule organizing center of the mitotic

spindle during mitosis [95]. In crm1 (a TgExportin1 homolog) mutant cells, the interphase

arrangement of centromeres is disrupted [95]. *S. pombe* CRM1 was first identified in a cold-

sensitive mutant screen[96]. This mutant presented deformed nuclear and chromatin

morphology. Based on the phenotypic characterization, and by determining that SpCRM1

localized at the periphery of the nucleus, the authors concluded that SpCRM1 "must be one of

those nuclear components that modify chromosome structures or regulate the nuclear

environment required for maintenance of higher order chromosome structures [96]."

Interestingly, characterization of the effect of temperature sensitive mutations identified that a

point mutation caused Crm1 to mis-localize to the cytosol[96], an effect that can be mimicked

on wild type Crm1 by Leptomycin B treatment [71, 72]. At the restrictive temperature the

overall chromatin organization seems affected and centromeres of SpCRM1ts mutant come

apart and disperse in the nucleus; an effect akin to what we observed in *T. gondii* upon

treatment with Leptomycin B*.*

Centromere clustering could be part of a more general organizational scheme of nuclear

elements in apicomplexan parasites, dependent on interactions with the nuclear pore complex.

The organization of nuclear territories could constitute a mechanism by which functional

domains are differentially regulated through development. Positioning of telomeres to specific

regions of the nucleus has been shown to be important to the biology of *Plasmodium*

*falciparum*. Var genes, which encode for the polymorphic PfEMP1 protein, and allow the

parasite to fool the host's immune response by antigenic variation, localize to sub- telomeric

regions. Repositioning of telomeres to active expression or silenced sites has profound

consequences on the biology of the malaria parasite. Although its functional significance has not

been established,  telomeres of *T. gondii* have been shown to localize to discrete foci at the

periphery of the nucleus [73]. Interestingly, a role for the nuclear pore in organization chromatin

elements has been extensively described for telomeres of other species. In yeast, the silent

mating-type loci and telomeres are regulated by interactions with components of the nuclear

periphery, including binding to Nup145 [97-99].

To conclude, we propose a model in which centromeres are "hung up" on the nuclear envelope by interacting with components of the nuclear envelope during interphase. Following entry into S-phase, centromeres are handed over to the mitotic spindle during mitosis. Upon mitosis exit, centromeres are re-positioned onto the nuclear envelope until the onset of the next round of division (Figure 2.12A).While our results shed light onto an important mechanism of organization, essential for parasite survival, there are still many unanswered questions. We have started to unravel the mechanism by which centromeres are held in position at the nuclear envelope, however, we do not yet understand how they are recruited to a specific site on the nuclear periphery. The localization of centromeres at the nuclear envelope is not random. The centrosome is consistently adjacent on the cytosolic side. Moreover, the centromere-centrosome association is maintained both in *T. gondii* and *P. falciparum*, regardless of the cell cycle stage. This suggests that the mechanism mediating this association extends beyond the biology of *T. gondii*.

Our "hanger" model offers a plausible explanation. One could imagine a scenario in which centromeres are handed over to the mitotic spindle upon its formation early in S-phase by kinetochore-microtubule interactions. The mitotic spindle in Apicomplexa forms immediately adjacent to the centrosome, within an intact nuclear envelope. Upon mitotic exit and mitotic spindle disassembly centromeres are released, and are able to re-associate with the closest nuclear pore by interacting with its components, for examples, TgExportin1. We showed that a "readily accessible" pore is found at the nuclear envelope near all centromeres, adjacent to the site of mitotic spindle assembly and disassembly.

The latter idea, however, falls short in explaining how all centromeres associate with the same set of nuclear pores, and how the distance between the centrosome and centromeres

remains practically unchanged during the progression of the cell cycle. Perhaps, chromatin factors keep centromeres associated not only to the nuclear envelope, but to each other. This would impose an additional level of physical constraint and could prevent centromeres from drifting away from each other in the absence of a spindle, forcing them all to associate with the same pore. TgSMC1 could potentially serve this function through its DNA cross-linking ability. Finally, it is reasonable to expect that a centrosome-associated factor could be involved in directing centromeres to a specialized nuclear pore. Further study of centrosome-associated factors could shed light on the identity of centrosome components with roles in targeting or maintaining the position of centrosome-associated nuclear components.

## MATERIALS AND METHODS

### Chromatin immunoprecipitation

ChIP was performed as described in [60, 100, 101]. Briefly, chromatin from SMC1-HA transgenic tachyzoites was cross-linked for 10 min with 1% formaldehyde at room temperature and purified after sonication yielding fragments of 500–1,000 bp. Chromatin was immunoprecipitated at 4 °C overnight using a HA polyclonal antibody (Abcam ab9110) and washed extensively. The DNA was treated with proteinase K for 2 h and subsequently purified using the Qiagen PCR purification kit. 100 ng of precipitated DNA was amplified using the DNA Genomeplex whole genome amplification kit (Sigma) and subsequently labeled using random primers coupled to a fluorochrome. Probes were hybridized to a tiled oligonucleotide array representing the complete *T. gondii* genome according to NimbleGen Systems procedures. The array was fabricated by NimbleGen Systems (http://www.nimblegen.com) and contained 740000 oligonucleotides representing version 4 of the Me49 genome with an approximate spacing of 80 bp between each oligonucleotide.

**Co-Immunoprecipitation (Co-IP) and Mass Spectrometry Analysis**

Approximately $1 \times 10^9$ SMC1_YFP, RHΔKu80 or the HA-tagged lines generated in this

study (TgImportin1-HA, TgExportin1-HA, TgSUN2-HA), were collected by centrifugation, and

washed once with PBS. Parasites were lysed by resuspension in hypotonic buffer (20 mM Hepes,

10 mM KCl, 400 mM Mannitol, 2 nM EDTA) supplemented with EDTA free protease inhibitor

(Roche) to approximately $5 \times 10^8$ parasites/ml, followed by 4 cycles of freeze/thaw with liquid

nitrogen. Efficient lysis was assessed by light microscopy. Debris and intact parasites were

pelleted by centrifugation at 10,000 g for 10 min at $4^0$C. Soluble fractions were incubated

overnight at $4^0$C with 20 µl of the antibody of interest. The next day, 100 µl of Sepharose bound

Protein A or Protein G (Santa Cruz) for rabbit or mouse antibody respectively, were added and

incubated at room temperature for 2 h. Complexes were washed six times with Co-IP wash

buffer (50 mM Tris pH 8, 200 mM NaCl, 2mM EDTA, 1% NP-40) supplemented with protease

inhibitor, then resuspended in 200 µl of SDS-PAGE loading buffer and boiled for 5 minutes.

Elution fractions were used either for mass spectrometry or western blotting. Negative controls

were performed using the pre-immune serum for each antibody or ProteinA/G Sepharose alone.

**Construction of tagged reporter parasites**

*Toxoplasma gondii* RH strain parasites were maintained by serial passage in human

foreskin fibroblast (HFF) cells and genetically manipulated as previously described [102]. To tag

the genomic locus of TgSMC1, TgExportin1, TgImportin1 and TgSUN2 with a 3xHA or a YFP tag,

approximately 1500 bp of the open reading frame ending before the stop codon were amplified

from *T. gondii* genomic DNA. All primer sequences used are shown in supplementary Table S2.2.

These amplicons were cloned via ligation independent cloning (LIC)[103] into the pLIC-HA-CAT

or pLIC-YFP-DHFR vector, respectively to create in-frame fusions [104]. Transgenic clones were

established by transfection of ΔKu80-TaTi parasites and chloramphenicol or pyrimethamine

selection respectively [104]. Integration was confirmed by PCR and western blot in all cases.

**Fluorescence *In Situ* Hybridization**

Intracellular parasites grown on glass coverslips for 24 hours were incubated with 10 nM

Leptomycin B or the equivalent volume of 70% methanol for 24-36 hours, and then fixed with

4% para-formaldehyde in PBS. Downstream sample treatment  and hybridization conditions

were done as described in [105].  Probes were amplified by PCR using genomic DNA as template

[73]. Labeling of probes with Alexa 488 or Alexa 594 was done using the FISH Tag DNA

Multicolor Kit (Molecular Probes) following the manufacturer's instructions. FISH-IFA was done

as described in [73] using anti-centrin1 for co-staining.

**Protein expression and antibody production**

Sequences encoding for the last 400 C-terminal amino-acids of TgSMC1 were amplified

from *T. gondii* cDNA and inserted into plasmid pAVA-421 6xHis [106].  Recombinant fusion

protein was purified on $Ni^{2-}$-NTA resin (Qiagen, Hilden, Germany) [107]. Rabbits were immunized

with 1 mg of purified protein, and serum was collected after 10 weeks (Cocalico Biologicals,

Reamstown, PA, USA).  Mice were immunized with 0.4 mg of purified protein, and serum was

collected after 3 weeks.

**Fluorescence microscopy**

For immunofluorescence assays, host cells (HFF) were inoculated onto coverslips and

infected with parasites. Coverslips were fixed 24 hours after infection, and 24-36 hs following

incubation with 10 nM LeptomycinB (Sigma-Aldrich), with 4% formaldehyde in PBS and

permeabilized with 0.2% Triton X-100 in PBS/3% BSA. Coverslips were then blocked in 3% bovine

serum albumin (BSA) in PBS as previously described [108]. Primary antibodies used were mouse

anti-alpha tubulin at a dilution of 1:1000 (12G10, a gift of Jacek Gaertig, University of Georgia),

rabbit anti-Centrin1 at 1:1000 (gift of Iain Cheeseman, Massachusetts Institute of Technology),

mouse anti-GFP at 1:1000-1:400 (Torry Pines Biolabs), rat anti-HA at 1:1000 (clone 3F10, Roche

Applied Science), mouse anti-IMC1 mAb 45.15 [109] at 1:1000 (gift of Gary Ward, University of

Vermont), mouse anti-TgChromo1 at 1:1000 [73], mouse anti-CenH3 [30] at 1:20, rabbit anti-

MORN1 [37] at 1:250, and rabbit and mouse anti-SMC1 at 1:1000 (generated in this study). The

secondary antibodies used were AlexaFluor 350, AlexaFluor 488, and AlexaFluor 546

(Invitrogen), at a dilution of 1:2000. Images were collected on an Applied Precision Delta Vision

inverted epifluorescence microscope using a UPlans APO 100×/1.40 oil lens. Images were

subjected to deconvolution and contrast adjustment using Applied Precision software

(Softworx). For quantitative image analysis (as described in the results section) a minimum of 50

vacuoles were scored for each out of at least three repeats. Super-Resolution images were

acquired using the Zeiss ELYRA S1 (SR-SIM) microscope. Images were collected and processed

using Zeiss Zen software.  Means and standard deviations were calculated and plotted using

Graph Pad Prism Version 5.0c (La Jolla, California, USA).

**Transmission Electron microscopy and Immuno-gold labeling**

Cells infected with SMC1-HA parasites were fixed in 4% para-formaldehyde/0.05%

glutaraldehyde in 0.1 M sodium phosphate buffer pH 7.4, blocked with 1% FBS in PBS (all RT),

followed by overnight infiltration in 2.3 M sucrose/20% polyvinyl pyrrolidone at 4°C. Samples

were frozen in liquid nitrogen, and sectioned with a Leica UCT cryo-ultra microtome. Sections

were blocked with 1% FBS and subsequently incubated with rat anti-HA (1:100), followed by

incubation with rabbit anti-rat (1:400), and finally 10 nM colloidal gold conjugated protein A.

Washed sections were stained with 0.3% uranyl acetate/2% methyl cellulose and viewed with a JEOL 1200 EX transmission electron microscope. Controls, omitting the primary antibody, were consistently negative at the concentration of colloidal gold conjugated protein A used. Infected cells were also fixed in 2% glutaraldehyde in sodium phosphate buffer 0.1M, pH7.4, followed by post-fixation with 1% osmium tetroxide in sodium phosphate buffer, alcohol dehydration and Epon resin embedding. Serial sections were obtained with a Leica UCT cryo-ultramicrotome and collected in carbon coated single hole grids.

**Western Blotting**

Western blotting was performed as previously described [110]. We used anti-HA (Roche) antibodies at a dilution of 1:1000, anti-tubulin at 1:1000, anti-GFP at 1:500, anti-CenH3 at 1:500 and anti-SMC1 antibodies at a dilution of 1:1000. Pre-immune sera for anti-SMC1 antibodies were used at a comparable dilution.  Horseradish peroxidase (HRP)-conjugated anti-rat, anti-mouse, or anti-rabbit antibody (Pierce) were used at a dilution of 1:20,000
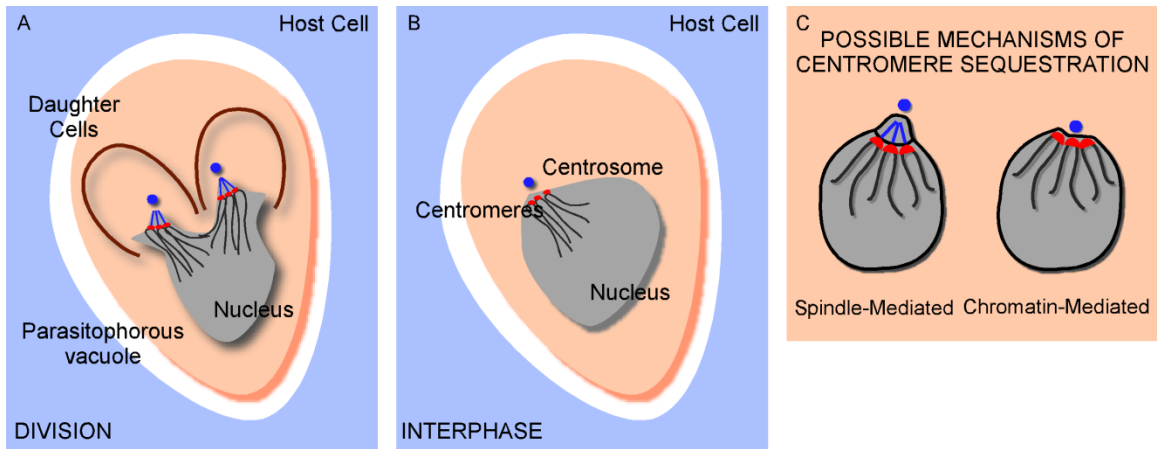
**Figure 2.1 Toxoplasma gondii sequesters centromeres in the periphery of the nucleus throughout the cell cycle. A.** *Toxoplasma gondii* divides by endodyogeny. Two daughter cells (orange) assemble within the mother cell. The nucleus divides by closed mitosis. The mitotic spindle (blue), organized by the centrosome (dark blue), assembles within the nuclear envelope and contacts the centromeres (red). **B.** During interphase (G1), centromeres cluster at the periphery of the nucleus, adjacent to the centrosome. The mechanism of this clustering and its significance for parasite biology is unknown. **C.** We propose two testable hypotheses for the mechanism of centromere sequestration. A mitotic spindle could persist throughout the cell cycle or, alternatively, chromatin-binding factors could mediate attachment of centromeres to the nuclear envelope.
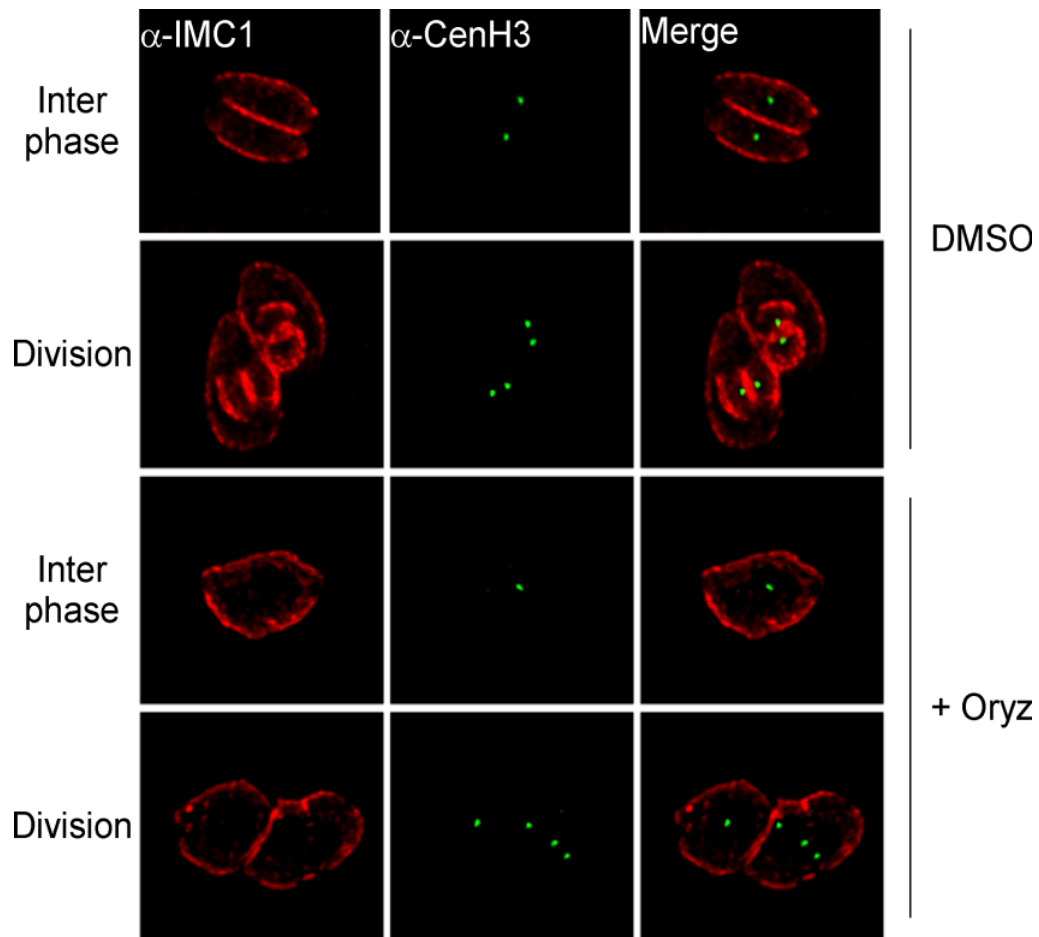
**Figure 2.2. Treatment with the microtubule-disrupting agent Oryzalin does not un-cluster centromeres**. Parasites were treated with DMSO (control) or 2.5 µM Oryzalin, fixed and stained with anti-IMC1 and anti-CenH3. Both in DMSO and Oryzalin treated samples, interphase parasites display a single TgCenH3 dot corresponding to clustered centromeres. In both samples, dividing parasites display duplicated TgCenH3 foci. However, in Oryzalin treated parasites no daughter cell structures can be detected and proper chromosome segregation is impaired as evidenced by the presence of multiple (>2) TgCenH3 foci within a single parasite.
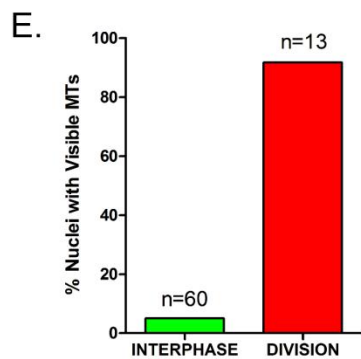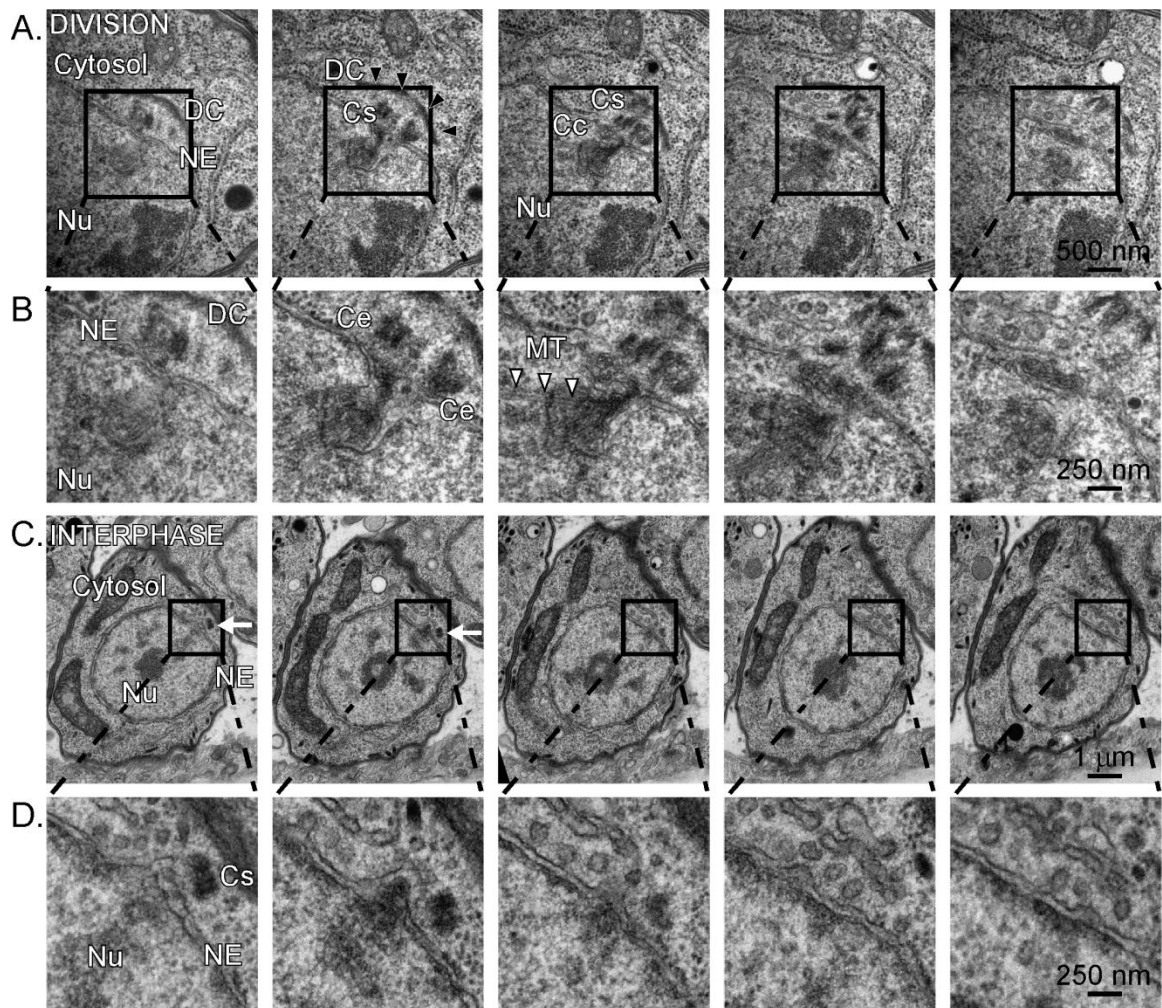
**Figure 2.3. TEM serial sections through dividing and interphase parasites reveal that spindle microtubules are only detectable in mitotic nuclei**. **A.** Panels show consecutive series through a dividing nucleus. A forming daughter cell (DC, black arrowheads) is detectable proximal to the nucleus (Nu) and the centrosome (Cs). The mitotic spindle organizes within the nuclear envelope

46

(NE) in a structure known as the centrocone (Cc). **B.** Zoomed in panels of the boxes indicated in

A. The microtubules (MT, white arrowheads) of the mitotic spindle are clearly visible. **C.** Panels

show consecutive series through a parasite in interphase containing a single centrosome (white

arrow). **D.** Zoomed in panels of the boxes indicated in C. Microtubules are not seen proximal to

the centrosome or the nuclear envelope at the site of centromere sequestration. Note that all

parasite serial sections were obtained from the same block, and thus were subject to identical

fixation and post-fixation treatments. **E.** Parasites present in TEM serial sections were classified

as "interphase" or "dividing", depending on the presence of a single or a duplicated centrosome

respectively, and scored for the presence of visible spindle microtubules.

**A.**

| | α-IMC1 | α-HA (SMC1) | DAPI | Merge |
|---|---|---|---|---|
| Interphase | | | | |
| Division | | | | |

**B.** α-Morn1

Interphase

Division

**C.** α-Chromo1

Interphase

Division
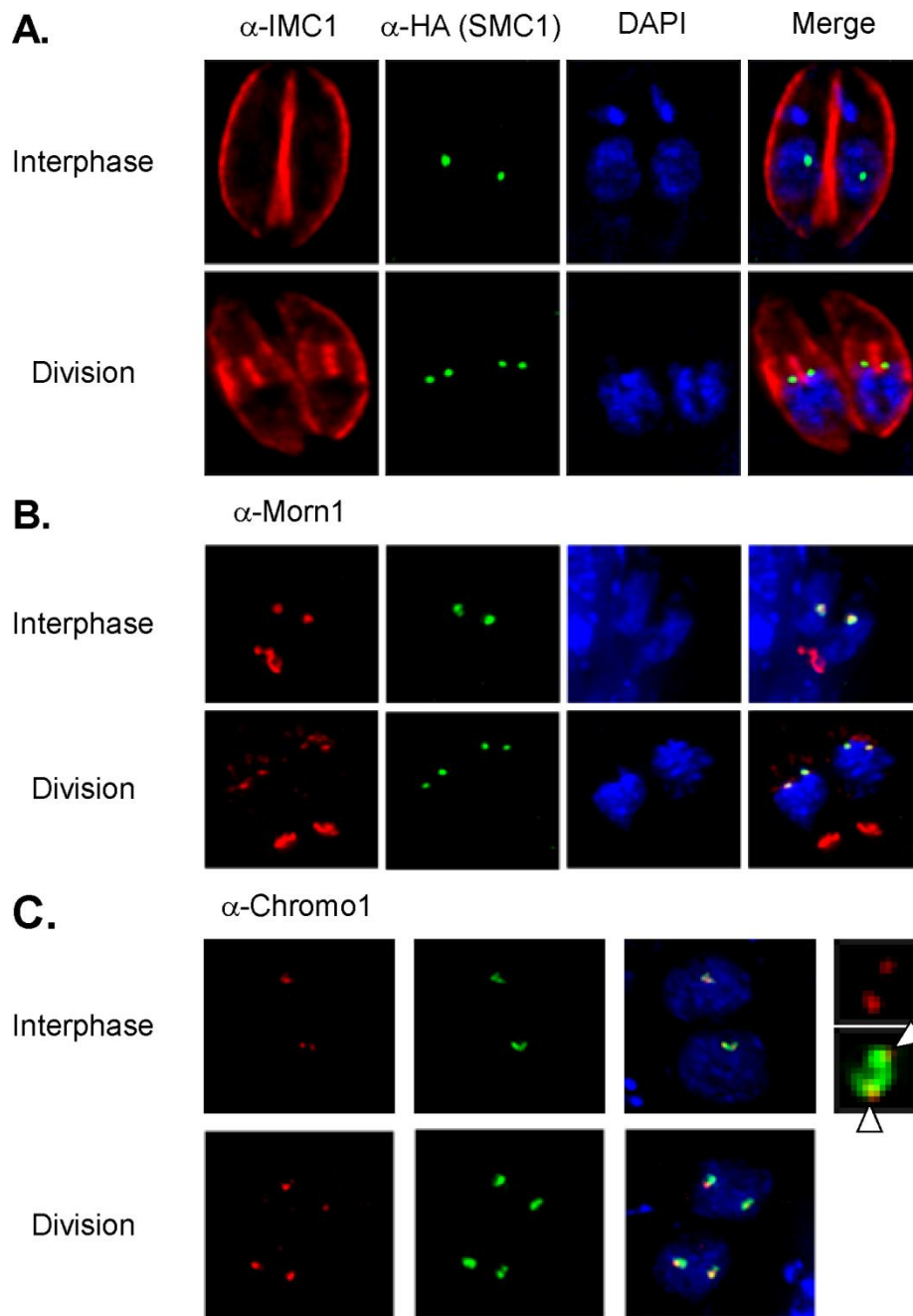
**Figure 2.4. TgSMC1 Localizes at the Periphery of the Nucleus, to a single dot in non-dividing and two foci in dividing parasites. A.** mmunofluorescence assay (IFA) of a strain in which TgSMC1 was endogenously tagged with a C-terminal 3x HA. Anti-HA antibodies were used in combination with anti-IMC1, which labels the parasite's outline.  TgSMC1 localizes to the periphery of the nucleus both in dividing (marked by the presence of daughter cell outlines) and

48

non-dividing (interphase) parasites**. B.** IFA of TgSMC1-HA parasites co-staining with anti-HA (green) and anti-TgMorn1 (red), a marker of the basal end of the parasite, and the centrocone. The centrocone is a specialized structure of the nucleus which houses the mitotic spindle during mitosis **C**. IFA of TgSMC1-HA parasites, co-staining with anti-HA (green) and anti- TgChromo1 (red), a peri-centromeric DNA binding protein. TgChromo1 appears to flank TgSMC1's localization (zoom, white arrowheads).
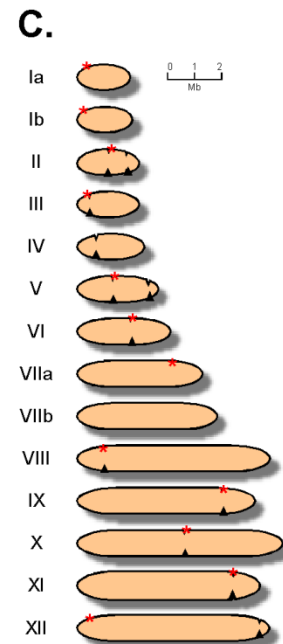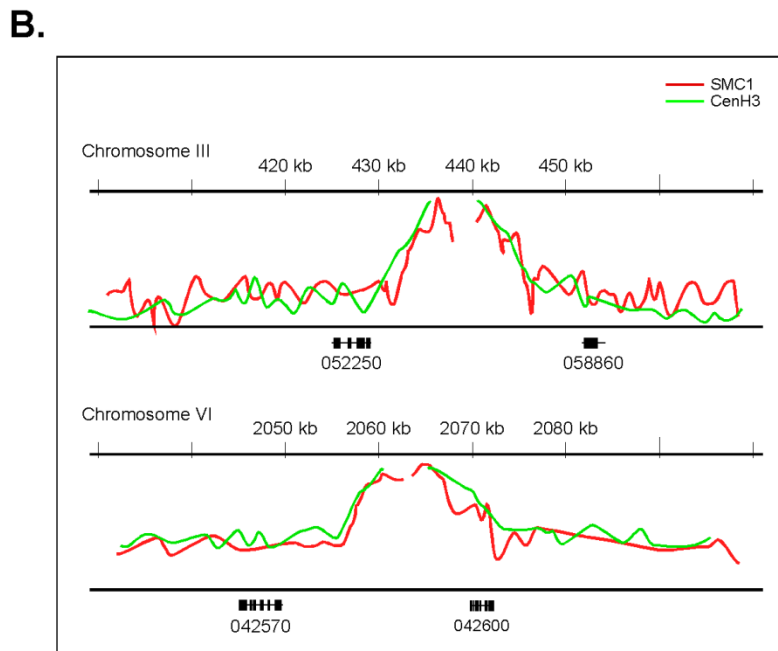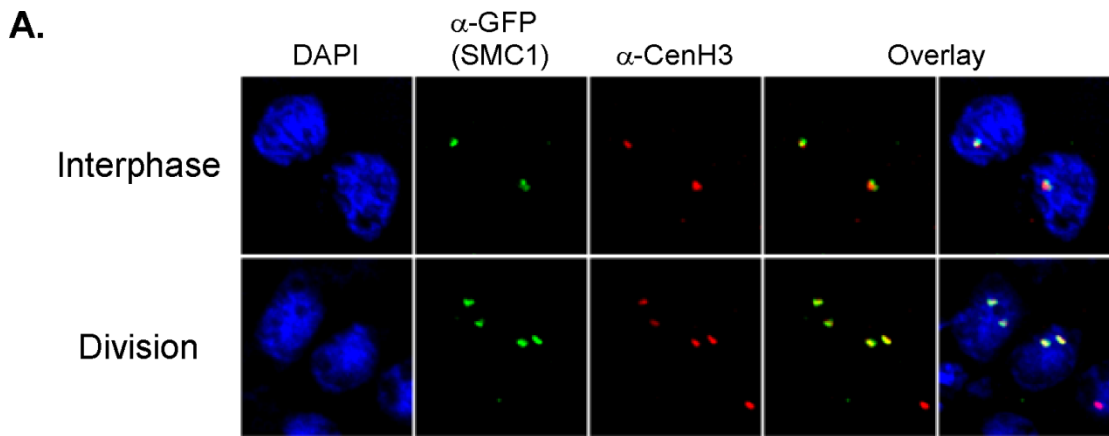
**Figure 2.5**. **TgSMC1 Co-localizes with TgCenH3 to the centromeres of *T. gondii*.**

**A**.Immunofluorescence assay. TgSMC1-YFP (green) was co-stained with anti-TgCenH3 antibodies

(green). The signals for TgSMC1 and the marker for the *T. gondii* centromeres show tight co-

localization throughout the cell cycle. **B.** Hybridization peaks on a microarray CHIP covering the

genome of *T. gondii*, of immunoprecipitated chromatin from the TgSMC1-HA cell line (red line).

Chromosomes III and VI are shown as representative examples. Our previous ChIP-CHIP results

using the TgCenH3-HA cell line (green line) are shown, overlaid, as reference. **C.** Schematic

representation of *T. gondii's* 14 chromosomes. Red asterisks indicate the position of the

centromeres, mapped previously, for each chromosome. Black arrowheads correspond to the

hybridization peaks obtained from  the TgSMC1-HA cell line ChIP-CHIP experiments for each

chromosome.
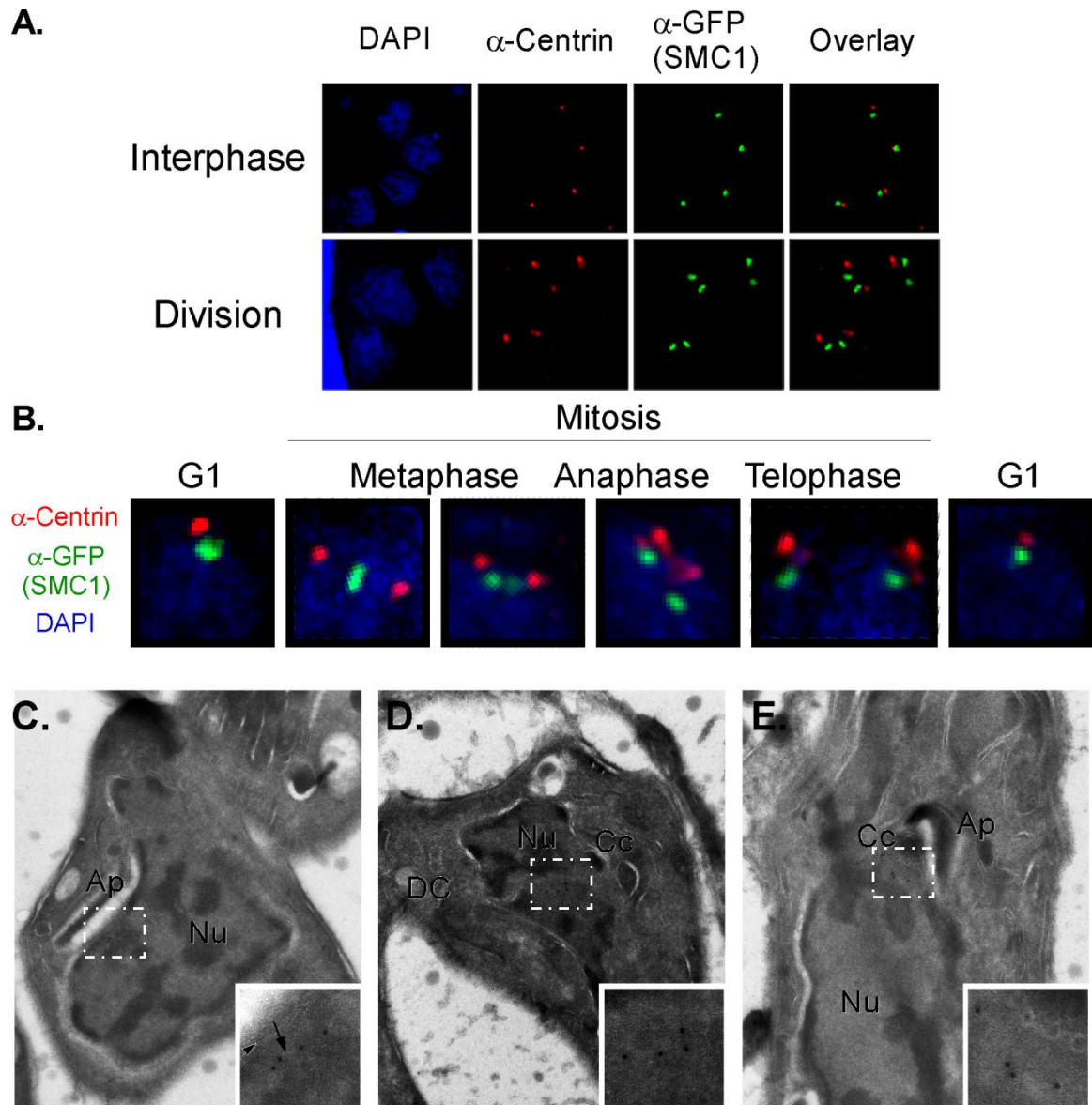
**Figure 2.6. TgSMC1 persists throughout the cell cycle in proximity to the centrosome**. **A**. Immunofluorescence assay. SMC1-GFP (green) localizes in the periphery of the nucleus (blue) and proximal to the centrosome (red) both during interphase and division  **B**. SMC1-GFP can be detected proximal to the centrosome throughout the cell cycle. **C-E.** Cryo-immuno gold detection of SMC1-HA visualized by transmission electron microscopy.  **C.** Interphase. Gold particles can be detected adjacent to the nuclear envelope (inset, arrowhead).  Gold particles appear to line up at the bottom of a  cleft of the nuclear envelope (inset, arrow).  **D**. Metaphase.

Gold particles c an be detected in between two centrocone (Cc) strucutres.  Two daughter cells

(DC) are assembled simultaneously. **E.** During division gold particles can be detected in the

proximity of the centrocone (Cc). Ap= Apicoplast. Nu=Nucleus.
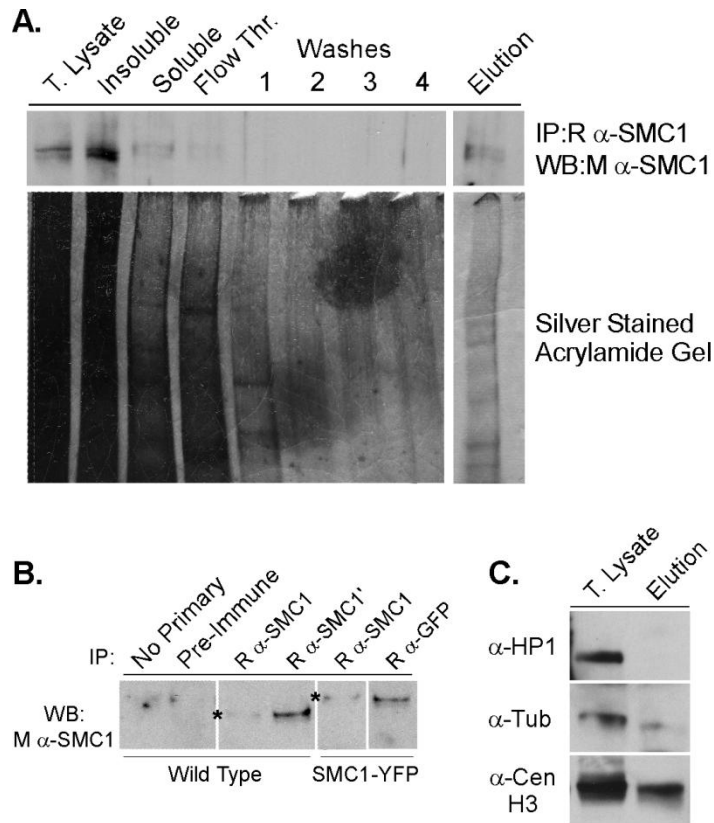


**Figure 2.7. TgSMC1 Co-Immunoprecipitation**. **A.** Western Blot. Elutions fractions of

immunoprecipitations using the antibodies indicated on the right, probed with anti-SMC1**. B.**

Representative western blot (upper panel) and silver stained acrylamide gel (lower panel) of an

immuno-precipitation experiment from parasite lysate using an anti-TgSMC1 antibody.  **C.**

Western blot. Parasite lysate or the elution fraction of an immuno-precipitation using anti-SMC1

were probed with the indicated antibodies. anti-HP1 recognizes TgChromo1, a chromodomain

protein which binds peri-centromeric DNA, and was used as a control for the specificity of our

pull downs.  The results of the Mass spectrometry analysis of elution fractions of multiple

immuno-precipitations can be found in Table 2.1.
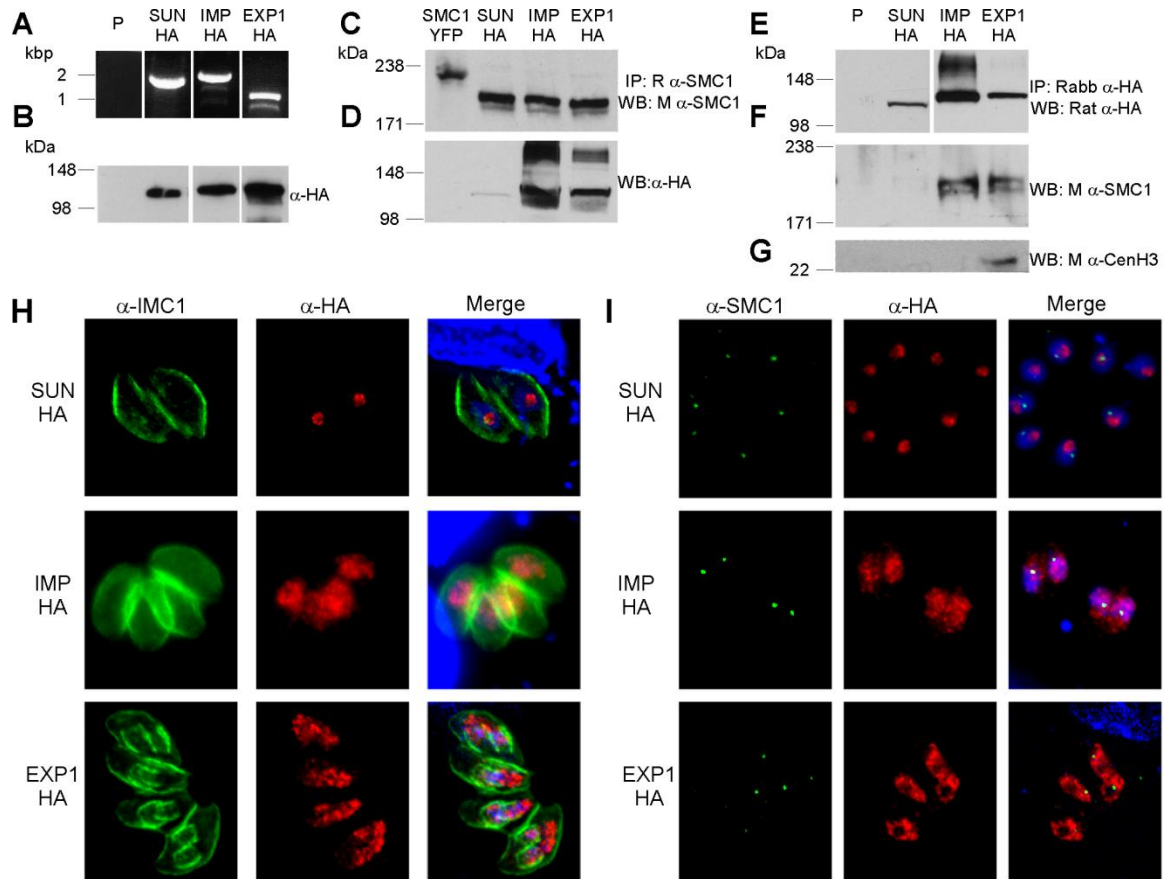


**Figure 2.8. TgExportin1 and TgImportin1 co-precipitate with TgSMC1 and localize to the**

**nucleus.**  TgExportin1 and TgImportin1 (TgME49_249530 and TgME49_253730 respectively),

which co-immunoprecipitated with TgSMC1, were endogenously tagged with a C-terminal 3xHA.

"SUN" (TgME49_288530) is annotated as a hypothetical protein containing a Sun domain. This

protein was represented by 2 peptides in the Mass spectrometry analysis of SMC1-YFP anti-GFP

Co-IP, but was not found in other samples, and was used as a negative control. **A**. PCR

verification of the endogenous tag insertion **B.** Western blot shows bands consistent with the

predicted molecular mass of each protein are recognized by anti-HA antibodies in each of the

tagged cell lines. **C-G** Western blots of reciprocal Co-immunoprecipitation. **C.** Western Blot.

TgSMC1 was pulled down using anti-SMC1 antibodies in the 3xHA TgImportin1, TgExportin1 and

TgSUN2 tagged cells lines, and probed with anti-HA (**D**). **E.** TgImportin1, TgExportin1 and

TgSUN2 were pulled down using anti-HA antibodies and probed with anti-TgSMC1. These results

recapitulate our MS results, and suggest that the interaction between TgSMC1 and either

TgExportin1 or TgImportin1 are real. **G**. In addition to co-precipitating with TgSMC1, TgExportin1

also co-precipitates with TgCENH3. **H-I**. Immunofluorescence assays using anti-HA in

combination with anti-IMC1 to labels the parasite's outline (**H**) or anti-TgSMC1 (**I**) to label the

centromeres.
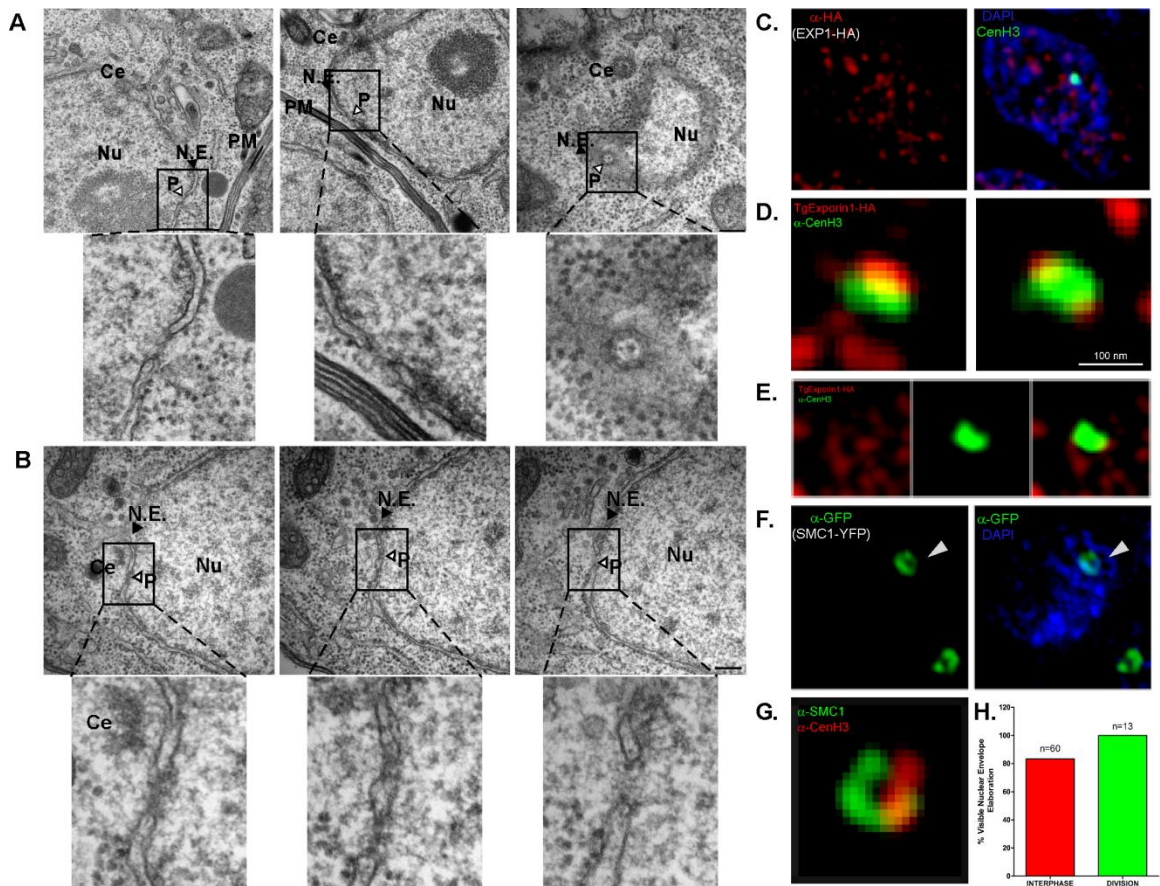


**Figure 2.9. A nuclear pore is found in the proximity of the centrosome. A.** Sections through

nuclei reveal the presence of nuclear pores (P, white arrowhead) visible as interruptions in the

nuclear envelope (NE, black arrowhead). The localization of the nuclear pores shown is not

54

associated with that of the centrosome (Ce), indicated as a reference. **B.** Serial section through

an interphase nucleus. An interruption of the nuclear envelope (NE, black arrowhead) is seen

adjacent to the position of the centrosome (Ce, white arrow). P, white arrowhead, indicates the

position of a centrosome-associated nuclear pore complex.  **C.** Super resolution imaging of

TgExp1-HA reveals that the protein localizes to the discrete foci in the nucleus **D** and **E.** TgExp1-

HA foci co-localize with, flank or surround the localization of TgCenH3. **F.** Super Resolution

microscopy reveals that TgSMC1 pattern of localization in the periphery of the nucleus appears

to be in the shape of a hollow oval (arrowhead) **G**. Super-resolution image. TgSMC1 surrounds

TgCenH3. **H.** The appearance of a "nuclear envelope elaboration" consisting of a discontinuous

fragment of the nuclear envelope proximal to the centrosome was quantified in serial sections

of both dividing (green) and non-dividing (red) parasites. Note that the mitotic spindle

penetrates and interrupts the nuclear envelope during division; hence an "opening" of the

nuclear envelope proximal to the centrosome is observable in the vast majority of the dividing

nuclei.
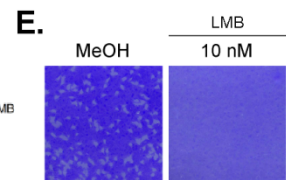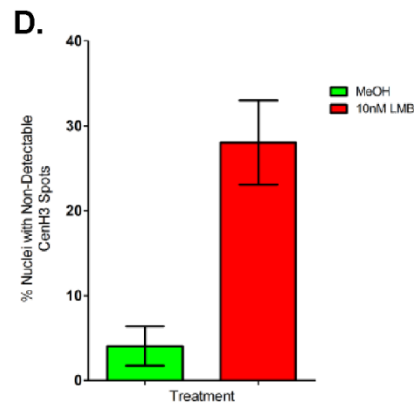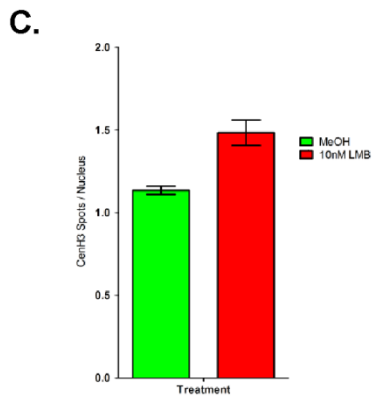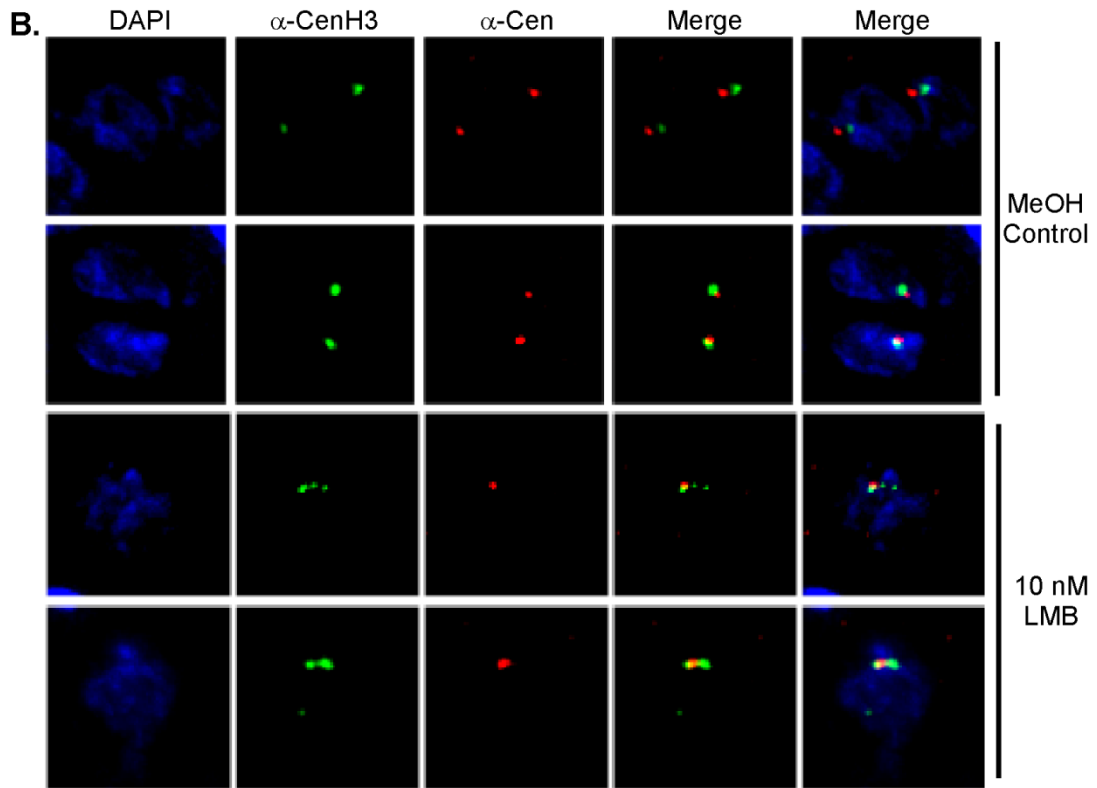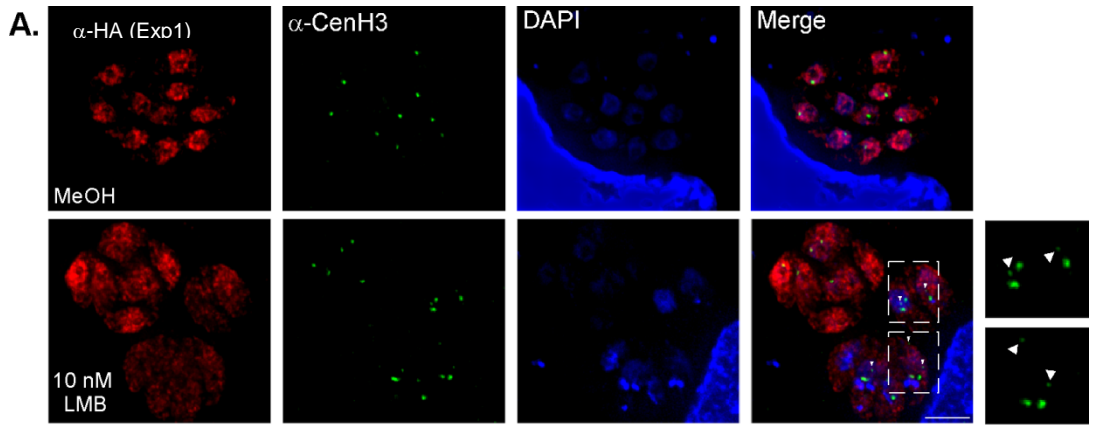
**Figure 2.10 Leptomycin B (LMB) treatment causes mis-localization of TgExportin-1 to the cytosol and centromere un-clustering** .**A**. Immunofluorescence assay of either untreated or 10 nM LMB treated TgExportin1-HA parasites (24h), labeled with anti-HA and anti-TgCenH3. Drug-treated parasites exhibit TgExportin1 cytosolic localization. LMB treated parasites in which TgExportin1-HA appears to be cytosolic, multiple CenH3 foci are visible (arrowheads, Zoomed panel) while those maintaining nuclear localization of TgExportin1 exhibit a single TgCenH3 focus.  **B.** Immunofluorescence assay of either untreated or 10 nM LMB treated TgExportin1-HA parasites (24h), labeled with anti-centrin (centrosome marker) and anti-TgCenH3. In LMB treated parasites, multiple CenH3 foci are visible in the presence of a single centrosome. Note that in many parasites TgCenH3 is not detectable (not shown) **C.** Quantification of number of CenH3 foci per nuclei whenever CenH3 was detectable **D.** Quantification of the percentage of nuclei with undetectable TgCenH3 staining, following 36-48h of 10nM LMB treatment. **E.** Plaque assays. Parasites treated with 10 nM Leptomycin B for 12 days are unable to lyse a monolayer of fibroblast, while control parasites are able to generate plaques (clearings). This suggests that Leptomycin B treatment is lethal to *T. gondii*.
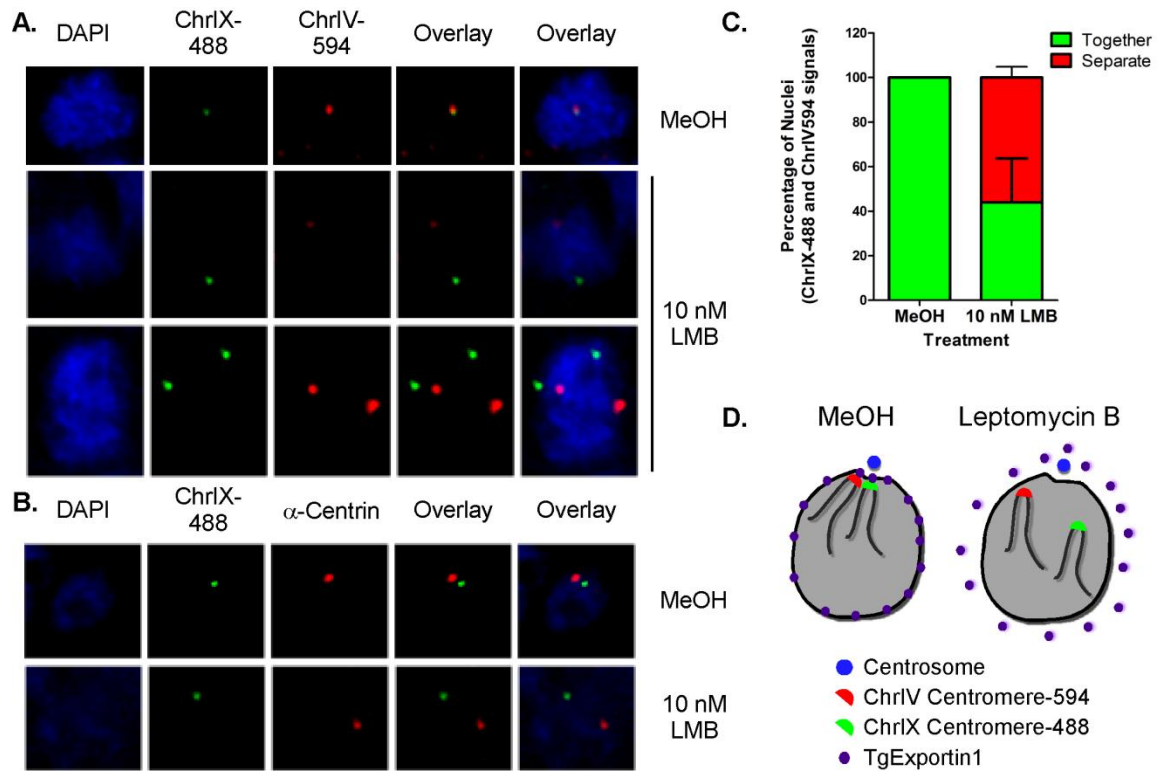
**Figure 2.11. Fluorescence *in situ* hybridization (FISH) of centromeres following treatment with Leptomycin B. A.** Parasites treated with methanol (control) or 10 nM Leptomycin B were hybridized with fluorescently-labeled probes complementary to the centromeres of chromosome IX (Alexa 488 labeled) and chromosome IV (Alexa 594 labeled). **B.** Control or Leptomycin B treated parasites were hybridized to an Alexa-488 labeled probe complementary to the centromere of Chromosome IX and processed for immuno-fluorescence with anti-Centrin1 to visualize the centrosome. **C.** Samples treated as in A were scored for the presence of co-localizing (together) signals corresponding to ChrIX and ChrIV centromeres or signals detected in separate regions of the nucleus. **D.** Schematic representation of the effect of Leptomycin B treatment on TgExportin1 localization and centromere clustering.
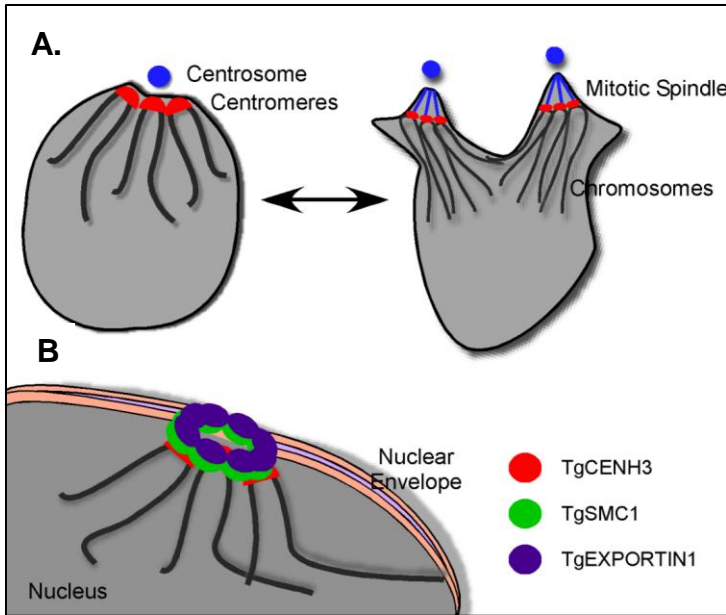
**Figure 2.12. A model: Handing over the centromeres; from the spindle to the pore, and back**.

We propose a model in which centromeres are "hung up" on the nuclear envelope by

interacting with components of the nuclear envelope during interphase. Centromeres are

handed over to the mitotic spindle during mitosis. Upon mitosis exit, centromeres are re-

positioned onto the nuclear envelope until the onset of the next round of division by interacting

with components of the nuclear pore such as TgExportin1.
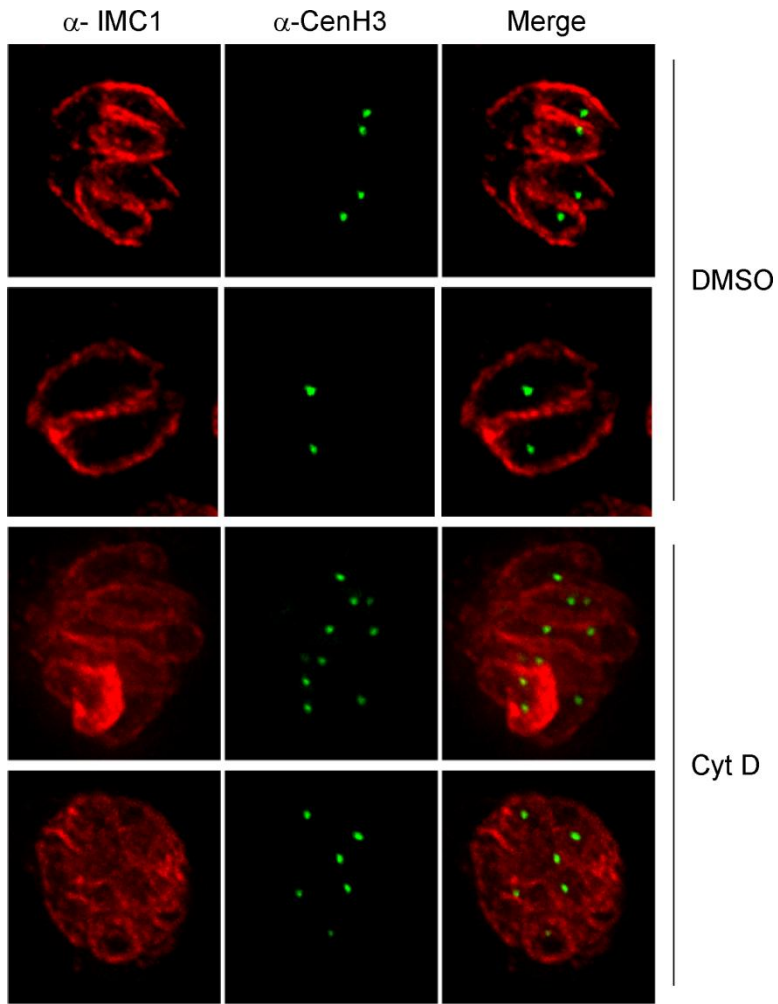
**Figure S2.1. Treatment with the actin-depolymerizing agent Cytochalasin D has no effect on centromere clustering**. Immunofluorescence assay of DMSO (control) or Cytochalasin D treated parasites with anti-IMC1 to label the parasites' outline and anti-TgCenH3 to label the centromeres. Centromeres remain clustered as one or two foci per parasite upon treatment with Cytochalasin D.
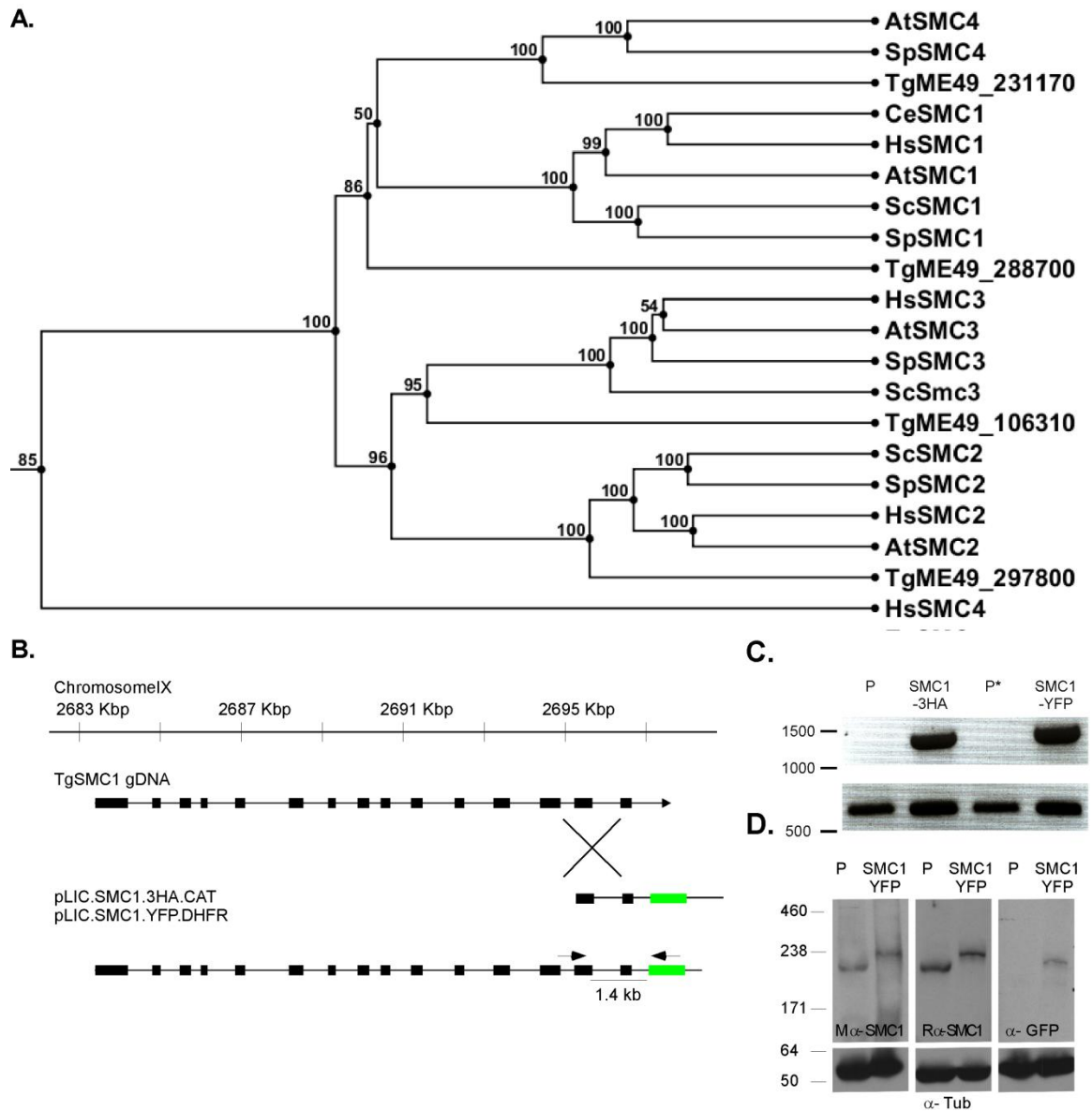
**Figure S2.2. Four Structural Maintenance of Chromosome (SMC) homologs are encoded in the**

***T. gondii* genome**. **A.** The genome of *T. gondii* encodes for four homologs of the Structural

Maintenance of Chromosome (SMC) family of proteins, each clustering with a distinct functional

clade. TgME49_297800 is an SMC1 homolog (TgSMC1), and clusters with other members of the

cohesin family. **B.** Two epitope tagged cell lines were generated by replacing the TgSMC1 3' end

with either a triple hemagglutinin (HA) or a yellow fluorescent protein (YFP). Arrows represent

the approximate position of screening primers used in C.  **C.** PCR confirmation of tag insertion.

The expected PCR product is detected in tagged cell line but not detected in parental cell lines. A
control set of primers amplifies a PCR product from a different genomic location in all cell lines.
**D.** Western blot shows that antibodies raised against the last 400 C-terminal amino-acids of
TgSMC1 recognize the expected molecular weight protein in wild type parasites, as well as in a
strain in which TgSMC1 was endogenously tagged with a C-terminal YFP (TgSMC1-YFP). Anti-GFP
recognizes TgSMC1-YFP.  Anti-tubulin was used as a control.
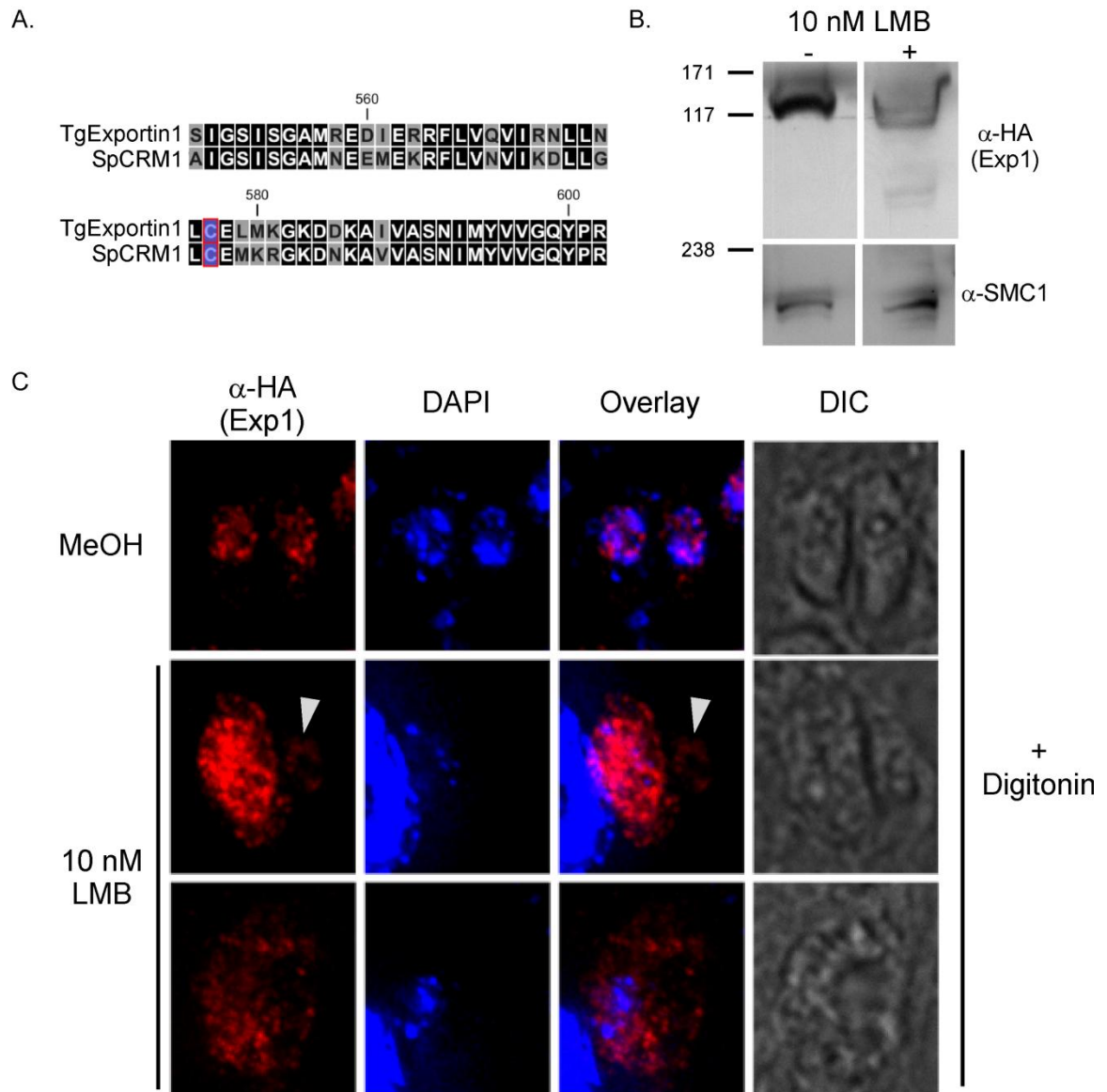
**Figure S2.3. Leptomycin B causes TgExportin1 to localize to the cytosol**. **A.** Partial protein

sequence alignment of TgExportin1 and SpCRM1. SpCRM1's cysteine 529, the target of

Leptomycin B, is well conserved in TgExportin1 (cysteine 577) (blue box). **B**. Western blot of the

elution fraction of an immunoprecipitation of TgExportin1-HA after treatment with methanol

(control) or 10 nM Leptomycin B. Multiple bands corresponding to TgExportin1 can be detected

in treated parasites. These might correspond to degradation products or to forms of TgExportin1

with an altered oxidative state which affects gel motility. **C.** Immunofluorescence assay of

TgExportin1-HA cells treated with Methanol (control) or Leptomycin B, and permeabilized with

low concentrations of the plasma membrane permeabilizing detergent digitonin, prior to

fixation. TgExportin1-HA is detectable around the nucleus in control parasites but can be seen

blebbing off the plasma membrane (white arrowhead) or in the parasitophorous vacuole in

Leptomycin B treated parasites.
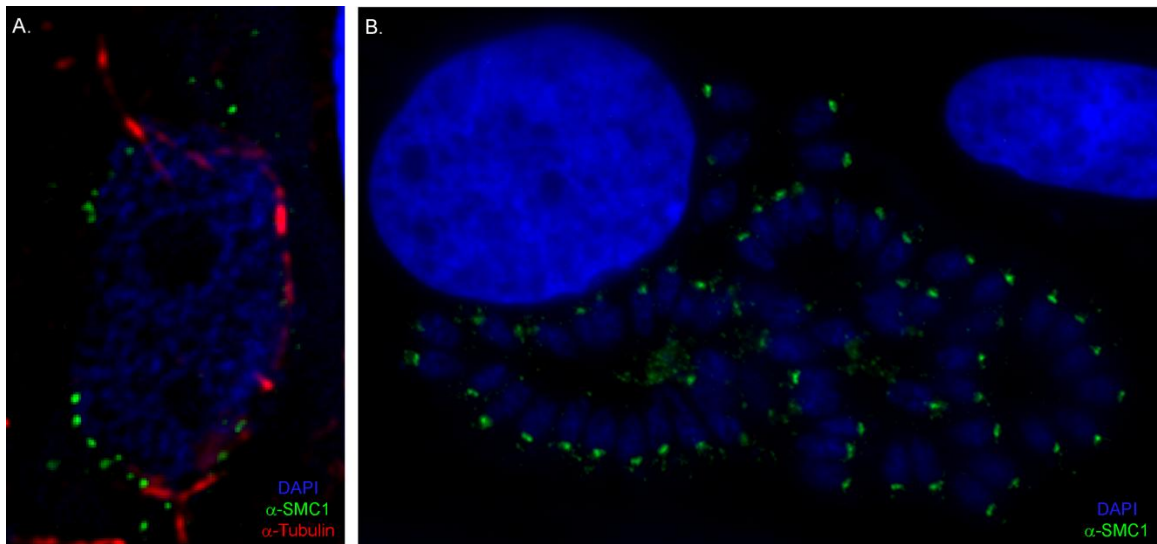


**Figure S2.4. Anti-TgSMC1 labels discrete foci in the nucleus of *Sarcocystis neurona*.** **A.** Anti-

TgSMC1 (green) labels punctuate in the periphery of the polyploid nucleus of a *S. neurona* cell

dividing by endopolygeny. **B.** The polyploid nucleus is parceled out into daughter cells

(merozoites) prior to cytokinesis. TgSMC1 labels a single focus at the periphery of individual

nuclei in *S. neurona*.

**TABLES**

**Table 2.1: Mass Spectrometry (LC-MS) Results of SMC1 Co-Immunoprecipitation**

| ToxoDB 8.1 Accession | Annotation | Av. Protein ID Prob. (%) | Mass (Da) | Av. Seq. Coverage (%) | Sample** (Unique Peptides) | | | |
|---|---|---|---|---|---|---|---|---|
| | | | | | α-SMC1 | α-SMC1* | α-GFP (SMC1-YFP) | (-) cont. |
| TGME49_200320 | hypoxanthine-xanthine-guanine phosphoribosyl transferase (HXGPRT) | 100 | 31485 | 27 | 6 | 6 | 8 | 0 |
| TGME49_203600 | hypothetical protein | 99 | 47215 | 6.35 | 0 | 2 | 2 | 0 |
| TGME49_205220 | U5 snRNP-associated subunit, putative | 75 | 122776 | 3.42 | 0 | 5 | 1 | 0 |
| TGME49_206670 | hypothetical protein | 61.5 | 218501 | 0.48 | 2 | 0 | 0 | 0 |
| TGME49_210360 | DEAD (Asp-Glu-Ala-Asp) box polypeptide 41 family protein | 99 | 73229 | 3 | 2 | 1 | 0 | 0 |
| TGME49_216050 | tetratricopeptide repeat-containing protein | 75 | 59519 | 0.765 | 0 | 2 | 1 | 0 |
| TGME49_219790 | pre-mRNA processing factor PRP3 | 98.5 | 76835 | 2.3 | 0 | 1 | 1 | 0 |

| | | | | | | | | |
|---|---|---|---|---|---|---|---|---|
| TGME49_222380 | importin-beta N-terminal domain-containing protein | 100 | 129490 | 18 | 8 | 19 | 17 | 0 |
| TGME49_224890 | hypothetical protein | 100 | 116710 | 9 | 5 | 14 | 3 | 0 |
| TGME49_226640 | zinc binding protein, putative | 94 | 14670 | 17.2 | 0 | 1 | 2 | 0 |
| TGME49_228760 | hypothetical protein | 87 | 49240 | 4.3 | 0 | 2 | 1 | 0 |
| TGME49_230960 | splicing factor 3b, subunit 3, 130kD, putative | 99 | 135745 | 2.96 | 2 | 7 | 1 | 0 |
| TGME49_235490 | hypothetical protein | 100 | 102120 | 12 | 4 | 8 | 6 | 0 |
| TGME49_240060 | hypothetical protein | 75 | 88534 | 1.35 | 0 | 1 | 1 | 0 |
| TGME49_244110 | nucleosome assembly protein (nap) protein | 100 | 48587 | 11 | 2 | 4 | 4 | 0 |
| TGME49_246340 | DnaJ domain-containing protein | 100 | 95361 | 2.55 | 2 | 1 | 0 | 0 |
| TGME49_246740 | hypothetical protein | 75 | 64742 | 2.15 | 0 | 2 | 1 | 0 |
| TGME49_247450 | hypothetical protein | 100 | 245873 | 2 | 3 | 2 | 2 | 0 |
| TGME49_249530 | exportin 1, putative | 100 | 129094 | 18 | 4 | 20 | 20 | 1 |
| TGME49_252510 | hypothetical protein | 100 | 80604 | 11 | 0 | 7 | 3 | 0 |
| TGME49_253730 | importin-beta N-terminal domain-containing protein | 100 | 115148 | 12 | 2 | 10 | 9 | 0 |
| TGME49_269990 | hypothetical protein | 100 | 216244 | 1.34 | 0 | 3 | 1 | 0 |

| | | | | | | | | |
|---|---|---|---|---|---|---|---|---|
| TGME49_280490 | U-box domain-containing protein | 100 | 121998 | 8 | 4 | 13 | 7 | 0 |
| TGME49_286080 | elongation factor 2 family protein | 100 | 113344 | 4.5 | 2 | 6 | 7 | 0 |
| TGME49_288530 | NOL1/NOP2/sun family protein | 100 | 87639 | 3.9 | 0 | 2 | 0 | 0 |
| TGME49_288700 | RecF/RecN/SMC N terminal domain-containing protein | 100 | 183132 | 16 | 16 | 14 | 22 | 0 |
| TGME49_289540 | hypothetical protein | 74 | 100518 | 4.7 | 1 | 1 | 7 | 0 |
| TGME49_293060 | SPRY domain-containing protein | 100 | 80292 | 1.6 | 0 | 0 | 1 | 0 |
| TGME49_293340 | ran binding family protein 1, putative | 100 | 24292 | 8.5 | 2 | 3 | 2 | 0 |
| TGME49_304680 | ubiquitin family protein | 87.5 | 56734 | 6.3 | 1 | 1 | 0 | 0 |
| TGME49_306600 | RNA recognition motif-containing protein | 99 | 21205 | 6.9 | 0 | 0 | 1 | 0 |
| TGME49_311690 | UBA/TS-N domain-containing protein | 100 | 45976 | 9.75 | 0 | 3 | 3 | 0 |
| TGME49_313670 | adaptin N-terminal region domain-containing protein | 89 | 107007 | 4.0 | 1 | 3 | 5 | 0 |
| TGME49_321650 | hypothetical protein | 100 | 153575 | 3.3 | 1 | 3 | 5 | 0 |

*Affinity Purified α-SMC1 antibody **Proteins shown on this table were either absent from the control sample and present in the positive samples, or showed 10-fold enrichment in number of unique peptides in at least one of the positive samples as compared to the negative control sample.

**Table 2.1: Name and sequences of all primers used in this study**

| Primer Name | Purpose | Sequence (5'→3') |
|---|---|---|
| SMC1_LIC_F (2035) | SMC1 3' replacement/ endogenous tagging | TACTTCCAATCCAATTTAATGCACCTAGGGACGAAGTCGACGCACC GCTCGACG |
| SMC1_LIC_R (2036) | SMC1 3' replacement/ endogenous tagging | TCCTCCACTTCCAATTTTAGCCTCCGCATTCTCGGAGGCCAGTAAG |
| LIC_YFP_R (2464) | Screening 3' replacement with YFP | CGGTGAACAGCTCCTCCGCCCTTGCTCAC |
| LIC_3HA_R (1595) | Screening 3' replacement with 3HA | GGATAGCCAGCGTAGTCCGGG |
| SMC1_Lic_screening _F (3529) | Screening - SMC1 3' replacement | TACTTCCAATCCAATTTAATGCAGCTAGCAGCGTTTGCTGCCTCTGC AATCTGTTGAG |
| SMC2_cDNA_F (2176) | SMC2 cDNA cloning for overexpression | GGATCCATGTACATCGAGGCAATTGTTCTCG |
| SMC2_cDNA_R (2177) | SMC2 cDNA cloning for overexpression | CCTAGGGTTCGGGTTCACCGCTGTCT |
| pAVA_SMC1_C_F (2549) | SMC1 cDNA cloning into pAVA for C-terminal peptide synthesis | GGGTCCTGGTCCGATGTGGGTCTACAGAGAAGAGAAAC |
| pAVA_SMC1_C_R (2548) | SMC1 cDNA cloning into pAVA for C-terminal peptide synthesis | CTTGTTCGTGCTGGGAGGCCAGTAAG |
| Exportin1_LIC_F (2938) | TgExportin1 3' replacement/ endogenous tagging | TACTTCCAATCCAATTTAATGCAAAGCTTTCAGACCGTCAACCAGAA A |
| Exportin1_LIC_R (2871) | TgExportin1 3' replacement/ endogenous tagging | TCCTCCACTTCCAATTTTAGCGTCATCGTCTCCTCCACGAACTGTC |
| Exportin1_LIC_Scree nF (3200) | Screening – TgExportin1 3' replacement | CCAAGGCAGAGCGCGCCTCGGATTT |

| Importin_LIC_F(3284) | TgImportin1 3' replacement/ endogenous tagging | TACTTCCAATCCAATTTAATGCACGTTGCTGCCACTCGTTAAATCAAC |
|---|---|---|
| Importin_LIC_R (3285) | TgImportin1 3' replacement/ endogenous tagging | TCCTCCACTTCCAATTTTAGCGAGACAAACAAAGGGAAGGAGAGGCGT |
| Importin_LIC_Scrn_F (3391) | Screening – TgImportin1 3' replacement | CGTCTGCACGGAATACTTACGTCTG |
| SUN2_LIC_F (3348) | SUN2 3' replacement/ endogenous tagging | TACTTCCAATCCAATTTAATGCACCACTGTACTGTTGATGCGTCTGTG |
| SUN2_LIC_R (3349) | SUN2 3' replacement/ endogenous tagging | TCCTCCACTTCCAATTTTAGCCGCACGCTTCTTAGAAATACTTGC |
| SUN2_LIC_ScreenF (3393) | Screening – SUN2 3' replacement | GTACGGACAGGCAGAGAGATTCCGT |

- Primer sequences used for amplification of FISH probes can be found in Gissot et. al. 2011[73]

CHAPTER 3


CELL DIVISION IN APICOMPLEXAN PARASITES IS ORGANIZED BY A HOMOLOG


OF THE STRIATED ROOTLET FIBER OF ALGAL FLAGELLA[2]

**ABSTRACT**

Apicomplexa are intracellular parasites that cause important human diseases including malaria and toxoplasmosis. During host cell infection new parasites are formed through a budding process that parcels out nuclei and organelles into multiple daughters. Budding is remarkably flexible in output and can produce two to thousands of progeny cells. How genomes and daughters are counted and coordinated is unknown. Apicomplexa evolved from single celled flagellated algae, but with the exception of the gametes lack flagella. Here we demonstrate that a structure that in the algal ancestor served as the rootlet of the flagellar basal bodies is required for parasite cell division. Parasite striated fiber assemblins (SFA) polymerize into a dynamic fiber that emerges from the centrosomes immediately after their duplication. The fiber grows in a polarized fashion and daughter cells form at its distal tip. As the daughter cell is further elaborated it remains physically tethered at it its apical end, the conoid and polar ring. Genetic experiments in *Toxoplasma gondii* demonstrate two essential components of the fiber, TgSFA2 and 3. In the absence of either of these proteins cytokinesis is blocked at its earliest point, the initiation of the daughter microtubule organizing center (MTOC). Mitosis remains unimpeded and mutant cells accumulate numerous nuclei but fail to form daughter cells. The SFA fiber provides a robust spatial and temporal organizer of parasite cell division, a process that appears hard-wired to the centrosome by multiple tethers. Our findings have broader evolutionary implications. We propose that Apicomplexa abandoned flagella for most stages yet retained the organizing principle of the flagellar MTOC. Instead of ensuring appropriate numbers of flagella, the system now positions the apical invasion complexes. This suggests that elements of the invasion apparatus may be derived from flagella or flagellum associated structures.

## INTRODUCTION

Apicomplexa are protozoan parasites responsible for numerous human and veterinary diseases. Human pathogens in this phylum include *Plasmodium*, the causative agent of malaria, *Toxoplasma*, an opportunistic pathogen which causes encephalitis in immunocompromised individuals and congenital toxoplasmosis, and *Cryptosporidium* one of the most important causes of severe early childhood diarrhea around the world. Apicomplexa are obligate intracellular parasites that follow a stereotypical propagation cycle. A motile zoite stage seeks out and invades a suitable host cell and in this process establishes a novel compartment, the parasitophorous vacuole, that houses the parasite during its intracellular development [111]. Parasites replicate and ultimately produce a new generation of zoites that destroys the host cell upon egress and fan out to infect new cells. Apicomplexans have adapted to tissue and host cell niches as varied as red blood cells, intestinal epithelial cells, macrophages and lymphocytes, or neurons.

The budding mechanism used by apicomplexans appears to be the key to their ability to scale their reproductive output to the size and biology of the specific host cell [25]. In this process, many species including the malaria parasite, deviate from the conventional cell cycle and pass through DNA synthesis and nuclear mitosis numerous times amassing a large number of genomes. Coinciding with the last round of mitosis, daughter buds are assembled and each nucleus is packaged into a new zoite. It is not understood how the parasites match the number of nuclear genomes with emergent daughter buds and how buds are placed and assembled correctly. The bud is scaffolded by microtubules that emanate from a newly formed apical microtubule organizing center (MTOC) [47] (shown in blue in Figure 3.1A for *T. gondii*). These microtubules anchor the inner membrane complex (IMC, purple), an assemblage of

membranous and cytoskeletal elements that establishes cell shape and is critical to the parasite's gliding motility [112]. The MTOC is thought to be a ring structure and can be further elaborated by additional elements including the conoid [31, 32, 47]. The MTOC also organizes the specialized apical secretory machinery that delivers proteins for host cell invasion and modification. Secretion of these organelles occurs at the extreme apex and through the ring [113, 114].

The centrosome has been demonstrated to organize parasite chromosomes and some organelles. Interestingly, both in *T. gondii* and *P. falciparum* chromosomal centromeres are constantly tethered to the centrosome [60, 64]. A similar physical association with the centrosome has been described for the apicoplast and the Golgi [56, 115, 116]. We hypothesized that a second tether linking the centrosome to the daughter bud MTOC and the associated invasion machine could provide a robust mechanism for cell assembly. In this study we use *T. gondii,* which divides using the simplest internal budding process in the phylum known as endodyogeny [55] as a model. We find that in *T. gondii* SFA proteins, whose orthologs are found in the rootlet associated with flagellar basal bodies of single celled algae, assemble into a highly dynamic fiber during cell division. The SFA fiber links the centrosome and daughter MTOC, and ablation of SFA by conditional knock out results in multinucleated cells which fail to initiate the formation of daughter cells.

## RESULTS

During cell division *Toxoplasma gondii* assembles two daughter cells with a complex microtubular cytoskeleton and secretory apparatus within the mother cell (Figure 3.1A). This process has to be coordinated with mitosis and organelle segregation to ensure that the emerging daughter cells not only are competent to invade a new host cells, but also carry the

genetic and metabolic machinery required to propagate. It is not well understood how each daughter cell inherits a complete set of essential organelles. Striated fiber assemblin (SFA) is the main component of striated rootlets associated with basal bodies in green algae [117-119]. In previous work, Lechtreck and colleagues identified genes encoding homologs of SFA in Apicomplexa, including *T. gondii* [62]. This was surprising because with the exception of the male gamete Apicomplexa lack flagella. Nonetheless, antibodies raised against SFA from the green alga *Spermatozopsis similis* revealed a spot in proximity of the centrosome in *T. gondii* [62]. Transcription of the *T. gondii* SFA genes is cell cycle-dependent with peak expression coinciding with DNA synthesis and mitosis (Figure 3.1B) [120, 121]. We therefore hypothesized that SFAs may function during division of apicomplexan parasites.

To define the function of SFA proteins in *T. gondii*, we first determined their localization. We focused on TgSFA2 and TgSFA3, two proteins that are expressed in the tachyzoite stage maintained in tissue culture. We engineered parasites in which the native TgSFA2 is tagged with a triple hemagglutinin (3xHA) at its C terminus. Southern blot analysis with a probe complementary to the 3'end of TgSFA2 confirmed the insertion of the tag into the locus (Figure S1A). Western blot showed a single band of the mass predicted for TgSFA2-3HA (30 kDa) to be recognized by anti-HA antibodies (Figure 3.1D). To study TgSFA3, we expressed the gene in *E. coli*, and raised antibodies against the recombinant protein. Independently, we also generated a strain in which TgSFA3 is endogenously tagged with yellow fluorescent protein (YFP) at its C-terminus. A Western blot with anti-GFP antibodies showed a fusion protein of expected mass in the TgSFA3-YFP cell line, but not in the parental cell line (Figure 3.1D). This band is also recognized by the anti-SFA3 antibody, which in wild type parasites recognizes native TgSFA3 (35 kDa) and the recombinant protein in bacterial lysates (rSFA3, Figure 3.1D). We next performed immunofluorescence assays (IFA) on TgSFA2-HA parasites using HA and anti-SFA3 antibodies to

detect both proteins simultaneously.  TgSFA2 and TgSFA3 largely co-localize and both reveal two short fiber-like structures per parasite cell (Figure 3.1E).

While observing endogenously tagged TgSFA2 or the labeling by the TgSFA3 antibody by immunofluorescence we noticed that only a fraction of the parasites showed staining. At a given time twenty four % of the parasites express TgSFA2, while 76 % do not (Figure 3.1C). These percentages closely match those previously reported for interphase and dividing parasites in asynchronous populations of *T. gondii* [58]. Next, we co-stained cells for TgSFA2-HA and with antibodies that detect markers of *T. gondii* cell cycle progression including centrin and IMC1. Centrin is a marker of the centrosome (Figure 3.2A-C, red), IMC1 (blue) is part of the cytoskeleton of the inner membrane complex of the pellicle and outlines the mother cell as well as the forming daughters [38, 122].  Most parasites appear to be in G1 or early S phase, as determined by the presence of a single centrosome per parasite. Consistent with our prediction, no SFA labeling is discernible in these interphase cells.  After centrosome duplication, SFA labeling becomes apparent as small punctuate structures which are very close to or overlap with centrosome labeling. In parasites that show anti-IMC1 stained daughter buds, TgSFA2 labels a long structure, extending away from the centrosome (Figure 3.2C). Notably, the SFA fiber is arched with a spiraling hook shape at its distal end. This pattern is also apparent in immuno-gold labeled cryosections of SFA2-HA parasites. Figure 3.2D shows the intra-nuclear mitotic spindle of *T. gondii*, an early step in the budding process [25, 55]. A short series of gold particles is visible at the bottom spindle pole. In parasites progressed further in division gold particles form an arched line that climbs into the apical end of the daughter bud (Figure 3.2E). We conclude that SFA2 and 3 form a structure early in mitosis, that extends into a fiber during budding, but is absent in interphase.

To test whether SFA proteins have a functional role in parasite division we generated mutants in which their expression can be manipulated (Figure 3.3A). We constructed a strain, iΔSFA3, in which the native promoter of SFA3 is replaced by a tetracycline-regulatable promoter [123, 124]. The targeting construct was derived from a cosmid clone carrying the SFA3 locus by recombineering [94, 123]. A corresponding strain for SFA2 (iΔSFA2) was also made. In this case we used a plasmid that was designed to introduce both a regulatable promoter and a transactivator into the locus (both strategies and the specific parental strains used are described in detail in the Materials & Methods section and supplementary Figure S3.2). Disruptions of the targeted loci were confirmed by PCR (Figure S3.2B and S3.2D). Mutant parasites were cultured in the presence of anhydrotetracycline (ATc) and targeted protein levels were measured by Western blots using anti-SFA3 antibodies or by RT-PCR for the SFA2 mRNA. We noted a marked decrease in the levels of the targeted SFA proteins or mRNAs after two days of ATc treatment (Figure 3.3B). In both mutant strains parasite growth was severely impaired in the presence of ATc, as documented by their inability to form plaques in a fibroblast monolayer (Figure 3.3C, note that plaque formation of the parental strains is not affected by ATc). We conclude that SFA2 and SFA3 are non-redundant and both are required for parasite viability.

We hypothesized that the growth arrest of mutants deficient in SFAs is caused by defects in cell division. We cultured the mutant parasites for 24 and 48 h in ATc and stained using anti-IMC1 antibody to outline cells and DAPI to visualize nuclei. As shown in Figures 3.4A and B, for both mutants ATc treatment resulted in excessively large cells bearing multiple nuclei. We quantified this phenotype in the iΔSFA3 strain (Figure 3.4D), 59% of parasite cells are multinucleated (≥2 nuclei per cell) after 24 h of ATc treatment. Parasites with numerous apparently normal nuclei are also readily observed by electron microscopy (Figure 3.4C). To evaluate nuclear division and chromosome segregation more rigorously we stained mutants

with a monoclonal antibody that we developed against the *T. gondii* centromeric histone variant CenH3. In Apicomplexans, centromeres are sequestered at the nuclear envelope in a centrosome-dependent manner and haploid and diploid nuclei have a single or duplicated CenH3 spot respectively [60, 64]. We quantified the nuclear ploidy and note that ATc treated mutants and controls are indistinguishable (Figure 3.5B). Moreover, we observed that every nucleus is associated with one or two centrosomes and that the centromere-centrosome association appears undisturbed (Figure 3.5A).

We next monitored daughter cell formation. Normally, IMC1 outlines the pellicle of both the mother and daughter cell (see Figure 3.2A and B). Strikingly, mutant parasites containing multiple nuclei showed aberrant or no daughter cells when stained with anti-IMC1 (Figure 3.4A). To test whether SFAs are required for the initiation or elaboration of daughters we stained mutants for the early marker of budding ISP1 (IMC sub-compartment protein 1). ISP1 labels the apical cap of the inner membrane complex and can be detected prior to IMC1 [43]. In ATc treated parasites ISP1 is visible in the mother cell pellicle but no daughter structures are discernible (Figure 3.5C). Taken together, these results suggest that loss of SFA proteins does not affect centrosome duplication and mitosis but severely impedes budding.

To better understand the mechanistic basis of the mutants' inability to bud, we monitored the localization of SFAs in relation to structures important for daughter cell assembly throughout division. Daughter cells are formed on a stereotypic scaffold of 22 sub-pellicular microtubules that arise from a circular apical organizing center, the apical polar ring [42]. In *Toxoplasma* this structure also includes the conoid a motile structure thought to be involved in host cell invasion [31, 32]. We examined the localization of the SFA fiber relative to that of alpha-tubulin, RNG1 (Ring1), a component of the apical polar ring [29], and ISP1 [43]. We

observed that the apical end of the SFA fiber consistently extends beyond the end of tubulin staining corresponding to the sub-pellicular microtubules (Figure 3.6A) and terminates at the apex of developing daughters, extending through the RNG1 staining and to the very tip of the ISP1 staining (Figure 3.6B and C). To unravel this complex architecture we imaged serial sections of dividing parasites by transmission electron microscopy (TEM). Figure 3.7A shows two consecutive sections through a daughter bud in which the conoid (Cn) and centrosome (Ce) are clearly identifiable. Spanning the area between them is an arching electron dense fiber (black arrowheads). The fiber terminates at a pair of microtubules that extend through the center of the conoid (arrow, [47]). Figure 3.7C-E shows a series of perpendicular sections through the conoid of a daughter cell. An electron dense fiber (arrowheads) curls up through the conoid coming into close contact with the apical rim of the structure and ending in the proximity of the central microtubule pair (arrow). A series of sections through a very early daughter bud shows the fiber to be already present at this stage (Figure 3.7F-I). Note that it again makes contact with the apical rim of the conoid (Figure 3.7G, arrowhead) and that it emerges from in between the two centrioles of the centrosome (Figure 3.7F and G, arrow). Our light and electron microscopic observations suggest that the SFA fiber physically connects the centrosome to the tip of the forming daughter cell.

To visualize the dynamic development of the SFA fiber we inserted a yellow fluorescent protein coding sequence into the genomic locus of SFA3 creating a C-terminal fusion protein. We time lapse imaged the SFA3-YFP strain and determined that SFA3 is visible for two hours and twenty minutes (n>5), a time frame consistent with the duration of mitosis in *T. gondii* under imaging conditions [58]. Moreover, we observed that the SFA structure is dynamic and its morphology changes with time. In order to have a spatial reference for the transition events of the SFA fiber we imaged SFA3-YFP in combination with Centrin1 fused to red fluorescent protein

(RFP). This allowed us to concurrently monitor the position of the SFA fiber and the centrosome [37, 70]. In time lapse imaging the YFP signal appears right on the centrosome (Figure 3.8A). The fiber then elongates away from the centrosome. When the fiber reaches about half of its final length a "hook" like shape at the tip away from the centrosome can be resolved (Figure 3.8A, 100'). The fiber reaches a maximum length of about 1 µm, at which point it appears to break close to its distal end (Figure 3.8A, 140-160'). This leaves a small dot (presumably associated with the tip of the daughter cell). The longer centrosome associated portion shortens from the distal end and finally, SFA3-YFP is no longer detectable leaving only the centrosome visible (Figure 3.8A, 200').

Polarized polymerization of subunits similar to microtubules or actin filaments could be a model for the growths of the SFA. To test this idea and to determine the direction of fiber extension we used fluorescence recovery after photo-bleaching. We chose SFA3-YFP parasites exhibiting two fibers of medium length (0.45 µm) and selectively bleached one of the two fibers using a diffraction limited 488nm laser spot (Figure 3.8C). Panel B in Figure 3.8 shows the target fiber prior to bleaching, note that the second fiber is not in the same focal plane as the target fiber and does not appear in this series of images. Panel C shows that after the laser pulse, the target fiber is no longer visible. We monitored the fluorescence of the bleached fiber after one hour, and found reappearance of the YFP signal (Figure 3.8D). While the unbleached fiber had practically doubled in size to 0.85 µm, the YFP signal on the bleached fiber was only 0.35 µm (Figure 3.8D and E). For reference we also imaged the apicoplast labeled with FNR-RFP (Ferredoxin/NADPH Reductase-RFP). During division the apicoplast shows close apposition to the centrosome (see Figure 3.8F) [116]. When compared to the control fiber SFA3-YFP labeling of the bleached fiber appeared to be polar and proximal to the apicoplast. Thus, it appears that the fiber grows out by polymerization and that the new subunits are added at the end proximal

to the centrosome which could be considered the "plus" end of the fiber. We note that we currently do not have a suitable probe to observe the bleached segment of the fiber, and thus cannot measure its entire length. We therefore cannot formally exclude proximal labeling due to laser induced stunting or breakage of the fiber.

Rootlet fibers are typically found in intimate contact with basal bodies or microtubules [117, 125]. Our observations are consistent with a polar SFA fiber that places and potentially governs the formation of the daughter cell and/or its MTOC. Alternatively, newly formed microtubules e.g. the central pair could be recruiting the fiber to the MTOC tethering the daughter in a secondary fashion. To distinguish between these two alternatives we tested whether daughter cell microtubules are required for SFA fiber formation or vice versa. We stained microtubules in the iΔSFA3 mutant using different tubulin antibodies. In Figure 3.9A we show antibody 6-11B directed against acetylated alpha tubulin as this antibody recognized daughter cell microtubules particularly well [126]. In mutants treated with ATc for 48h no daughter microtubules are detectable. Note that these particular cells (Figure 3.9F) are already multinucleated and undergoing another round of mitosis as indicated by the presence of two centrosomes per nucleus. Microtubules of the mother cell are readily detected. Conversely we treated SFA3-YFP or SFA2-HA parasites with 2.5 µM of the microtubule disrupting agent oryzalin [65]. As previously reported [63] oryzalin treated parasites fail to produce daughter cells, note the lack of daughter IMC1 staining in Figure 3.9B. However, in these parasites SFA fibers are still detected (Figure 3.9A and B, green). In fact fibers are noticeably more abundant; 60% of vacuoles exhibit SFA fibers after 24 h of oryzalin treatment while only 25% of the control parasites do (Figure 3.9C). We further noticed that in oryzalin treated parasites SFA fibers remain shorter and show a more uniform size distribution when compared with untreated parasites (Figure 3.9D). We conclude that daughter cell microtubules are not required for SFA

fiber formation but that microtubule elongation may be required for the fiber to extend to its full length, break and disappear. Alternatively, fiber elongation might require licensing by a checkpoint controlled by daughter cell growth.

## DISCUSSION

Flagella provide motility and sensory functions to a large variety of single and multicellular eukaryotes. They are anchored in the cell by the basal body [127]. Flagellar basal bodies are embedded within a complex cytoskeletal system known as the flagellar rootlet system or basal body cage which has been studied in most detail in the green alga *C. reinhardtii* [125]. There is evidence that these structures not only position the flagella but also define cellular axes of symmetry and asymmetry [128, 129]. The rootlet is composed of several types of biochemically and structurally distinct fibers some of which are made of microtubules. In *Chlamydomonas,* centrin based fibers (also known as contractile fibers) interconnect basal bodies and connect the basal bodies to the nucleus [130]. Sinister fibers, first described in *Spermatozopsis similis,* connect the basal bodies to two of the four microtubules of the flagellar rootlet and to cytoplasmic microtubules [131]. Striated fibers are made up from a single SFA protein and run along microtubules, emerging close to basal bodies in post mitotic cells, and are thought to guide and stabilize their associated microtubules [62, 119]. It has been proposed that the mechanism by which SFA binds microtubules is related to the structure of a rod domain found in the protein which consists of 29 amino acid repeats. The periodicity of this repeat confers the characteristic striation pattern found in SMAFs, and also fits the spacing between tubulin subunits in microtubules [62].  Striated fibers are also found in association with basal bodies in mammalian cells (e.g. various receptor cells), but the proteins isolated from these fibers do not appear to be homologous to SFA proteins [132].

In this study we show that striated fiber assemblins play a critical role in the cell division of the apicomplexan parasite *T. gondii*. We identified a fiber that is made up of at least two proteins, TgSFA2 and 3. This structure becomes apparent as soon as the centrosome is duplicated; it emerges from in between the two centrioles and grows away from the centrosome. Its distal end is intimately associated with the apical tip of the daughter cell (Figure 3.10 D summarizes our current ultrastructural understanding). Interestingly, the SFA fiber is not only a tether between centrosome and the daughter; it is required for daughter assembly. In conditional mutants lacking the SFA fiber we do not detect daughter buds even using the earliest markers available. The "birth" of the daughter is the establishment of the apical MTOC. We propose that the distal end of the SFA fiber initiates and thus positions the daughter MTOC. Could the fiber itself be an MTOC? Several studies have demonstrated the ability of algal rootlet complexes to initiate microtubule assembly in vivo and in vitro [133, 134]. It is tempting to note the peculiar shape of the end of the *Toxoplasma* fiber in the context of the circular MTOC found in these organisms and to speculate that the structure of the fiber may template the microtubule arrangement of the daughter pellicle. Further biochemical work is required to test this hypothesis in vitro. *Chlamydomonas* SFA has been demonstrated to have the intrinsic ability to self-assemble and self-organize; recombinant SFA forms striated fibers in vitro [135]. Why does a cell in a stage lacking flagella use a budding system that depends on elements of the flagellar rootlet? We believe this to be a consequence of the evolutionary history of Apicomplexa. The assembly of the flagellum and the mitotic spindle share deep evolutionary roots. The centrioles, which are at the core of many, but not all mitotic spindle poles, are homologous to the basal bodies [127]. In fact, in many cells the very same structure performs both functions. In *Chlamydomonas*, during interphase two closely apposed basal bodies organize the organisms' two flagella [125]. These flagella are resorbed upon entry into cell

division and the basal bodies become associated with the poles of the mitotic spindle. Following division both daughters assemble a transition zone onto the centrioles and reform flagella (Figure 3.10 B). The rootlet (shown schematically in white in Figure 3.10 A) appears to be important in both roles setting up division and symmetry planes and positioning the centrosome and the flagellum relative to each other as the cells move through their replicative cycle [128, 129]. Apicomplexa are believed to have an evolutionary past as photosynthetic aquatic algae. They are part of the Chromalveolata, a large branch of the eukaryotic tree of life that emerged from the endosymbiosis between a flagellated protist and a red alga [136]. The most conspicuous holdover of this past is a chloroplast-like organelle [10]. We hypothesize that the ancestors of Apicomplexa, as their present day kin likely depended on the rootlet to organize the relationship of their flagellar and mitotic MTOCs. As they adapted to intracellular parasitism they developed specialized cytoskeletal and secretory organelles that allow them to attack other cells [111]. Some precursors of these organelles are found in closely related flagellated protists that are fully or partially symbiotic, predatory or parasitic – in all these cases the organelles are found in close proximity to the flagellar basal body [137-139]. We propose that Apicomplexa subsequently abandoned the flagellum for most stages yet retained the organizing principle of the MTOC. Instead of ensuring that daughter cells have appropriate numbers of flagella the system now measures out and positions the apical invasion complexes (Figure 3.10 C). Overall this suggests that elements of the invasion apparatus may be derived from flagella or flagellum associated structures.

In combination with the recently described tethering of the nuclear genome and other organelles [60, 64, 116] a remarkably hard-wired model for the assembly of infective parasite stages emerges. The role of the SFA fiber is crucial in this context, a self-organizing polar fiber that will initiate a daughter in the proximity of each centrosome once its components are

82

expressed. The elegance of this mechanism is its scalability and independence of ploidy. It satisfyingly explains how *T. gondii* can form two daughters per round of budding, while *P. falciparum* forms ten to twenty in the red cell, and many thousands during liver cell infection. Direct evidence for the control of zoite formation by the flagellar rootlet is currently limited to the experiments with *T. gondii* presented in this study. However, we note that SFA homologs are encoded in the genomes of all apicomplexans for which sequence is available (and many other chromalveolates [61]). Furthermore electron dense structures comparable to those identified as SFA fibers in this study have been observed in previous ultrastructrual reports in *Eimeria* and *Plasmodium* [36, 140, 141]. Many mechanistic questions remain, some of them directed towards the relationship between the structure of the fiber and its function. There are also intriguing problems associated with the spatial and temporal control of initiation and breakdown of the structure, and how they are integrated into the parasites mechanisms of cell cycle control, which remain to be deciphered.

## MATERIALS AND METHODS

### Construction of tagged reporter parasites

*Toxoplasma gondii* RH strain parasites were maintained by serial passage in human foreskin fibroblast (HFF) cells and genetically manipulated as previously described [102]. To tag the genomic locus of TgSFA2 (genbank accession XM_002367757) with a 3xHA tag, 585 bp of the open reading frame ending before the stop codon was amplified from the *T. gondii* genomic DNA. All primer sequences used are shown in supplementary Table S1.  Similarly, 3000 bp upstream of the stop codon of XM_002370621.1 were amplified to tag TgSFA3 with YFP. These amplicons were cloned via ligation independent cloning (LIC)[103] into the pLIC-HA-CAT or pLIC-YFP-DHFR vector, respectively to create in-frame fusions [104]. Transgenic clones were

established by transfection of ΔKu80 parasites and chloramphenicol or pyrimethamine selection respectively, as previously described [104]. Integration was confirmed by PCR or Southern blotting as previously described [110]. A probe complementary to the 3' region of the SFA2 gene was amplified by PCR. Cen1-RFP [37] was introduced into SFA3-YFP parasites by transient transfection. FNR-RFP [110] was transfected into SFA3-YFP parasites and stable transgenics were isolated by fluorescence activated cell sorting [102].

**Construction of conditional SFA2 and SFA3 knock out parasites**

To target SFA2  1500 base pairs immediately up and downstream of the start codon were amplified and introduced into vector piKO in order to flank an HXGPRT selectable marker [142], a transactivator (TaTi) and the tetracycline regulatable T7S1 promoter (this plasmid was a kind gift of Dominique Soldati, University of Geneva). The final construct was linearized using NcoI/SpeI and transfected into ΔKu80 parasites. Clones were obtained after mycophenolic acid selection and screened for locus insertion by PCR screen (see supplementary Figure S3.2C and S3.2D).  Mutants were grown in 0.5 µg/ml of ATc (Sigma-Aldrich) for 1 to 4 days, total RNA was isolated (RNAeasy, Qiagen, Hilden, Germany), reverse transcribed (Invitrogen, Carlsbad, CA, USA), and RT-PCR was performed using SFA2 specific and control primers (Table S3.1).

For SFA3, a cosmid (PSBLE51) was modified by recombineering [94] to replace the native promoter by a regulatable promoter. A suitable cassette was constructed by inserting a gentamycin marker [94] into the promoter replacement plasmid *pDT7S4_087270* [123] The resulting plasmid (*pGDT7S4_087270*) was used as template to amplify the modification cassette using 50 bp homology flanks for insertion into SFA3 (Figure S3.2A). The Modified cosmid was isolated by double selection on gentamycin

and kanamycin [94] and transfected into TATiΔKu80 parasites [123], clones were isolated after pyrimethamine selection and tested for promoter replacement by PCR (supplementary Figure S3.2A and S3.2B).

**Protein expression and antibody production**

The complete coding region of TgSFA3 was amplified from the *T. gondii* genomic DNA and inserted into plasmid pAVA-421 6xHis [106].  Recombinant fusion protein was purified on Ni$^{2-}$-NTA resin (Qiagen, Hilden, Germany) [107]. Rabbits were immunized with 1 mg of purified protein, and serum was collected after 10 weeks (Cocalico Biologicals, Reamstown, PA, USA). The sequence encoding for amino-acids 1-110 of TgCENH3 [60] was amplified and cloned into the same expression vector and purified in a similar fashion as SFA3. Mice were immunized with 0.4 mg of purified protein, and serum was collected after weeks.

**Fluorescence microscopy**

For immunofluorescence assays, host cells (HFF) were inoculated onto coverslips and infected with parasites. Coverslips were fixed 24 hours after infection with 4% formaldehyde in PBS and permeabilized with 0.2% Triton X-100 in PBS/3% BSA. Coverslips were then blocked in 3% bovine serum albumin (BSA) in PBS as previously described [108]. Primary antibodies used were mouse anti-alpha tubulin at a dilution of 1:1000 (12G10, a gift of Jacek Gaertig, University of Georgia), rabbit anti-Centrin1 at 1:1000 (gift of Iain Cheeseman, Massachusetts Institute of Technology), mouse anti-GFP at 1:1000-1:400 (Torry Pines Biolabs), rat anti-HA at 1:1000 (clone 3F10, Roche Applied Science), mouse anti-IMC1 mAb 45.15 [109] at 1:1000 (gift of Gary Ward, University of Vermont), rabbit anti-IMC3 [59] at 1:500, mouse anti-ISP1 mAb 7E8 [43, 143] at 1:1000 (gift of Peter Bradley, University of California, Los Angeles), rabbit anti-MORN1 [37] at

1:250, anti-aceytlated tubulin (Sigma) at 1:1000, and rabbit anti-SFA3 at 1:1000 (generated in this study). The secondary antibodies used were AlexaFluor 350, AlexaFluor 488, and AlexaFluor 546 (Invitrogen), at a dilution of 1:2000. Images were collected on an Applied Precision Delta Vision inverted epifluorescence microscope using a UPlans APO 100×/1.40 oil lens. Time-lapse imaging was performed on the same Delta Vision microscope in a climate controlled chamber at 37 C. Cells were grown and imaged on glass bottom Wilco culture dishes (Wilco Wells, Amsterdam, The Netherlands). Images were obtained every 10 minutes for 4 hours, and processed to correct for cell drifting. Photobleaching of SFA3-YFP was performed on a Delta Vision microscope using a single 600 ms pulse with a 488 nm laser set at 20% power, on a specified, diffraction-limited, region. Images were subjected to deconvolution and contrast adjustment using Applied Precision software (Softworx). For quantitative image analysis (presence/absence of fibers, and number of nuclei/cell or centromeric clusters/nucleus, as described in the results section) a minimum of 50 vacuoles were scored for each out of at least three repeats. Averages and standard deviations were calculated and plotted using Graph Pad Prism Version 5.0c (La Jolla, California, USA). Fiber length measurements were done using Volocity (Perkin-Elmer, Rodgau, Germany) on images taken of SFA3-YFP parasites under oryzalin or DMSO control treatment. Each point represents the average fiber length in one imaging field. Measurements were done for at least 18 fibers (and up to 81) per image. 4 images from 3 independent replicates were used.

**Electron microscopy**

Cells infected with SFA2-HA parasites were fixed in 4% para-formaldehyde/0.05% glutaraldehyde in 0.1 M sodium phosphate buffer pH 7.4, blocked with 1% FBS in PBS (all RT), followed by overnight infiltration in 2.3 M sucrose/20% polyvinyl pyrrolidone at 4 °C. Samples

were frozen in liquid nitrogen, and sectioned with a Leica UCT cryo-ultra microtome. Sections were blocked with 1% FBS and subsequently incubated with rat anti-HA (1:100), followed by incubation with rabbit anti-rat (1:400), and finally 10 nM colloidal gold conjugated protein A. Washed sections were stained with 0.3% uranyl acetate/2% methyl cellulose and viewed with a JEOL 1200 EX transmission electron microscope. Controls, omitting the primary antibody, were consistently negative at the concentration of colloidal gold conjugated protein A used. Infected cells were also fixed in 2% glutaraldehyde in sodium phosphate buffer 0.1M, pH7.4, followed by post-fixation with 1% osmium tetroxide in sodium phosphate buffer, alcohol dehydration and Epon resin embedding. Serial sections were obtained with a Leica UCT cryo-ultramicrotome and collected in carbon coated single hole grids.

**Western Blotting**

Western blotting was performed as previously described [110]. We used anti-HA antibodies at a dilution of 1:1000, anti-tubulin at 1:1000, anti-GFP at 1:500 and anti-SFA3 antibodies at a dilution of 1:1000. Pre-immune sera for anti-SFA3 antibodies were used at a dilution of 1:1000. Horseradish peroxidase (HRP)-conjugated anti-rat or anti-rabbit antibody (Pierce) was used at a dilution of 1:20,000.
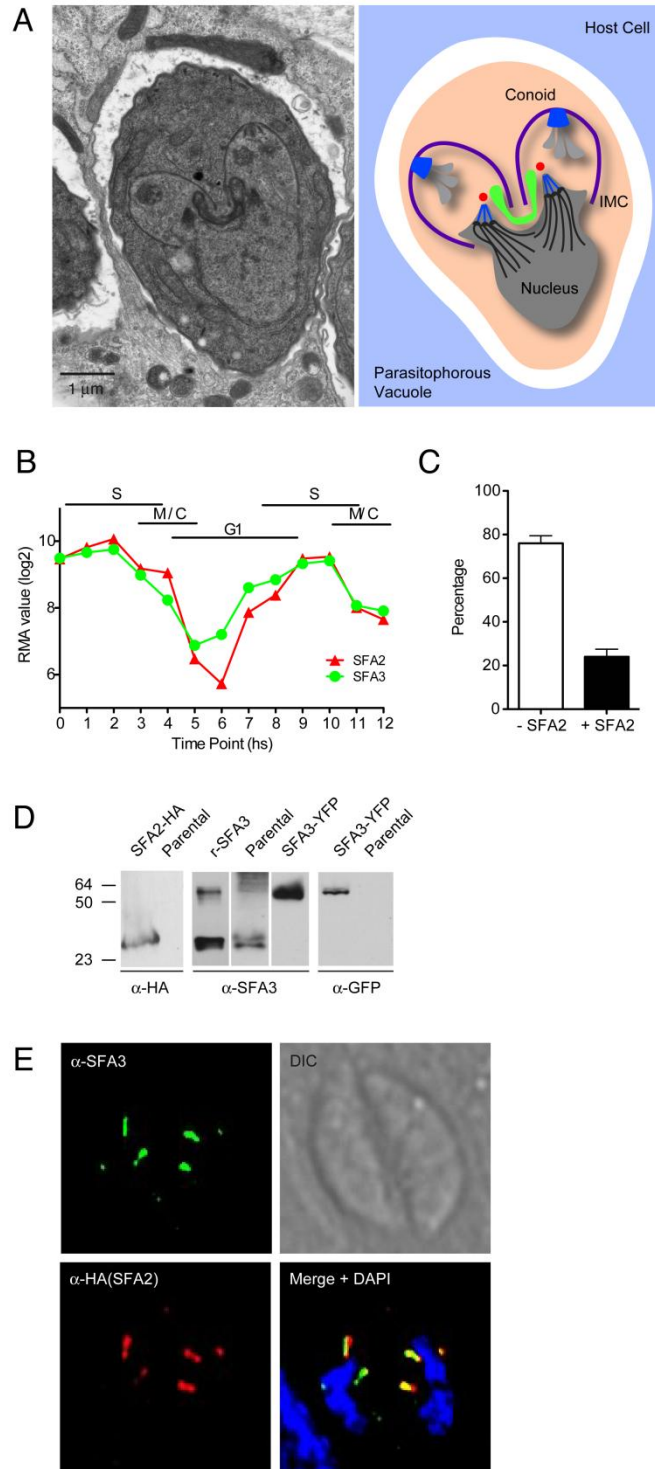
**Figure 3.1.** *T. gondii* **tachyzoites express two striated fiber assemblins that localize to a structure close to the nucleus. A.** Electron micrograph and schematic representation of a dividing *T. gondii* parasite. Two daughters are assembled within a mother cell. Centrosomes are shown in blue, apicoplast in green. **B.** Robust multi-array averages of SFA2 and SFA3 transcripts over two consecutive division cycles based on data set collected by Behnke and colleagues [120, 121]. **C.** Parasites do not express TgSFA2 at all times. Parasites expressing SFA2-HA were scored by immunofluorescence assay using anti-HA antibody in an asynchronous parasite population (n=250). **D.** Western blot analysis shows a 30 kDa band when probed with anti-HA antibody in SFA2-HA transgenics but not the parental strain. Anti-SFA3 antibodies recognize the recombinant protein used for immunization (rSFA3), as well as the native protein in parental parasites. Lower mobility bands of approximately 60 kDa likely correspond to dimers formed both by the recombinant and native SFA3 proteins. Anti-SFA3 antibodies also recognize YFP tagged SFA3 in the endogenously tagged TgSFA3-YFP strain. The expected masses for SFA3 and SFA3-YFP are 36 kDa and 56 kDa respectively. Anti-GFP antibodies specifically recognize SFA3-YFP in the endogenously tagged strain, but not in the parental strain. E. Immunofluorescence assay of SFA2-HA parasites stained with anti-SFA3 and anti-HA antibody and DAPI. Note that both SFA proteins localize to two fiber-like structures per parasite.
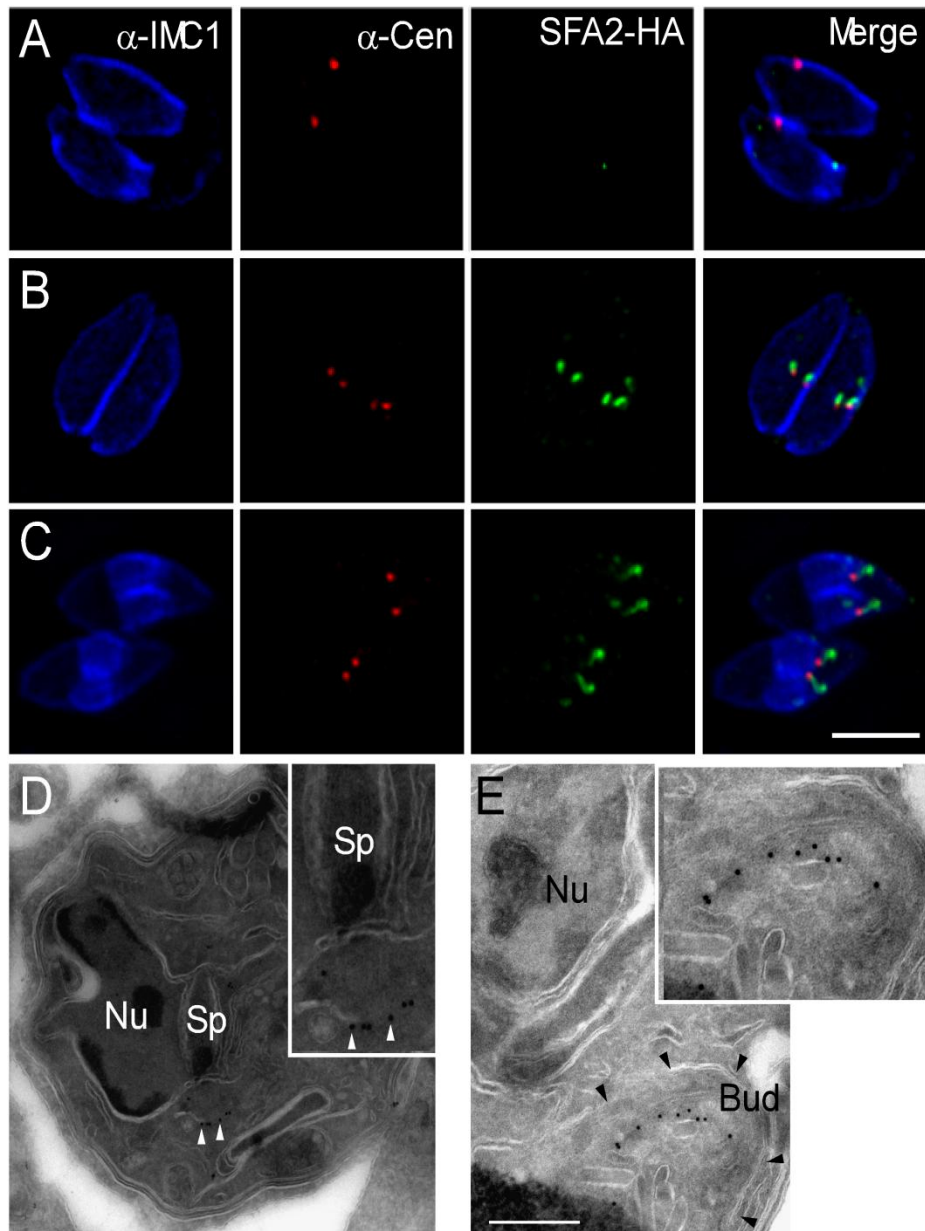
**Figure 3.2. *T. gondii* SFAs are expressed only during cell division. A-C.** Immunofluorescence

assays of SFA2-HA. Parasites were labeled with anti-HA (green), in combination with anti-IMC1

(blue) and anti-centrin (red). IMC1 labels the inner membrane complex in both the mother and

the daughter cell and centrin is a marker of the centrosome. Robust HA staining is only apparent

in parasites with duplicated centrosomes. Scale bar = 5 µm. **D** and **E.** SFA2-HA parasites were

fixed, cryo-sectioned, and probed with anti-HA antibody, followed by incubation with gold

conjugated protein A. **D.** The spindle (Sp) is visible in an invagination of the envelope of the nucleus (Nu), note vertical white lines representing spindle microtubules. Gold particles are highlighted by white arrowheads **E.** Inner membrane complex outlining a daughter bud is highlighted by black arrowheads. Scale bar= 500 nM. Insets show further enlargements for detail.
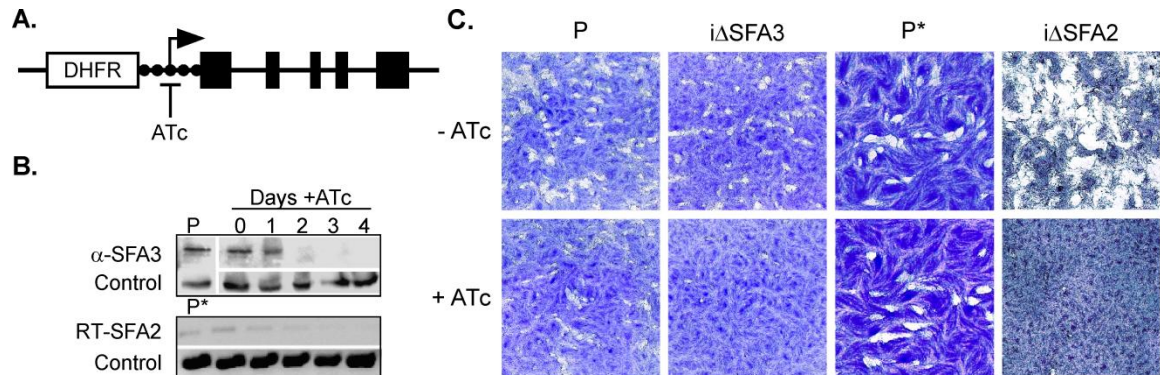


**Figure 3.3. TgSFA2 and TgSFA3 are required for parasite growth. A.** Simplified schematic representation of iΔSFA3 promoter insertion mutant (see supplemental materials for further detail). Promoter activity is inhibited by addition of anhydrotetracycline (ATc) to the growth medium. **B.** Top, Western blot using anti-SFA3 antibodies to measure SFA3 in the iΔSFA3 strain upon ATc treatment (P, parent; tubulin is shown as a loading control). Bottom, reverse transcriptase PCR analysis of SFA2 transcript in the iΔSFA2 strain upon ATc treatment (RT-PCR of TGGT1_021600 transcript is shown as control). Note that the expression of both targeted genes is susceptible to ATc. **C.** Plaque assay measuring growth of mutants and parental strains in the presence (+) or absence of ATc (-). Note that both mutant strains fail to form plaques (clearings) in a monolayer of fibroblast in the presence of ATc in the medium. The parental strains and untreated cultures of all strains are shown for comparison. The asterisk indicates that the parental strains (P and P*) of the mutants are distinct (see supplementary materials).
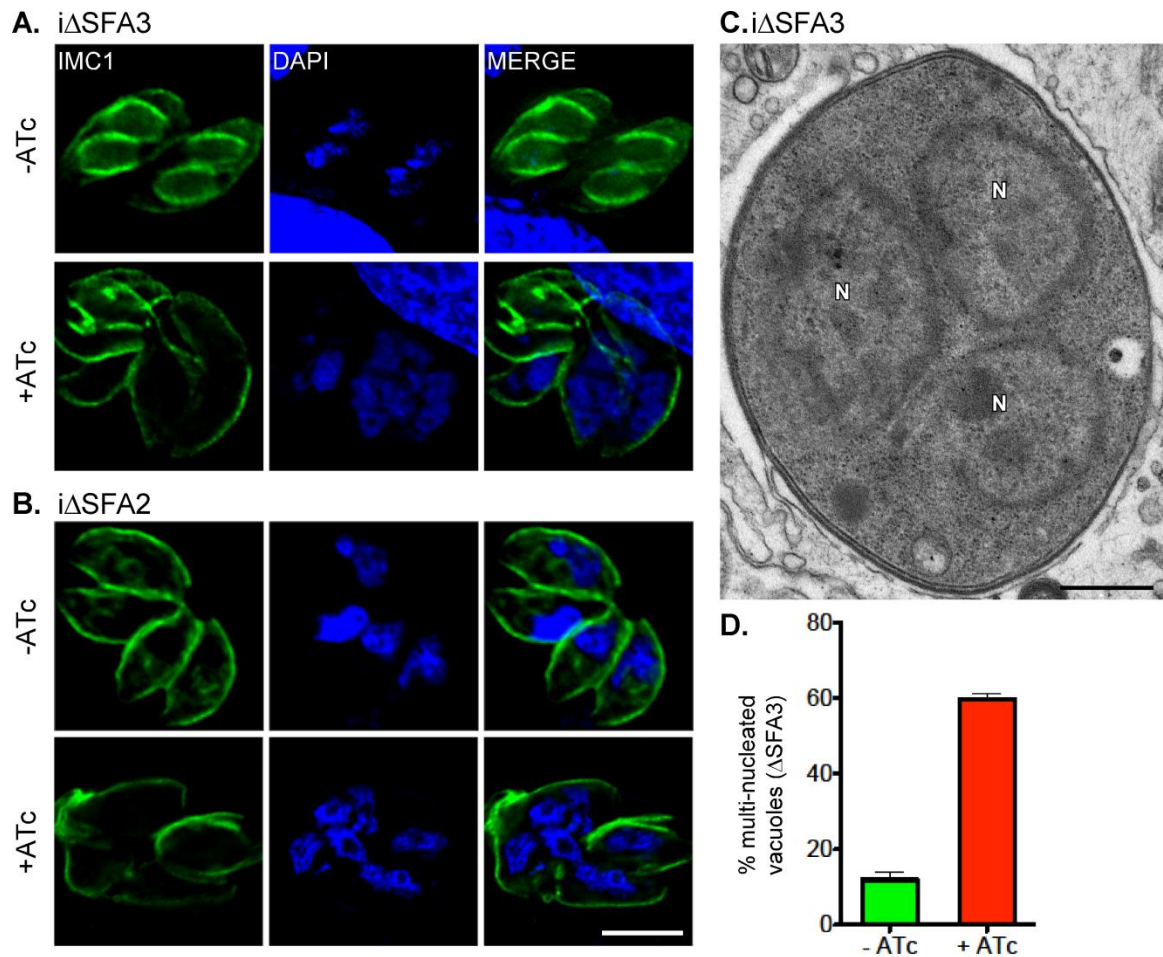
**Figure 3.4. Parasites lacking TgSFA2 or TgSFA3 show a pronounced cell division defect. A-B.**
Immunofluorescence assays of cells infected with iΔSFA3 (A) or iΔSFA2 (B) mutant parasites
cultured for 48 hs in presence or absence of ATc prior to fixation. Note that both mutants
accumulate multiple nuclei (blue), and fail to form proper buds (IMC1, green) under knock down
conditions. Untreated controls divide normally. **C.** Transmission electron micrograph of iΔSFA3
parasites grown in presence of ATc for 48 hs. This section through a cell shows three nuclei (N;
scale bar= 500 nm). **D.** Multi-nucleated (≥2) parasites were quantified for iΔSFA2 parasites (48 hs
+/- ATc) using DAPI and IMC1 staining. 30 randomly chosen fields were counted and the
percentage of vacuoles containing parasites with multiple nuclei is graphed.   Error bars
represent standard deviation (n=3).
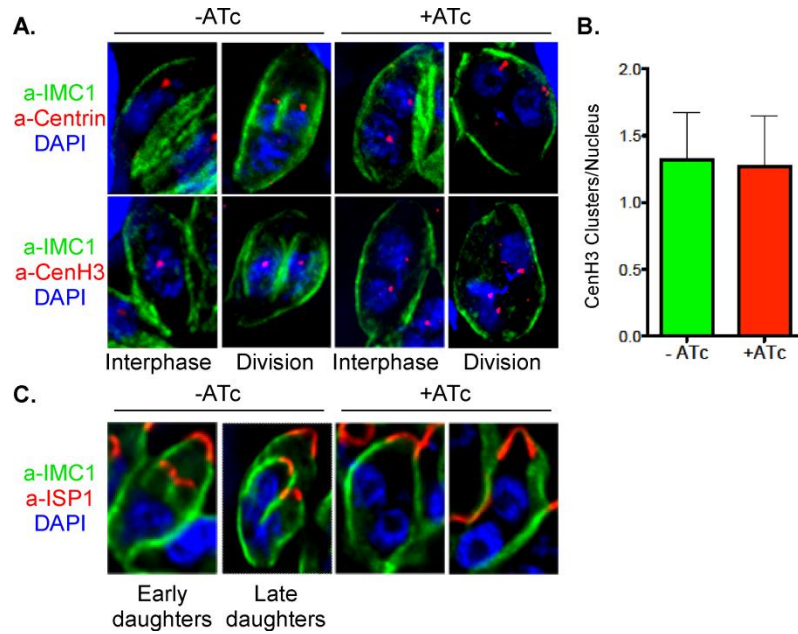
**Figure 3.5. Parasite lacking SFA go through mitosis normally but fail to form daughter cells. A.**
iΔSFA2 parasites grown in the presence or absence of ATc for 24 hs were labeled with anti-IMC1 (green) and DAPI (blue) anti-centrin (red, centrosomes, upper panels) or anti-CenH3 (red, centromeres, lower panels). Representative examples are shown for cells in interphase or division. Interphase nuclei associate with a single centrosome, while larger 2N nuclei associate with two. This is unchanged by ATc treatment. Interphase nuclei contain a haploid genome and exhibit one CenH3 dot representing a cluster of the centromeres of all 14 chromosomes bundled in the nucleus in close proximity to the centrosome (see [60]). Dividing nuclei exhibit two CenH3 dots representing duplicated chromosomes. Again, this labeling pattern is not affected in the mutant when judged on a per nucleus basis. Note though that in both cases the ATc treated cell is already tetraploid with no sign of cytokinesis **B.** The number of CenH3 dots per nucleus was quantified in IFA experiments for untreated or ATc treated iΔSFA2 parasites. The number of CenH3 dots, representing the number of chromosome sets per nucleus, is graphed, error bars show standard deviation (>50 parasite vacuole per experiment counted, n=3). **C.** Immunofluorescence of iΔSFA2 parasites after 48 hs ATc treatment showing IMC1 (green), DAPI

93

(blue), and anti-ISP1 (red). ISP1 (IMC sub-compartment protein 1) labels the apical cap of the IMC of both mother and daughter cells and is an early marker of budding [43]. ISP1 staining for daughter cells is absent in the ATc treated mutant. Note that the nuclei have completed mitosis in these cells and compare to a similar stage shown for untreated parasite.
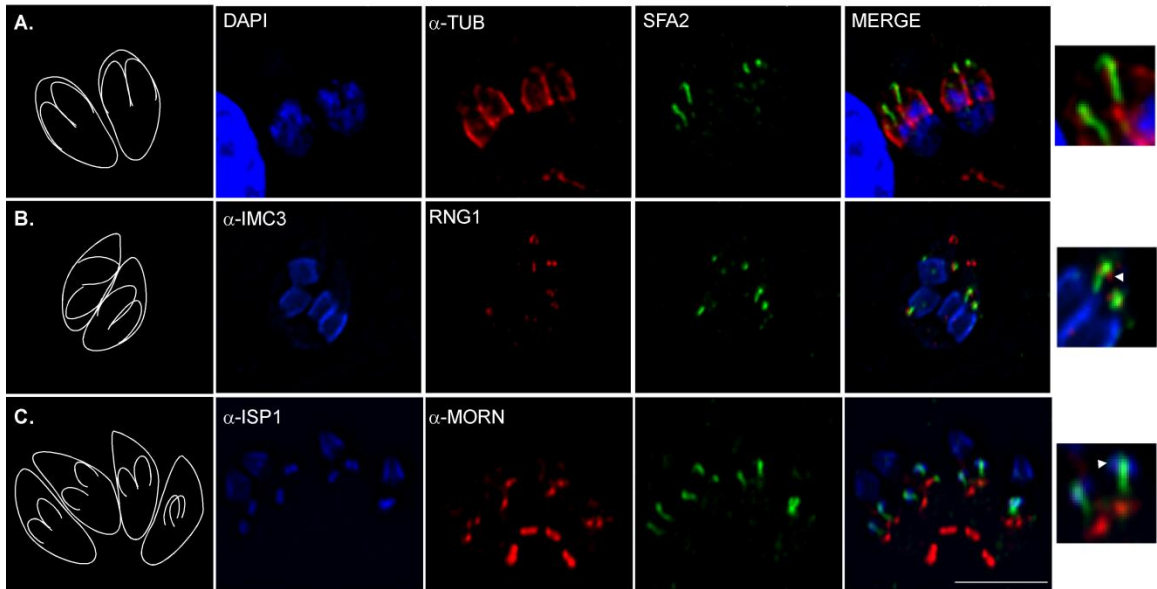


**Figure 3.6. The SFA fiber extends in the apex of the forming daughter.** Immunofluorescence assays showing SFA2-HA stained with anti-HA (green) in combination with markers for daughter bud. **A.** anti-tubulin (red) labels the sub-pellicular microtubules. SFA2 staining extends beyond the sub-pellicular microtubules and into the conoid. **B.** Anti-IMC3 (blue) labels the inner membrane complex of emerging daughter cells and is shown as a reference for the position of daughter cells. RNG1-YFP was detected using anti-GFP antibodies (red). RNG1 is a marker of the conoid [29]. The SFA2-HA signal extends into and slightly beyond the ring of RNG1 staining**. C.** anti-ISP1 (blue) labels the apical cap of the IMC. Anti-Morn1 (red) labels the basal complex of both the mother's and the daughter's IMC, as well as, a nuclear structure in immediate proximity of the centrosome [37, 70]. The SFA2-HA signal spans from the centrosome region to the apex of the daughter bud.  Scale bars = 5µm.
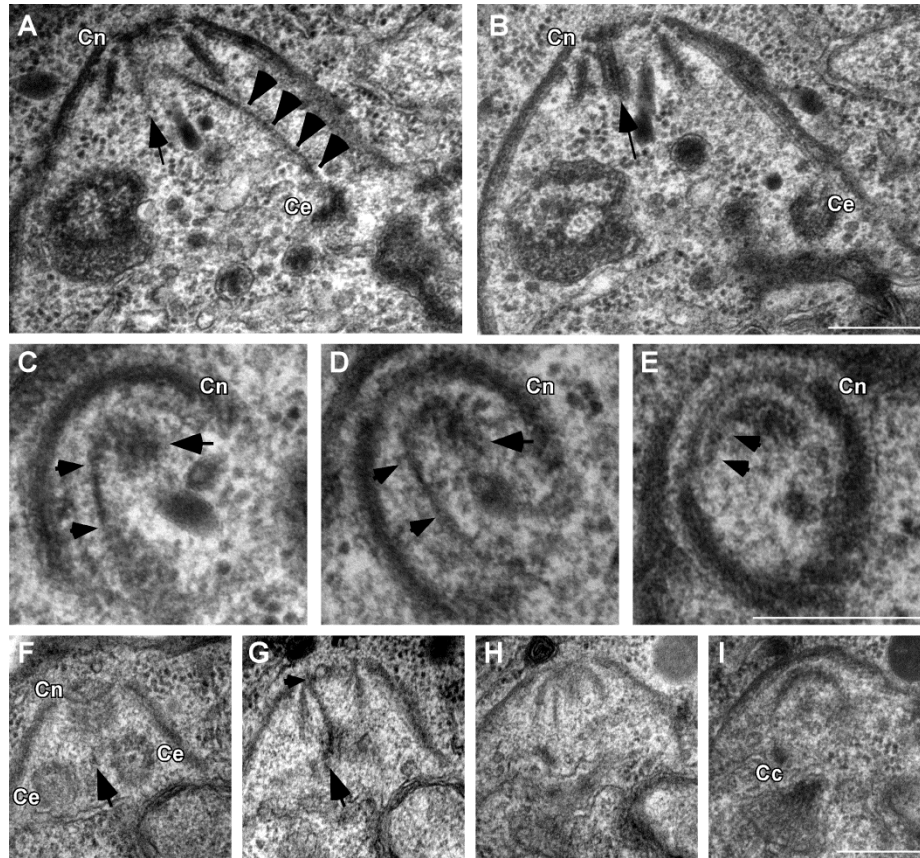
**Figure 3.7. A fiber links the centrosome and the apical complex of the daughter bud.** Transmission electron micrographs of serial sections of dividing wild type parasites. **A-B**. Two consecutive sections through a daughter cell are shown. An electron dense structure is highlighted in panel A (arrowheads, note some striation in this section, in particular toward the conoid end) emanating from close to one centriole (Ce, B) and reaching up to the conoid of the daughter cell (Cn, A and B). The structure ends in close proximity of the central pair of microtubules within the conoid (arrow, A and B). **C-E.** Three consecutive sections perpendicular to the conoid and the orientation of the parasite depicted in panels A and B are shown. A bent electron dense structure (arrowheads) runs within the conoid (Cn) towards the apical ring. The end of this structure appears in contact with the conoid-associated microtubule pair (arrow, also see Fig. 10 for a schematic outline). **F-I**. Four consecutive sections through an early daughter

cell. Both parallel centrioles (Ce) of the centrosome can be seen in F. A fiber is visible reaching into the conoid and touching the apical ring (Cn, F-H). The fiber emerges between the centrioles (arrow, F and G). The last section shows intra-nuclear microtubules as part of the centrocone (CC, a nuclear envelope structure associated with centromere organization in Apicomplexa); these link the kinetochores of the chromosomes to the centrosome. Scale bars = 250 nM
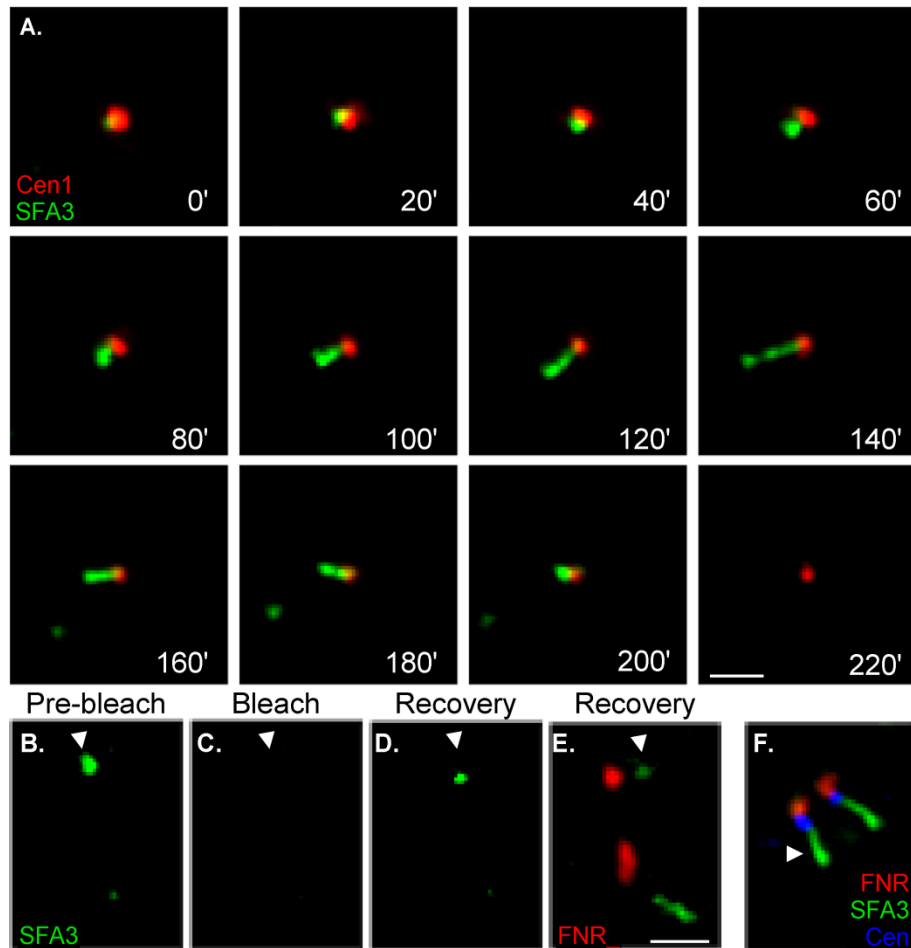


**Figure 3.8. The SFA fiber grows in a polar fashion away from the centrosome A.** Time lapse imaging of SFA3-YFP parasites expressing Centrin1-RFP. Images were taken every 10 minutes for 220 min. Note that SFA-YFP forms a centrosome associated spot which extends away from the centrosome (min 60-120). The fiber breaks at its distal end (min 140-160) and then shortens in reverse order. See supplementary move M2 for an animated version. **B-E**. Photo bleaching assay

of TgSFA3-YFP parasites expressing FNR-RFP (Ferredoxin/NADPH Reductase-RFP) **B.** The fiber in the focal plane (arrowhead) was 0.45 µM prior to bleaching. **C.** The target fiber was bleached using a 488 nm laser and is no longer visible after the laser pulse. **D.** Images of the photo-bleached fiber were taken after one hour to monitor recovery of the YFP signal. YFP labeling of the fiber can again be appreciated spanning 0.35 µM. **E.** Image showing the YFP labeled fiber after bleaching, its sister unbleached fiber, and FNR-RFP for reference. The right most fiber (unbleached) spans 0.85 µM. The bleached fiber appears shorter and that (new) labeling appears proximal to the FNR-RFP signal. **F.** Immunofluorescence assay showing the close proximity and relative orientation of apicoplast (FNR-RFP, red), centrosome (blue) and SFA fiber (green). The apicoplast (FNR-RFP) associates with the centrosome during division [116], and was used as a marker for the position of the centrosome.  Scale bar = 1 µm
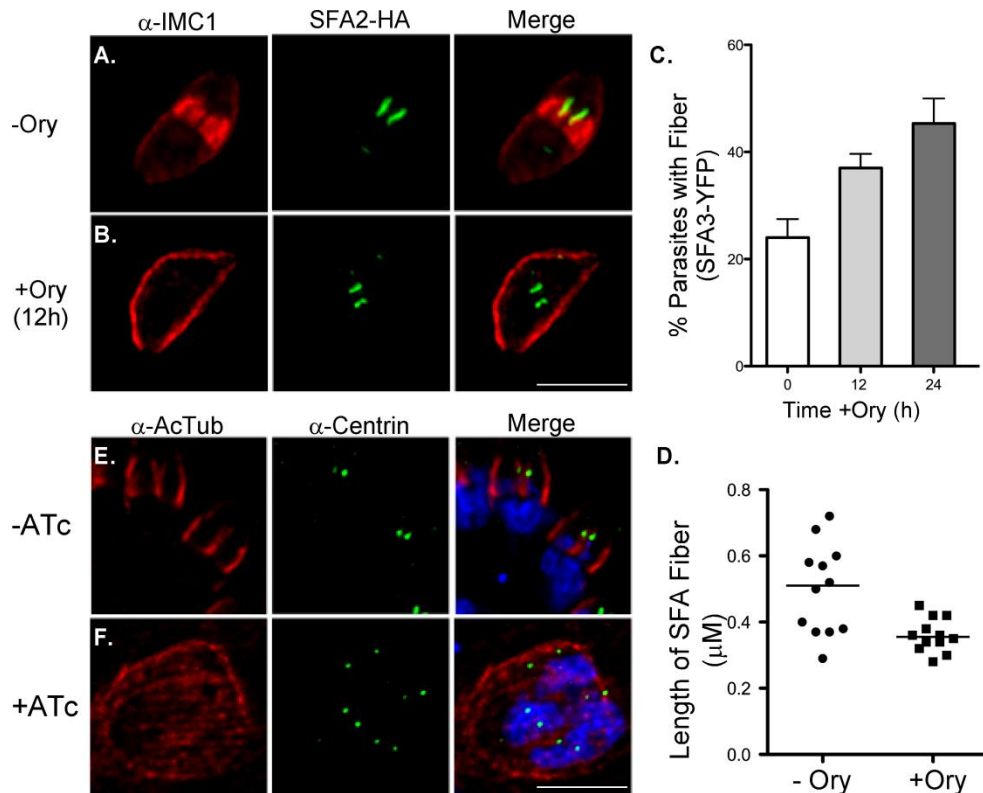
**Figure 3.9. Daughter microtubules depend on SFA fiber, but the fiber does not depend on microtubules. A** and **B**. Immunofluorescence of SFA2-HA parasites treated with oryzalin, a microtubule disrupting agent that prevents formation of new microtubules in daughter cells, and that has a more moderate effect on existing stable microtubules in the mother [63, 65]. Note that after 12 hs of treatment parasite cells fail to assemble buds (B) and compare to the matched control (A). SFA2-HA fibers are nonetheless detected. Note that in untreated parasites, daughter cells are normally detectable when similar fibers are observed **C.** SFA3-YFP parasites were treated with oryzalin and scored for the presence of SFA3-YFP after 0, 12 or 24 hs of treatment. Note that treated parasites accumulate fibers. **D.** Fiber length was measured in control parasites and parasites treated with oryzalin for 24 hs. Data points reflect the mean fiber length per field of view scored (n= 18-81 fiber/field, 4 fields for each of 3 independent repeats). Fibers of treated parasites are overall shorter and more uniformly distributed in size. **E .** iΔSFA2 parasites were grown in the absence or presence of ATc and stained for acetylated tubulin (red), centrin (green) and DAPI (blue). The anti-acetylated tubulin antibody labels daughter buds strongly (as do antibodies to unmodified tubulin) in untreated mutants. ATc treated iΔSFA2 parasites exhibit acetyl-tubulin staining exclusively in the mother cell cytoskeleton (note that two mutant cells are shown with microtubules encaging each entire cell; the cells are abnormally large due to the block in budding). No daughter microtubular-skeletons are discernible in these cells despite the fact that each cell shown has 2 nuclei, both of which are entering mitosis as indicated by the duplicated centrosomes. Scale bars = 5µm.
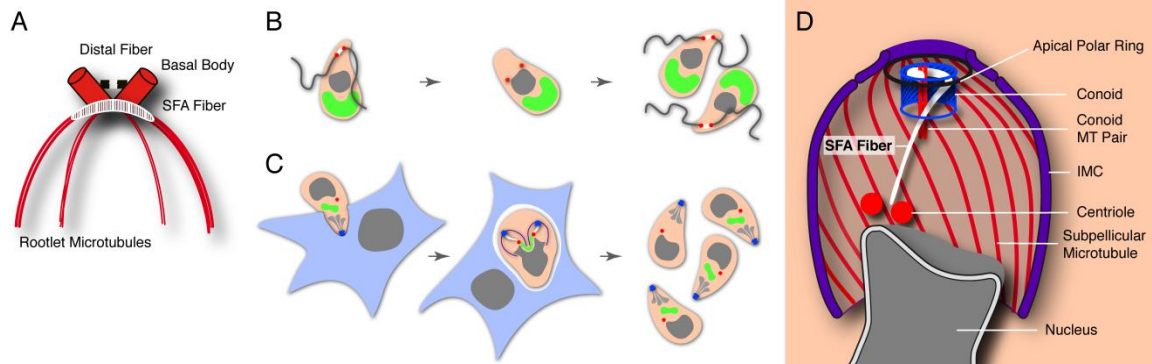
**Figure 3.10. Is the apical host cell invasion complex derived from the flagellum of the algal ancestor? A.** Schematic representation of the flagellar rootlet system of *Chlamydomonas* (simplified after [65]). The two flagellar basal bodies are coordinated by rootlet fibers (only SFA and distal fibers are shown here) and bundles of rootlet microtubules (2 or 4 microtubules each) **B.** Schematic outline of cell division in the hypothetical flagellated algal ancestor of Apicomplexa. Basal bodies of the flagella also serve to organize the mitotic spindle (flagella are resorbed or shed during mitosis in some flagellated algae, note that number and behavior of flagella in the apicomplexan ancestor is hypothetical). Rootlet fibers (white)  may have additional roles in division [125, 128, 129]. **C.** Apicoplast, green; nucleus, grey; SFA fiber, white; basal body/centrosome, red; conoid, blue, rhoptries (secretory component of the apical invasion apparatus), light grey. Apicomplexans are intracellular parasites and have lost flagella in most stages. SFA rootlet fiber is only expressed during division and coordinates the centrosome with the MTOC of the daughter bud. This suggests that the system that controlled the positioning and assembly of flagella in the ancestor now organizes the assembly of the apical host cell invasion complex. D. Schematic representation of the SFA fiber and its relationship to other cellular structures during *T. gondii* cell division (only a single daughter bud is shown for simplicity).
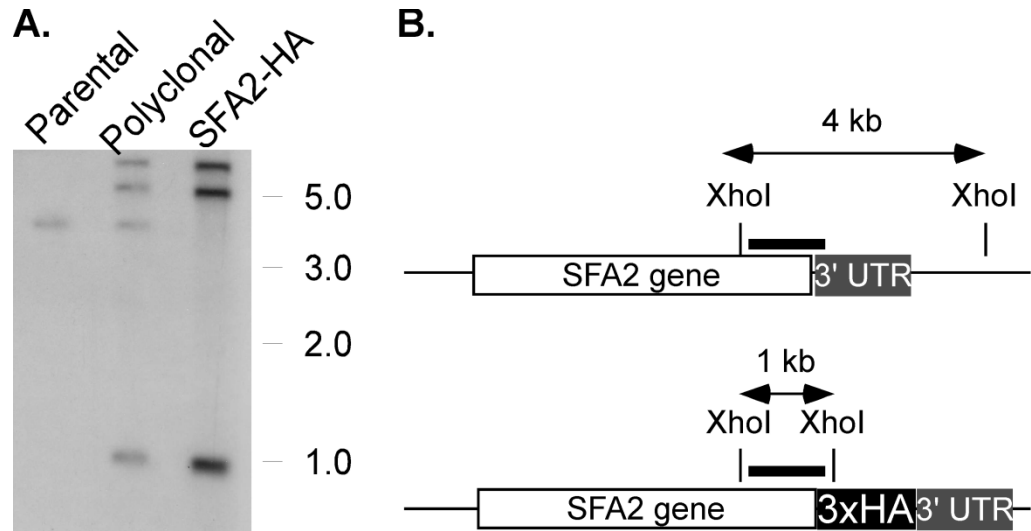
**Figure S3.1. Confirmation of the insertion of a triple hemagglutinin (HA) tag at the endogenous locus of TgSFA2. A.** Southern blot of the parental strain, the polyclonal transfected population, and the SFA2-HA clone used in this study is shown. **B.** A radioactively labeled probe complementary to the 3' end of TgSFA2 was used for hybridization and is represented with a black bar. Insertion of the triple HA tag in the native locus creates an XhoI restriction site, absent in the parental cell line. This generates a 1.0 kb hybridization fragment in the SFA2-HA strain, while the probe hybridizes to a 4 kb fragment in the parental cell line. Note that in the polyclonal population both the 1.0 and 4.0 kb hybridization fragments are detected representing successful and unsuccessful insertions of the triple HA tag in the native locus respectively.  Also note additional integration products that were not further investigated
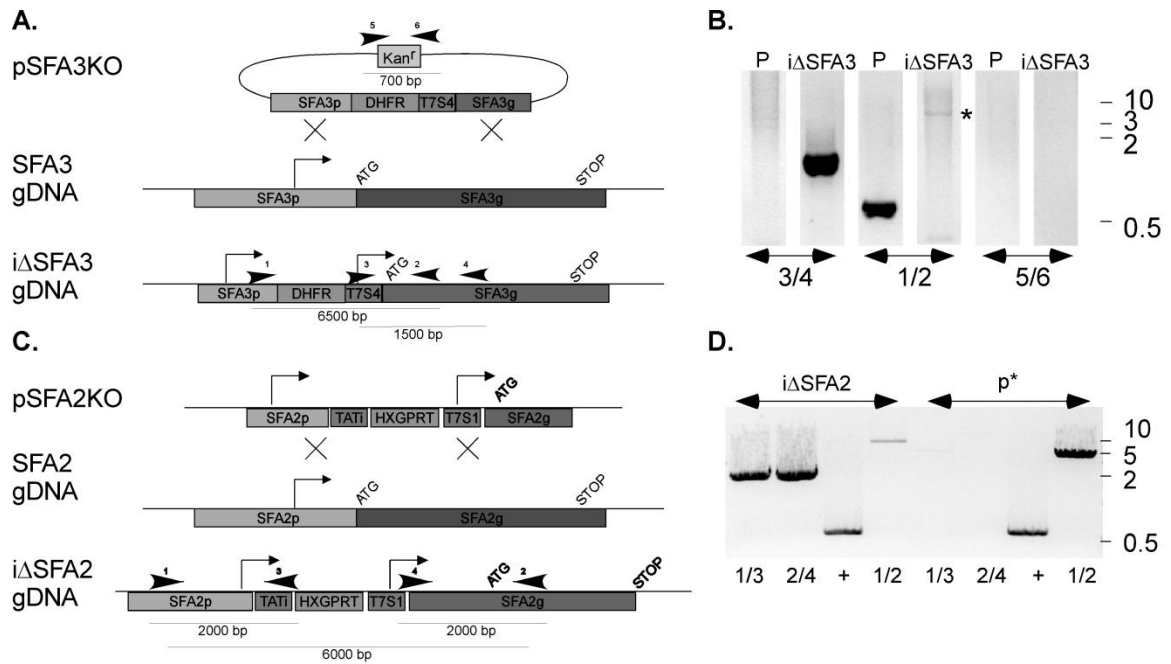
**Figure S3.2. Schematic representation of the constructs engineered for obtain the iΔSFA3 and iΔSFA2 conditional knock out strains and PCR screens.** **A.** Cosmid PSBLE51 containing the entire TgSFA3 gene (TgME49_ 018880) and several kilo bases upstream of the start codon was modified by recombineering a mutagenic cassette positioning an inducible promoter immediately upstream of the start codon, as well as a pyrimethamine resistance cassette for selection of transgenic parasites. Double homologous recombination of the construct into the TgSFA3 gene in the parasite yields iΔSFA3. The approximate location of primers used for PCR screen of clones is represented with arrow heads. **B.** PCR screen of a successful transfectant shows that the TgSFA3 native locus is modified by insertion of a regulatable promoter between the endogenous promoter and the TgSFA3 gene coding sequence. The parental strain used for transfection (ΔKu80TaTi) is shown as a control. Note that primer pair 4/5 control for the absence of an episomal copy of the modified cosmid piΔSFA3 (double homologous recombination into the genome causes loss of the kanamycin cassette) **C.** Schematic of the construct engineered to generate a conditional knockout of TgSFA2 (TgME49_005670), iΔSFA2. Upon successful

insertion into the TgSFA2 locus, the expression of TgSFA2 is controlled by the inducible promoter T7S1, while the expression of the transactivating protein (TATi) is under the control of the TgSFA2 endogenous promoter. The approximate location of screening primers in the genome of the resulting mutant is represented with arrow heads. **D.** PCR confirmation of successful insertion of the knock out construct piΔSFA2 into the TgSFA2 genomic context in the clone used for all experiments shown in this study. The parental strain used for transfection (ΔKu80) is shown as a control.

**TABLES**

**Table 3.1. Name and sequences of all primers used in this study**

| Number | Primer Name | Primer Sequence 5'-3' |
|--------|-------------|----------------------|
| 1 | SFA2 LIC F | tacttccaatccactatggggcaagg |
| 2 | SFA2 LIC R | tcctccagttccaatttcgaaggccc |
| 3 | SFA3 LIC F | tacttccaatccaatttaatgcggccttgcttggacaatgtacc |
| 4 | SFA3 LIC R | tcctccacttccaattttagcggctgtcgtgacgagacg |
| 5 | SFA2 3' F | gctaaatcatctgaaaaaggacatcg |
| 6 | SFA2 3' R | cagcgagtgcttatatctgtggaac |
| 7 | SFA2 Prom F | agatctatggcgggggctgcagggtcgtgca |
| 8 | SFA2 Prom R | actagtctcgagctcaaactgttccttcagcg |
| 9 | SFA2 Gene F | ccatggcacgtgtaaaccttgtcgaagcag |
| 10 | SFA2 Gene R | gctagcaatgcacggccctcctgtggaaa |
| 11 | SFA2KO Screen 1 | catatgcacacatataccaagacaccgggaa |
| 12 | SFA2KO Screen 2 | cctaggtggagcctgccaaaaccgctcacat |
| 13 | SFA2KO Screen 3 | tgagcgagtttccttgtcgtcag |

| 14 | SFA2KO Screen 4 | atggagcagaagctcatctccgag |
|---|---|---|
| 15 | SFA2 RT PCR F | cgctgaaggaacagtttgagctcga |
| 16 | SFA2 RT PCR R | ggctgtcgtgtactggttgatagca |
| 17 | RT PCR Control F | tcgatacatttcgttcgcgtag |
| 18 | RT PCR Control R | tcgtccgctctgtcgccttgc |
| 19 | Gent F | gggattaatgcggccggccgctgaagttcc |
| 20 | Gent R | cccattaattgcaggaagttcctattctctagaaag |
| 21 | SFA3 Cosmid F | cagtccacgcggtcgaagctcgcggtgttgagcgaacggattcatggtttgaatggtaaccgacaaacgcgttc |
| 22 | SFA3 Cosmid R | gctttcgtctgtcttcaaccagatcttgaaaagcagatggagtctgaggccaagcagagaagggagagtgaagaga |
| 23 | SFA3KO Screen 1 | atcaaggaagccatcacga |
| 24 | SFA3KO Screen 2 | cacgaagatggaagacagc |
| 25 | SFA3KO Screen 3 | cgccttggcgaatgttcatgac |
| 26 | SFA3KO Screen 4 | gtgttcacgggtcgaagggataaa |
| 27 | SFA3KO Screen 5 | atgattgaacaagatgg |
| 28 | SFA3KO Screen 6 | tcagaagaactcgtc |
| 29 | SFA3 pAVA F | gggtcctggttcgctgaggccaagca |
| 30 | SFA3 pAVA R | cttgttcgtgctgtgtcgtgacgaga |

CHAPTER 4

CONCLUSION

**INTRODUCTION**

Apicomplexan parasites cause numerous important human and veterinary diseases

including malaria, toxoplasmosis, cryptosporidiosis, coccidiosis, and Texas and East Coast fever.

Apicomplexa are obligate intracellular parasites and their ability to replicate appropriately

within different host cell niches is crucial to pathogenesis. The products of the intracellular

replication are motile stages, primed to invade new cells to spread and perpetuate the infection,

causing tissue damage and inflammation in the process.

How Apicomplexa invade cells has received significant attention as the licensing step to

establishing a successful infection. Through these studies, a detailed understanding of the

process and its pathogen and host components has been developed. [21, 144] Once the parasite

has successfully invaded the host cell, it replicates, divides and assembles daughter cells. These

events are less well understood than the invasion process.  The fundamental structural aspects

of apicomplexan division and replication were established in pioneering transmission electron

microscopy work more than 30 years ago.[36, 55, 145, 146]  However, the molecular

mechanisms underlying the assembly and regulation of these structures only began to emerge

recently and are the focus of this review. Apicomplexans infect a variety of host cells and can

scale the number of progeny to suit different niches. Key to this ability is a highly flexible cell

and division cycle. Here we summarize the latest molecular advancements in our understanding

of these events. We propose that the flexibility and scalability of apicomplexan division is based

on three organizational principles outlined in Figure 4.3. First, cell cycle progression has initial

local and late global control elements and control is spatially linked to the centrosome. Second,

the nucleus is highly structured into defined nuclear territories. Positioning distinct chromatin

domains, in particular the centromeres and telomeres ensures genome and epigenome integrity

through the intracellular growth phase and division. Third, daughter cells are assembled in a

stepwise and highly ordered process that is temporally and spatially guided by cytoskeletal self-

organization that emanates from and is tethered to the centrosome.

**The Apicomplexan Cell Cycle**

Eukaryotic cells divide by mitosis and the period between divisions is known as

interphase. Chromosomes replicate in the synthesis or S-phase of interphase, which is flanked

by gap or G-phases in which the cell sets the stage for the complex tasks of genome replication

(G1) or mitosis (G2). These events are often depicted as a cycle. Figure4.1 introduces the

eukaryotic cell cycle using the example of a mammalian cell and highlights key structural and

regulatory elements. Progression through the cell cycle is controlled by checkpoints at the end

or start of individual phases and an elaborate regulatory network of protein phosphorylation

and protein degradation.

The apicomplexan cell cycle is composed of three phases; G1, S and M, with G2 being

brief or absent.[25, 147-149] Centrosome duplication marks the boundary between the end of

G1 or interphase, and the start of S phase and division. [57, 58, 150] Centrosomes are the poles

and microtubule organizing centers (MTOC) of the mitotic spindle. Spindle microtubules contact

the centromeres of chromosomes through the kinetochore and segregate chromosomes during

mitosis (Figure 4.1). Centrosomes also function outside of mitosis in controlling cell polarity,

motility, and protein trafficking [151]. Mammalian centrosomes consist of a pair of centrioles,

microtubules arranged in cylindrical structures, surrounded by a pericentriolar matrix made up of more than 200 different proteins.[152, 153] Electron microscopy established early on that apicomplexan centrosomes structurally differ from those found in most model systems. In *Eimeria* and *Toxoplasma* centrioles are parallel compared to the orthogonal arrangement found in most other cells.[36] These centrioles are shorter than their animal counterparts (200 x 200 vs 700 x 250 nm) and exhibit 9+1 singlet microtubule symmetry (Figure 4.4B) compared to the typical 9+2 triplet arrangement [35, 36, 47]. Some species like *Plasmodium* appear to lack centrioles, but centriolar plaques are present in *Plasmodium,* and can be identified e.g. by using antibodies to the centrosome protein centrin.[145, 154, 155]

Apicomplexa divide by mechanisms quite different from those used by their hosts. In mammalian cell division the nuclear envelope gives way upon formation of the mitotic spindle, and chromosomes are pulled to opposite sides of the cell during mitosis. This is followed by fission of the cell during cytokinesis. In most cell types, division gives rise to two progeny.  In contrast, apicomplexans use closed mitosis of the nucleus, which leaves the nuclear envelope intact. Cytokinesis occurs through budding that can occur at the surface of the parasite cell or deep in its cytoplasm (external and internal budding). These mechanisms produce two to thousands of progeny. DNA replication and nuclear mitosis can occur several times during the intracellular growth of the parasite with no concomitant daughter cell assembly or cytokinesis, thus producing polyploid cells with multiple nuclei. Based on the extent and timing of nuclear division prior to cytokinesis, three distinct replication mechanisms have been described: endodyogeny, schizogony, and endopolygeny.

Endodyogeny is the simplest of the three and used by *Toxoplasma*.  A single round of DNA replication and nuclear mitosis is followed by assembly of two daughter cells and

cytokinesis. This is similar to mammalian cells in that it results in two progeny, however, note

that, unlike mammalian cells, daughter cells do not arise by fission of the mother cell but instead

assemble within the mother cell (Figure 4.2). Parasites such as *Plasmodium falciparum,* the

causative agent of malaria*,* or *Eimeria tenella*, which infects poultry, divide by schizogony.

Schizonts, a multinucleated form the parasite, arise through multiple nuclear divisions, resulting

in a syncytium. Surprisingly, while these multiple nuclei share one cytoplasm, they often divide

in an asynchronous fashion resulting in non-geometric expansion (the resulting number of nuclei

is not a power of 2). [156] The last round of mitosis however is synchronous and coincides with

simultaneous assembly of daughter cells (Figure4.2). In a yet another twist of the mechanism,

endopolygeny, parasites such as *Sarcocystis neurona* replicate their genome several times

resulting in a polyploid nucleus. Daughter cells then form at the surface of the mother cell,

coinciding with the last round of mitosis and karyokinesis that parcels the polyploid nucleus into

haploid nuclei to be packed into daughters.[56, 157] Apicomplexans can use more than one

form of division to adapt to the biology and size of their host cell as they move through their

complex multi-host lifecycles. For example, *T. gondii* divides by endodyogeny in the tissues of its

intermediate hosts but uses schizogony in the intestinal epithelium of the cat.[158] This suggests

overlapping regulatory mechanisms between different division modes that the parasites can

modulate to adapt to different niches.

While our focus here is on pathogen mechanisms of division we note that for some

species the host makes important contributions. *Theileria* lives free in the cytosol of host

leukocytes and subverts the host division machinery to aid its own propagation (Figure 4.2).

*Theileria* transforms leukocytes, immortalizing these cells and inducing continuous unchecked

proliferation very similar in appearance to a blood cancer like leukemia.[159]  Within these

transformed cells *Theileria* segregates into daughters upon host cell division by association with

the host centrosome. The parasite recruits host polo-like kinase 1, which controls centrosome

maturation and establishment of the mitotic spindle in the host to its surface to complete its

own division.[160] Other apicomplexans interact with the host cell centrosome but this appears

to mainly serve to prevent division of infected cells.[161, 162]

**REGULATION OF THE CELL CYCLE**

**Global Regulation of the Cell Cycle**

Progression through the cell cycle and its various checkpoints in mammalian cells is

controlled by a regulatory network of protein phosphorylation and protein degradation. Some

of the most important players in this complex network are the cyclin dependent kinases (CDKs)

and their regulatory cofactors the cyclins. The levels of individual cyclins change dramatically

along the cell cycle providing a clock mechanism. These cyclin waves are the result of changes in

cyclin transcription and even more importantly of ubiquitin mediated protein degradation.[163-

165] The Skip-Cullin-Fbox complex and the anaphase promoting complex (APC) are two

important degradation complexes responsible for irreversible transitions between stages of the

cell cycle.[166] Cyclin-CDK activity is further modulated by activating and inhibitory kinases as

well as cyclin-binding proteins.[164]

**Global Control by Kinases**

Three main types of cyclin-CDK pairs have been identified in mammalian cells. G1

Cyclins-CDKs control the entry into S phase by phosphorylating transcription factors required for

transcription of the DNA replication machinery.[167] S phase cyclins-CDKs pairs are synthesized

in late G1, and control events of the DNA replication process during S phase. Mitotic cyclin-CDKs

phosphorylate and activate microtubule-attachment proteins, kinetochore proteins and

additional kinases that initiate chromatin condensation and nuclear envelope breakdown. Other

kinases, such as NIMA (never in mitosis) participate in spindle assembly, spindle pole maturation

and nuclear import of cyclin-CDK complexes to the nucleus. The APC promotes mitotic exit by

phosphorylation of proteins in the mitotic spindle targeting them for degradation including

securin (which ensures sister chromatid cohesion) and Polo-like kinase.

Cyclins a variety of kinases and cell cycle specific transcription factors have been

described in Apicomplexa and these canonical regulators of cell cycle progression have been

recently reviewed. [168-170] Apicomplexan genomes encode a number of CDKs[168-170], and

homologs of the A/B family of cyclins, which can functionally complement cell cycle progression

mutants in yeast.[170] The specificity of cyclin-CDK pairing in apicomplexans, however, may

digress from what was observed in other eukaryotic cells, as the homolog of cyclin H of *T. gondii*,

which normally associates with CDK7 during division in yeast, is able to complement a *S.

cerevisiae* cyclin G1 mutant.[171] Mitotic CDK activators, such as CDC25 are not readily

identifiable in apicomplexans, in contrast, CDK inhibitors such as homologs of the CDK-inhibitory

kinase Wee1 have been noted.[170] NIMA kinases, required for completion of the cell cycle,

have been identified both in *T. gondii* [170] and in *P. falciparum.*[172] Homologs of components

of the APC have also been shown to operate in apicomplexans.[170]

**Global Transcriptional Control**

Microarray analysis in *P. falciparum* demonstrated that regulation of transcription

follows hardwired gene activation and silencing cascades as parasites transit through the

different stages (ring, trophozoites, and schizont) of their intracellular development in the red

blood cell. [173, 174] Genes are transcribed "as needed" within a relatively narrow window to

deliver proteins at the time they are used for the specific stage of the cell cycle. Temporal and

functional annotation has been derived from the analysis of expression clustering. In *T. gondii*

transcription can be clustered into two main waves, one transcribing genes for growth and

house-keeping functions during G1, and a second one coinciding with transition into S phase

that encodes proteins required for daughter assembly and invasion.[120, 175]

In *P. falciparum* and *T. gondii* the gene expression cascade is believed to be driven by a

cascade of Apetala2-type transcription factors (AP2). AP2s are transcription factors with well

defined DNA binding domains that were first described in plants.[176] Apicomplexa express AP2

homologs known as ApiAP2s which have been shown to bind DNA elements of co-regulated

genes exerting promoting as well as repressing effects.[120, 177-179] Tripping off the

transcription of each successive wave of ApiAP2s these factors could organize not only groups of

co-expressed genes but also script the self organized unfolding of developmental

progression[178]. In addition to transcription factors splicing factors like TgRRM1, were shown

to play critical roles in cell cycle progression.[180]

## LOCAL REGULATION OF CELL DIVISION

In parasites dividing by schizogony, cell division appears to follow a bi-modal scheme.

We will refer to this here as the growth and the budding phase. During the growth phase

multiple rounds of nuclear mitosis occur out of synchrony resulting in non-geometric expansion

(Figure4.3A). In the budding phase all nuclei of the schizont undergo a last, and importantly,

synchronous round of mitosis that coincides with the coordinated assembly of daughter cells.

Cyclins-CDKs and other factors that typically freely diffuse through the cytoplasm could

coordinate the events of the budding phase as all nuclei act in unison. However, the progression

of the first portion of the cell cycle is inconsistent with control mechanisms acting across the

entire cytoplasm as nuclei cycle independently from each other.[181] There appears to be

additional regulation that operates locally at the level of each nucleus.[148] We propose that the centrosome is the hub of this local control. Under this model regulatory proteins would be restrained in their reach to single nuclei by constraining the proteins to the centrosome. Furthermore, key structural components are physically tethered to the centrosome thus guiding the self assembly of new cells (see below).

**Centrosomes as Regulators of the Apicomplexan Cell Cycle**

Centrosome division marks the boundary between G1 and S phase both in mammalian cells and in Apicomplexa**.** Centrosome division in mammalian cells is controlled by regulatory kinases including Nek2, Aurora, and Cdk2, in *T. gondii* Nek1 was found to be required for centrosome duplication. Nek1 mutants show stalled centrosome replication and blocked parasite division[182],  Interestingly, they assemble a single daughter cell from their unduplicated centrosome.[183] A homolog of Aurora in *P. falciparum*, Pfark-1 localizes to paired dots which flank the mitotic spindle labeled with anti-$\alpha$-tubulin at the entry of M-phase. Pfark-1 likely co-localizes with the centrosome.[184] Importantly, this association is limited to a subset of nuclei within each schizont, consistent with the observed lack of synchrony of nuclear division in schizogony [184].

**Apicomplexan Mitosis and Centromere Clustering**

Apicomplexa divide their nuclei by closed mitosis.[25, 185, 186] Centrosome duplication is followed by the formation of short mitotic spindles. In *Plasmodium*, centriolar plaques associate with a pore of the nuclear membrane, duplicate, and move to opposite sides of the nucleus to give rise to a complete spindle. [146, 154, 187] Similarly, in *T. gondii*, an intranuclear spindle separates the centrosomes. This spindle forms within a funnel-like invagination of the nuclear envelope, breaks into two hemi-spindles that penetrate through pores in the nuclear

envelope to contact the kinetochores (Figure 4.5). As a result kinetochore microtubules are housed within a conical structure of the nuclear envelope, known as the centrocone. The exact function of this structure is not known but it may help to confine regulatory factors. Well defined centrocones are found in coccidian Apicomplexa such as *Toxoplasma gondii, Sarcocystis neurona* and *Eimeria spp*.[36, 37] In *Sarcocystis*, spindles can be observed throughout the intracellular development of this parasite, suggesting that the mitotic spindle persists for the entire cell cycle in these species or that G1 is extremely short resulting in the appearance of an essentially constant S and M phase.[56]

Mitosis has been difficult to observe and analyze in Apicomplexa due to a shortage of molecular markers and the lack of appreciable DNA condensation of apicomplexan mitotic chromosomes. During mitosis the spindle engages each chromosome by attachment to a microtubule. This attachment is facilitated by a large protein complex, the kinetochore, which assembles at a single site of the chromosome know as the centromere. Centromeres are marked by unique chromatin composition. In eukaryotes DNA is wound onto nucleosomes and centromeric nucleosomes are defined by the presence of specialized variant of histone H3, known as CenH3 or CenPA. A *T. gondii* strain bearing an epitope tag in CenH3 [60] now allows to follow chromosome segregation and to identify key mitotic phases. This marker also revealed that the centromeres of the fourteen *Toxoplasma* chromosomes cluster in one spot in the periphery of the nucleus (Figure 4.5). Moreover, this cluster is not only present during mitosis but maintained throughout the cell cycle, and its position remains close to the centrosome. In *P. falciparum* centromeres are similarly clustered and also show constant association with the centrosome.[64] This suggests that centromeres are physically tethered to the centrosome. The mechanism of tethering is not fully understood [60]

We hypothesize that the physical tethering of centromeres provides the short spindle microtubules ready access to kinetochores during division in a crowded nucleus filled with uncondensed chromatin.[60] It may also establish a nuclear sub-compartment in which DNA replication and condensation of the centromeres may be regulated differentially from the bulk of the chromatin due to intimate proximity to regulatory factors associated with the centrosome. Lastly, hanging on to the centromeres at all times ensures that parasites preserve a full complement of chromosomes even when using complex division modes that include polyploid nuclei. We propose centromere clustering to depend on interaction with the nuclear envelope rather than spindle microtubules (Figure 4.5), but this has not been formally demonstrated.

## SPATIAL ORGANIZATION OF CHROMATIN DURING THE CELL CYCLE

### Centromere Organization

Centromeres in *Toxoplasma* have an average size of 16 kb and appear to lack obvious primary sequence features like repeats, but the annotation of these particular segments may be incomplete.[60] *P. falciparum* centromeres are limited to 4-4.5 kb regions, encompassing a 2-2.5 kb AT and repeat rich core.[64, 188] In *P. berghei* centromeres are 6-12 kb and show no obvious sequence features.[64, 189] Identification of *Plasmodium* centromeres allowed the construction of artificial chromosomes, which segregate faithfully through cell division and have served as tools for the genetic manipulation of *P. berghei, yoelli and falciparum.* [189, 190]

The spatial organization of chromatin in the nucleus is intimately linked to the state of chromatin condensation and the presence of various histone variants and histone post-translational modification. Such epigenetic marks can alter chromatin structure and localization and thus effect differential gene expression and other specialized functions [191-194]. Overall

there are significant epigenomic differences between Apicomplexa and their mammalian hosts. Apicomplexan appear to lack DNA methylation and double stranded RNA interference[195, 196] and exhibit unique histone variants.[197] In this context we note that regions flanking the centromeres of *Toxoplasma* are characterized by the abundance of epigenetic markers associated with gene silencing (H3K9me2 and H3K9me3) and are devoid of activating marks associated with promoter activity (H3K4me3 and H3K9Ac).[60, 73] These epigenetic marks may not only influence transcription, but may also have important roles in defining the centromeres and influence their dynamic interactions with the nuclear envelope as the parasites move through the cell cycle. Curiously in *P. falciparum,* centromeres seem not to be flanked by heterochromatin but instead, are enriched for the histone H2 variant PfH2A.Z.[64, 192, 198] Homologs of the yeast Heterochromatin Protein 1 which binds H3 di and tri methylated chromatin at the centromere and the telomere were identified in *T. gondii* and *P. falciparum.* [73, 198] Consistent with the distinct heterochromatic environment in these parasites, TgChromo1 was shown to bind regions flanking the centromeres, whereas PfHP1 was not found near the centromeres. [73, 198] Both TgChromo1 and PfHP1 localize to sub-telomeric and telomeric regions of the chromosomes.[73, 198]

**Telomeres: Clustering and Repositioning**

Centromeres are not the only chromosomal domains with specific nuclear localization in apicomplexans. Telomeres are clustered into multiple foci at the nuclear periphery [73, 199] and in *P. falciparum* this clustering is used to silence virulence genes, in particular the *var* gene family, which are localized in the sub-telomeric regions. Apicomplexans are haploid for most of their life cycle; gamete fusion is immediately followed by meiosis in a division process known as

sporogony. During the meiotic division of *Eimeria tenella,* telomeres cluster in a specific region of the nuclear periphery.[200] Telomeres are arranged into multiple discrete clusters and interact with the inner nuclear membrane via an attachment plaque. The functional consequence of this arrangement could be an increase in the frequency of recombination due to the physical proximity of telomeres.[200] Clustering of telomeres is also seen in *Plasmodium* throughout the cell cycle, and thought to be linked to the very high rate of recombination between *var* genes, thus increasing population wide immune evasion through diversification of *var* gene products, which are important targets of the host immune response.[201, 202]

**Maintenance of the Nuclear Organization during the Cell Cycle**

Chromatin binding factors are obvious candidates to participate in the higher order organization of the nucleus in Apicomplexa. A steadily increasing number of parasite proteins that bind DNA, histones, or modified histones is emerging from bioinformatic [194, 203] and proteomic [204] screens for nuclear proteins, largely in *Plasmodium* and further functional analysis will likely lead to an understanding of their individual contributions to nuclear architecture. In addition to chromatin, the nuclear cytoskeleton and envelope probably play a role in defining specific regions of the nucleus. A mutation in the nuclear actin ARP4 leads to temperature sensitivity, abnormal nuclear division and chromosome missegregation in *T. gondii* (homologs are found in all Apicomplexa). [67] Antibodies raised against human lamin, a structural protein important for providing physical support to the inner nuclear membrane, label the nuclear envelope of *E. tenella* during meiosis.[200] Lamin homologs, however, are not readily identifiable by similarity searches in the genomes of Apicomplexa. Intriguingly, changes in the distribution of nuclear pores on the nuclear envelope occur concurrently with chromatin re-organization and changes in gene expression during the intracellular development of

115

*Plasmodium falciparum*.[93] Redistribution of nuclear pore complex during the replicative cycle of *Plasmodium* is also important for the proper segregation of pre-formed nuclear pore complexes to the daughter nuclei.[93]

## DAUGHTER CELL ASSEMBLY

Mitosis in mammalian cells is followed by cytokinesis, the actual cell division. In this process the body of the cell is split into two by a constrictive ring that typically forms at the midpoint of the spindle ensuring that each daughter cell inherits a nucleus (Figure 4.1). In apicomplexans cytokinesis occurs through budding and may split the mother cell in many more than two cells.

### Initiation of Cytokinesis

Daughter cells begin to assemble early after centrosome duplication and separation, coinciding with the start of S phase.[57, 58] Apicomplexan cytokinesis thus initiates well before mitosis is completed reflecting the complexity of the assembly process and the time required to accomplish the task. New cells are built on a polarized microtubule scaffold that is further elaborated with cytoskeletal and membrane components; this architecture is conserved throughout apicomplexans. The apex of the daughter is defined by the apical polar ring (APR), which acts as the MTOC for the microtubule scaffold that ultimately spans much of the length of the parasite (Figure 4.4E). [26, 27, 47, 205, 206] A recent study in *T. gondii,* identified RNG1, a proline-rich protein as the first molecular marker for the APR.[29] RNG1 is the first molecular marker of the APR described, but is not found in all apicomplexans. While RNG1 was found to be essential for parasite replication it only associates with the APR late in budding.[29] Comparative genome mining identified two additional APR components.[207] Unlike RNG1, these proteins appear very early during division. [207]   In addition to the apical ring, a subgroup

of apicomplexans known as coccidians (*Toxoplasma, Eimeria* and *Sarcocystis*) also possess a conoid (Figure 4.4D and E)[27, 31] a cylinder of atypical tubulin filaments capped by two pre-conoidal rings.[27, 47, 206] The conoid is a highly motile structure, able to extend and retract from its position in the apical end of the parasite in a calcium-dependent manner. Though its function has not been directly demonstrated, a role in invasion is frequently ascribed to this structure, as it extrudes prior to and during host cell invasion

Daughter cell assembly initiates in close physical proximity to the centrosome.[32, 55] Recent work in *T. gondii* revealed that the daughters are physically linked to the centrosome by a fiber. This fiber is made up of two homologs of the algal striated fiber assemblin (SFA) protein and grows out from the centrosome immediately following its duplication (Figure 4.4F).[30] *Chlamydomonas* SFA was shown to self-organize into polar fibers in vitro in a way that resembles actin polymerization.[135] Assembly of the SFA fiber at the centrosome precedes and is required for initiation of the daughter cell MTOC and the subsequent deposition of cytoskeletal and membrane components.  The SFA fiber is curved upon itself at the distal end, and it is tempting to speculate that this curvature may serve as a template for the ring shaped MTOC. SFA homologs are found in all apicomplexans. See Figure 4.7 for the evolution of the SFA fiber from algal ancestry to parasite present.

**Formation of the Inner Membrane Complex**

The microtubule scaffold of the budding daughter cell is further elaborated by flattened membrane sacks, known as alveoli or inner membrane complex (IMC), that are linked to each other by skeletal elements that form lattices, seams and membrane anchors.[38, 42] The plasma membrane is the outermost component of this layered assembly and acquired from the mother cell during cytokinesis.[55, 170]  The complete assembly is often referred to as pellicle.  The IMC

is linked to the sub-pellicular microtubules, anchors the gliding motility machinery[38-40], and tethers organelles to the pellicle.[41] Many of the IMC proteins are broadly conserved among Alveolata well beyond apicomplexan parasites.[208-212] The IMC is fascinating in that its proteins assemble in a temporally and spatially defined pattern and sequence during daughter cell formation. IMC proteins are expressed in a cell cycle dependent "just-in-time" fashion at exactly the time they are required for assembly. They take spatial clues from the microtubular scaffold of the forming daughter and interference with the MTOC or inhibition of microtubule polymerization largely blocks IMC assembly.[63] Furthermore they show hierarchical assembly in which deposition of 'early' proteins appears to guide the recruitment of 'late' factors.[43, 44, 48] IMC sub-compartment proteins (ISPs) separate specific domains within the IMC network and determine their boundaries.[43, 44] The specific functions of IMC sub-compartments are not well understood. However, a deletion mutant of the *Toxoplasma gondii* ISP2 protein shows defects in daughter cell assembly, suggesting that ISP proteins may not only have structural roles but also might participate in regulating aspects of division. [43, 44] As the daughter pellicle matures IMC proteins experience proteolytic modification. [59, 213]  Some of these modifications likely rigidify the structure or distinguish daughter from mother pellicle, thus helping to selectively disassemble the mother's pellicle and allowing the daughters to emerge. Posttranslational modification in the form of acylation is critical to spatial recruitment of IMC proteins. [43-45, 214] The specificity of this process is not fully understood, but likely involves compartment specific acyl-transferases[45] (see below).

Both the apical and the basal end of the IMC are capped, and feature a specialized set of proteins. The basal complex has received particular attention for its active role in budding, organelle division and cytokinesis. [32, 70] Morn1 is the best characterized component of the basal complex, but also found at various other sites in which the IMC or the nuclear envelope is

118

interrupted by an opening.  [37, 182, 215] The protein carries numerous membrane organization

recognition nexus (MORN) repeats, which in other eukaryotes enable protein-protein and

protein-membrane interactions. In mature parasites, Morn1 forms rings at the apex and base of

the cell. During division, daughter Morn1 rings assemble early and in close proximity of each

centrosome. [37, 122] As division moves forward, the rings move to the posterior driven by

microtubule polymerization, and then constrict at the end of the budding process.[37] Myosin

B/C [37]  and centrin2 [70]  have been shown to co-localize with Morn1 in this process and are

candidate motors to drive the constriction. Consistent with an important role in basal complex

organization, conditional mutants in Morn1 show incomplete abscission of daughters, multi-

headed cells, and poor growth. [215] However, null mutants have been obtained using Cre-lox

technology, suggesting that loss can be compensated for.[216] In *Plasmodium* Morn1 is

expressed in late schizonts during the budding cycle and localizes to the basal end of the

emerging daughter cell. Morn1 is prominently detected in male gametes suggesting an

additional role in sexual development.[182]   The localization and timing of expression of the

multiple pellicle proteins involved in daughter cell assembly of *T. gondii* have been recently

reviewed .[46]

**Loading Daughter Cells with the Invasion Machinery**

Apicomplexans use a battery of secretory organelles, including rhoptries, micronemes

and dense granules, to invade their various host cells. [217] These organelles are assembled de

novo and positioned within each daughter cell.[28, 55, 150, 218] Their assembly is aided by the

highly polarized organization of the apicomplexan secretory pathway. Proteins flow from the ER

to the nuclear envelope, to the Golgi apparatus, and to precursors of mature rhoptries and

micronemes. [219, 220] Importantly, the ER-exit site is confined to a small region of the nuclear

envelope close to the centrosome [221] (Figure 4.4A). The Golgi, which faces the exit site, also

shows close association with the centrosome. Coinciding with mitosis both ER-exit site and Golgi

divide by lateral extension and fission (for the Golgi). As a consequence both organelles localize

within the confines of the forming daughter from the beginning. The IMC, which demarks the

daughter is thought to actually be derived from the Golgi.[222]

To fully arm the invasion machinery secretory organelles, such as the rhoptries and

micronemes, need to associate with the apical complex at the apical tip of the parasite, through

which they deliver their contents. This is thought to depend on cytoskeletal elements that act as

tracks for molecular motors that carry secretory organelles to the apex during daughter cell

assembly and likely also replace or replenish organelles that have been discharged during gliding

and invasion in mature parasites. Several candidates are under consideration; two microtubules,

the central pair, extend from the apical tip into the bulk of the cell and molecular markers

distinguishing this structure are now available.[223]  Super-resolution microscopy of

micronemes reveals a pattern that is reminiscent of subpellicular microtubules[33]  and the

striated fiber has been proposed to act as a similar track for rhoptries in *P. berghei* based on

electron microscopy.[140] Most recently, genetic studies tie rhoptry tethering to actin/myosin.

An Armadillo Repeats-Only (ARO) protein was identified on the surface of rhoptries in *T. gondii*

and *P. falciparum,* this protein interacts with the motor myosin F. [224] Interference with ARO

or actin polymerization leads to scattering of rhoptries throughout the cytoplasm and impairs

invasion. [224] [34, 45] ARO is synthesized as a soluble protein and recruited to the rhoptry

membrane by acylation. This organelle-specific recruitment depends on the rhoptry localized

palmitoyl-transferase TgDHHC7.[34, 45, 224] Overall organelle specific acyl-transferases emerge

as a major principle of apicomplexan self assembly for a variety of membranous organelles. The

acyltransferase is targeted to the organelle via the secretory pathway and subsequently recruits

additional factors from the cytoplasm[34]. We do not understand the mechanistic basis for the

specificity of the process. Compartment-specific palmitoyl-transferases have been identified

both in *T. gondii* and *P. berghei* [45], but how do these enzymes recognize and distinguish their

targets? One possibility may be that acylation affirms and finalizes the initial contact established

through protein-protein interaction between other factors (Figure 4.6B).

**Inheritance of Symbiont Organelles**

In addition to a mitochondrion most Apicomplexa also harbor an apicoplast[11], a

descendent of a red algal endosymbiont (see Figure 4.7). While photosynthesis was lost, the

apicoplast still provides essential metabolites to the parasite. Most of the apicoplast genes were

horizontally transferred to the nucleus, but the organelle maintains a 35 kb genome. The

mechanisms that govern apicoplast biogenesis and division are a direct reflection of the complex

ancestry of the various compartments of the organelle[11]. The apicoplast genome is localized

at the lumen and maintained and replicated by proteins of bacterial origin [225-227] In contrast,

apicoplast segregation and fission depends on mechanisms contributed by the host. The plastid

is segregated into individual daughter cells by association with the centrosome. [25, 56, 115,

116, 228, 229] Division of the organelle occurs in two steps. The basal complex produces an

initial constriction, which then recruits a specialized dynamin-related protein to the site

resulting in apicoplast fission.[37, 215, 230] Mitochondrial division is not well understood in

apicomplexans. Segregation of the mitochondria occurs late during division, the organelle is

highly motile and appears to invade daughters right before the completion of budding.[150]

**FUTURE DIRECTIONS**

The intracellular development of apicomplexan parasites is remarkably hardwired and

occurs in predictable waves of co-expression and self-assembly. Individual components and

compartments of the parasite cell are linked by physical tethers that stage and guide the

assembly process. All components are directly or indirectly wired to the centrosome, which has

emerged as the true master of proceedings. Not only are key elements of the new cell directly

linked to centrosome, but so are regulatory proteins, and experimental manipulations that lead

to a loss or disorganization of centrosome produce a catastrophic breakdown of the

apicomplexan cell cycle. While we have made considerable progress in unraveling the molecular

components and function of the various cellular structures, our knowledge of how they are

regulated is still limited. Key to progress will be a detailed understanding of the centrosome and

its direct nuclear and cytoplasmic vicinity. What are the centrosome-associated master

regulators, how are they recruited to this compartment, and how are they turned over during

cell cycle progression? This is similarly true for the physical tethers that tie organelles to the

centrosome. Another central task will be to test and flesh out the phased cell cycle model. Most

importantly, how does the handover from local to global control occur, and how is this

coordinated in the different division modes?  So far much of what we know is based on *T. gondii*

taking advantage of the excellent genetics and microscopy offered by this model. Significant

technical advances in light microscopic resolution as well a conditional mutagenesis protocols

for different *Plasmodium* species should allow us to broaden the scope, which will be of

particular interest with respect to cell cycle control. Nuclear organization is obviously critical for

many of the phenomena discussed here, but how this organization is preserved during mitosis

and inherited by the daughters is unclear. Finally, while we have focused on the rigidity and

predictability of the process here, there has to be some flexibility and adaptation to changes in

the host cell and along the developmental lifecycle. We do not understand the mechanisms

used by the parasite to sense and to respond to such changes.

A deeper understanding of the intracellular development of the parasites also

potentially opens the door to new therapeutics. Drugs that interfere with the structural and

regulatory components of mammalian cell division are mainstays of cancer and immunosuppressive therapy. They should provide a similarly rich source of targets in apicomplexan parasites that has not been fully explored yet. The pronounced differences in the mammalian and apicomplexan division machinery may help in the identification of parasite specific compounds.

## ACKNOWLEDGEMENTS
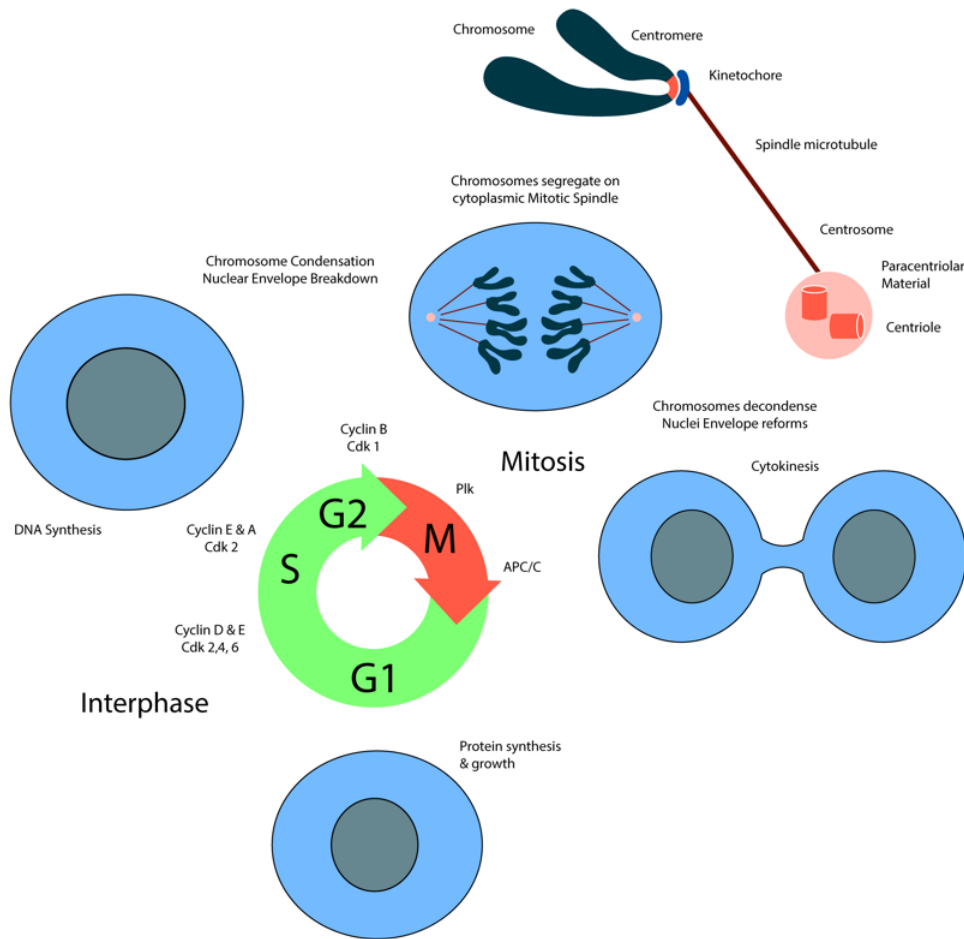
**Figure 4.1. The Mammalian Cell Cycle: Stages and Control.** The mammalian cell cycle

consists of four distinct phases known as G1, G2, S and M. G1, or interphase lasts for 9 hours in

human cells and it is the non-dividing stage of the cell cycle in which the cell "prepares" for

division. During G1 RNA and proteins are synthesized and the cell grows in size. During S phase,

chromosome replication occurs. In human cells, this phase lasts for 10 hours. G2 follows S

phase. During G2, the "second gap," checkpoints ensuring the proper replication of

chromosomes stall the cell cycle until the cell is ready to enter mitosis. Mitosis in human cells

occurs rapidly, in just about 30 minutes. M phase can be further divided into prophase,

metaphase, anaphase and telophase. Prophase marks the entry into mitosis. In mammalian

cells, chromosomes condense, the nuclear envelope retracts into the endoplasmic reticulum,

and the Golgi breaks down into vesicles. The mitotic spindle, nucleated by the centrosome,

starts forming. During metaphase, kinetochore components assemble onto the centromeric

regions of chromosomes and associate with microtubules of the mitotic spindle. Chromosomes

align. Anaphase is marked by the separation of sister chromatids, pulled apart by motor proteins

and the dynamics of the mitotic spindle. Telophase is the last stage of mitosis in which the cell

resumes division and goes back to normal; the mitotic spindle disassembles, chromosomes

decondense, and the nuclear envelope reforms. Division ends at the onset of cytokinesis, which

occurs concurrently with reformation of the Golgi in each daughter cell.
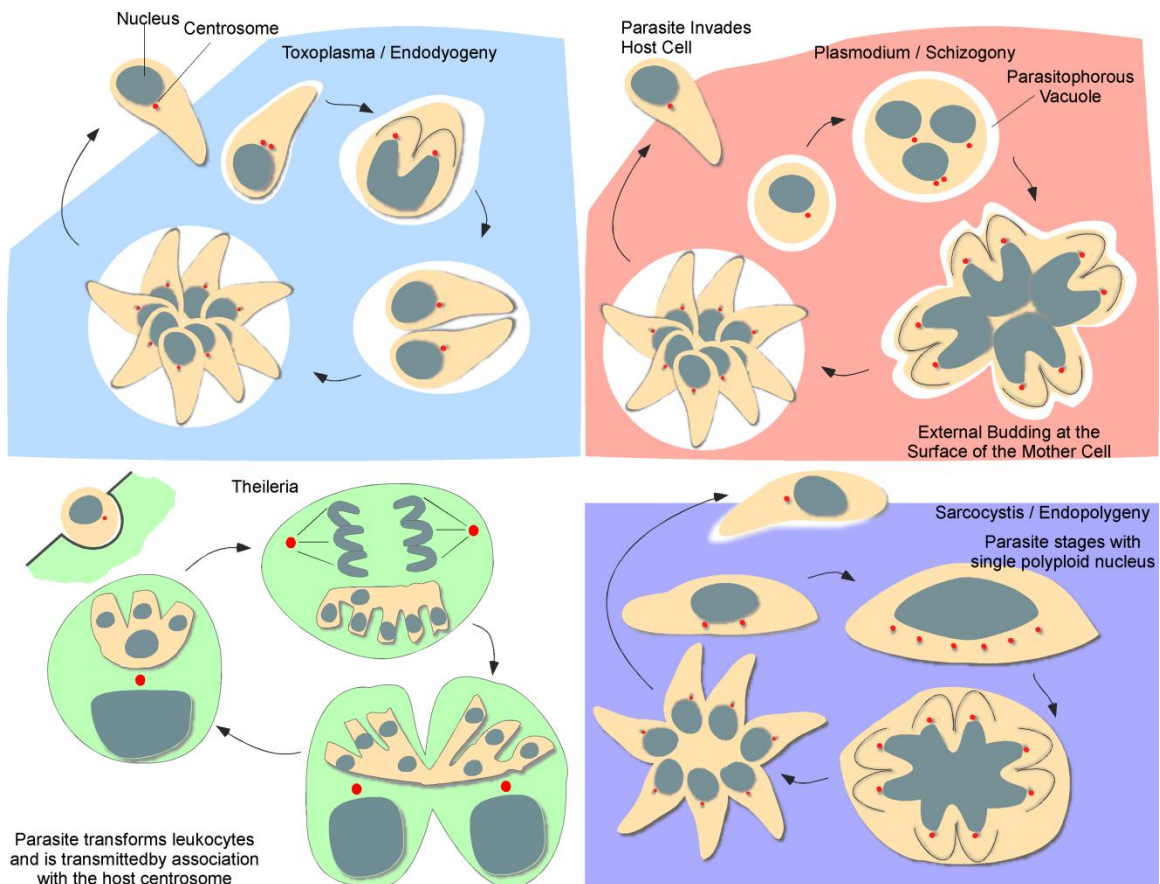
**Figure 4.2. Replication Cycles of Different Apicomplexan Species. A.** *T. gondii* replicates by endodyogeny. Each DNA replication cycle is followed by mitosis and budding. **B.** *Plasmodium* infects red blood cells and divides by schizogony. Initial nuclei multiply by asynchronous rounds of mitosis. The last round is synchronous for all nuclei and coincides with budding at the parasite surface. **C.** *Theileria* sporozoites infect leukocytes following the bite of an infected tick. The parasite transforms the leukocytes and divides exploiting the host's mitotic and cytokinetic machinery. **D.** *Sarcocystis* replicates DNA without nuclear division using multiple synchronous mitotic spindles. The final mitotic cycle coincides with budding and emergence of a new generation of merozoites (endopolygeny). Note that *Toxoplasma* and *Plasmodium* replicate with a parasitophorous vacuole while *Theileria* and *Sarcocystis* are free in the host cell cytoplasm.
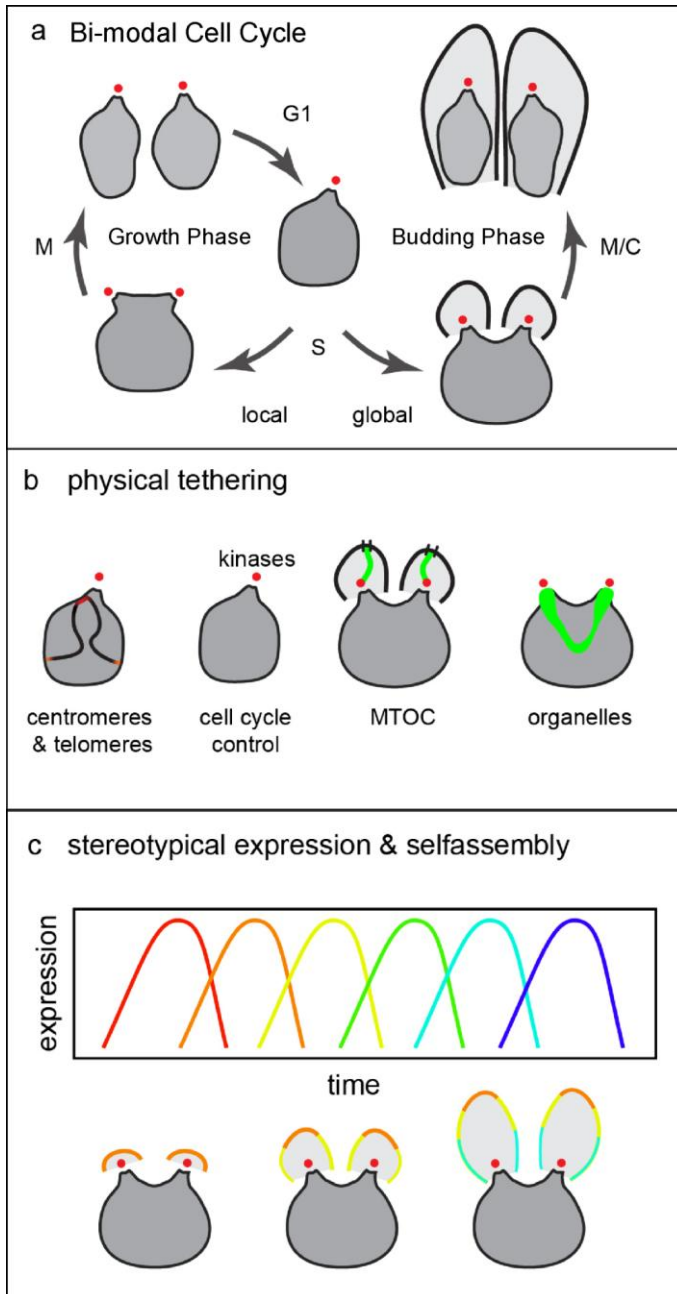
**Figure 4.3. Organizational Principles of Apicomplexan Replication. A.** Apicomplexa exhibit

remarkable cell cycle flexibility. Conceptually their various division modes can be unified using a

two-phase model (exemplified here for schizogony). This bi-modal scheme of division consists of

a "growth" phase and a "budding" phase. During the growth phase the parasite amplifies the

copy number of its genome through successive rounds of DNA replication and mitosis (S/M/G1).

Cell cycle control appears to rest with individual nuclei. The budding phase is synchronous and combines mitosis and cytokinesis (M/C). **B.** Numerous structural and regulatory elements of the apicomplexan cell are physically linked during replication and daughter assembly. Most of these tethers tie directly or indirectly to the centrosome. **C.** Cell cycle progression and budding is orchestrated by a gene expression cascade regulated largely at the transcriptional level. Budding includes numerous elements of self-assembly and self-organization.
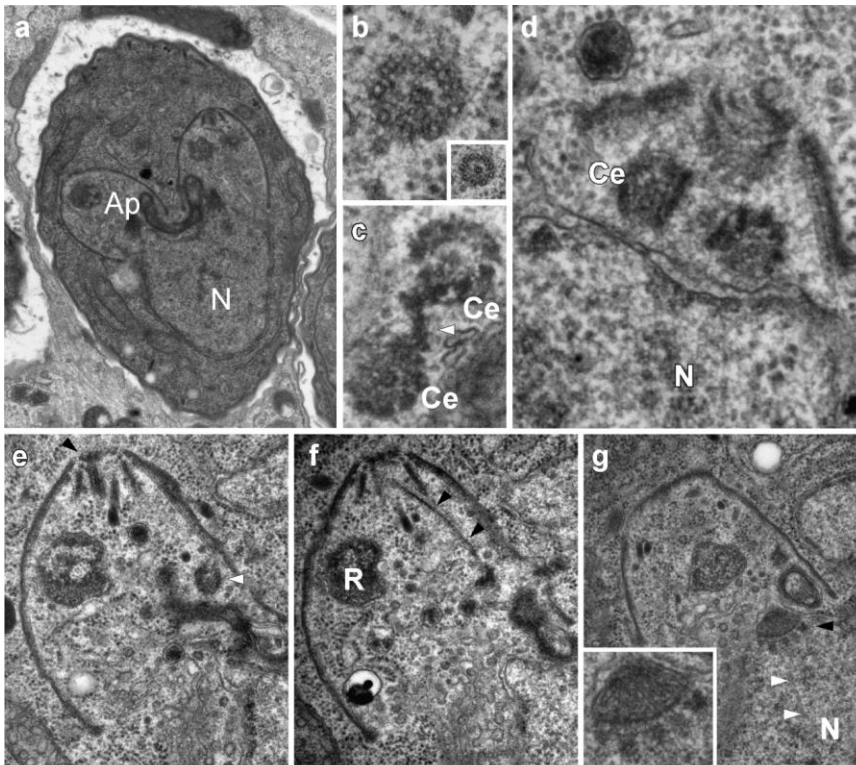


**Figure 4.4. Electron microscopic detail of mitosis and budding in *T. gondii*. A.** Endodyogeny in T. gondii. Note that nucleus (N) and apicoplast (Ap) co-segregate into daughters. ER exit site and Golgi apparatus are contained within the bud. **B**. The *T. gondii* centriole has 9 + 1 singlet symmetry. Inset shows an outline for the position of each microtubule of the centriole. **C.** Mother and daughter centriole (Ce) are physically linked by a v-shaped structure (white arrowhead). **D.** An emerging daughter cell assembles in the proximity of the centrosome (Ce).

Two parallel centrioles can be seen **E-G.** Three micrographs from a serially sectioned series

through a daughter cell highlighting different aspects of budding. **E.** Apicomplexan cells have

two MTOCs, the centrosome (white arrowhead) and the apical ring (black arrowhead). **F.** The

apical MTOC is coordinated with the centrosome through the striated fiber (black arrowheads).

Secretory organelles form within the daughter de novo (R, rhopty precursor). **G.** The

centrosomes of chromosomes (black arrowhead) are tethered to a specialized portion of the

nuclear envelope, the centrocone. Inset shows the centrocone enlarged. Microtubules

penetrate deep into the nucleus (white arrowheads).
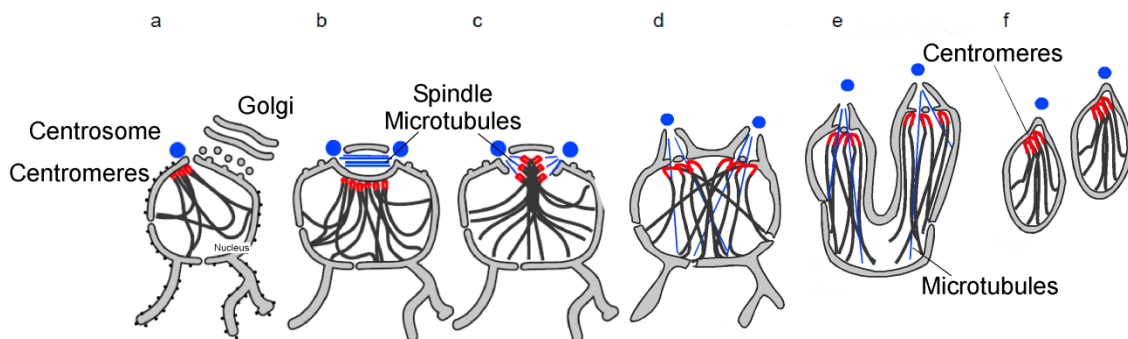


**Figure 4.5. Apicomplexa Divide by Closed Mitosis**. **a.** The interphase nucleus of apicomplexans

is highly organized and the centrosome (blue) is the reference point for this organization. Within

the nucleus the centromeres (red) are clustered and tethered to an opening in the nuclear

envelope that is in close proximity to the centrosome. Telomeres also have been found to

cluster and this may occur close to nuclear pores. Note that the ER-exit is a specialized region of

the nuclear envelope opposing the centromere cluster. **B.** The mitotic spindle is intranuclear

within a tunnel formed by the envelope. **C.** Progressive perforation of this tunnel allows

interaction of centromeres and kinetochore microtubules followed by metaphase and anaphase.

**D-F.** Two centrocones form at each centrosome. The centrosomes reengage the nuclear

envelope and spindle microtubules penetrate deep into the nucleus pushing the nucleus into

two lobes that undergo fission. Note that centromere tethering persists with the brief

intermission of microtubule interaction during mitosis.
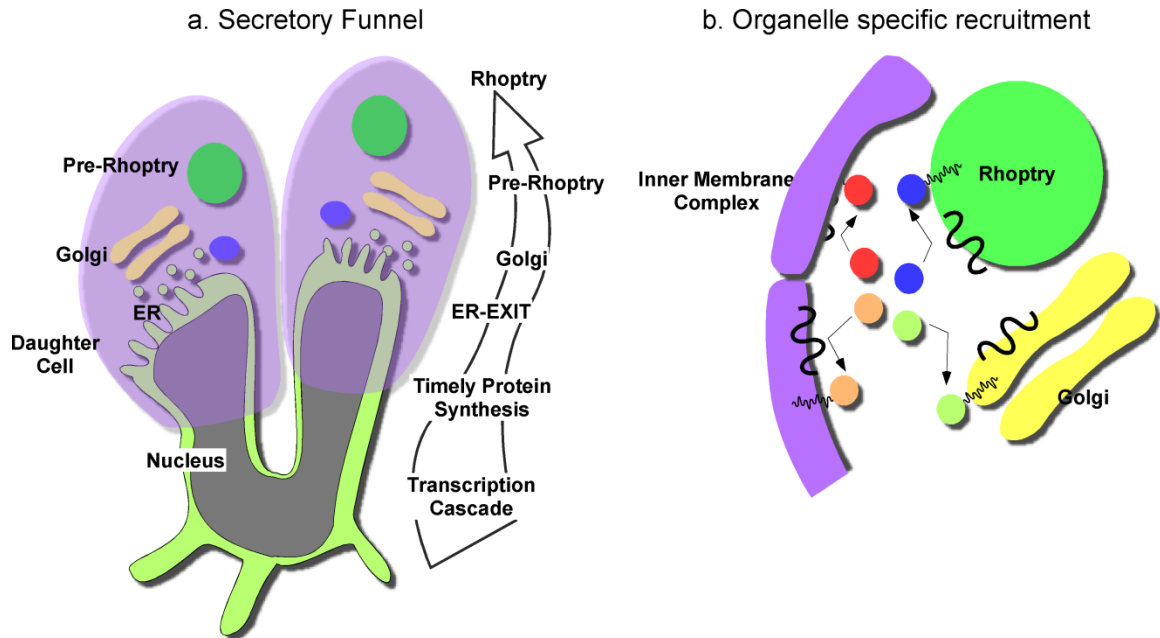


**Figure 4.6. Organization of Parasite Budding. A.** A number of membranous organelles are

formed de novo during budding including the inner membrane complex, rhoptries and

micronemes. The secretory pathway is highly polarized and key elements are tethered to the

centrosome. This organization gives rise to an effective secretory funnel targeting proteins and

membranes directly into the newly forming daughter cells. **B.** Apicomplexa use several elements

of recruitment and self-organization to assemble daughters. A battery of organelle specific

palmitoyl-transferases recruits cytoplasmic proteins to different compartments by tethering

them to the membrane through fatty acylation.

Auxotroph
Flagellate

Secondary
Endosymbiont

Red Alga

Free-living Photoshynthetic
Chromalveolate

**Striated Fiber Organizes Flagella**

Flagellum

Basal Body

Striated
Fiber

Rootlet Microtubules
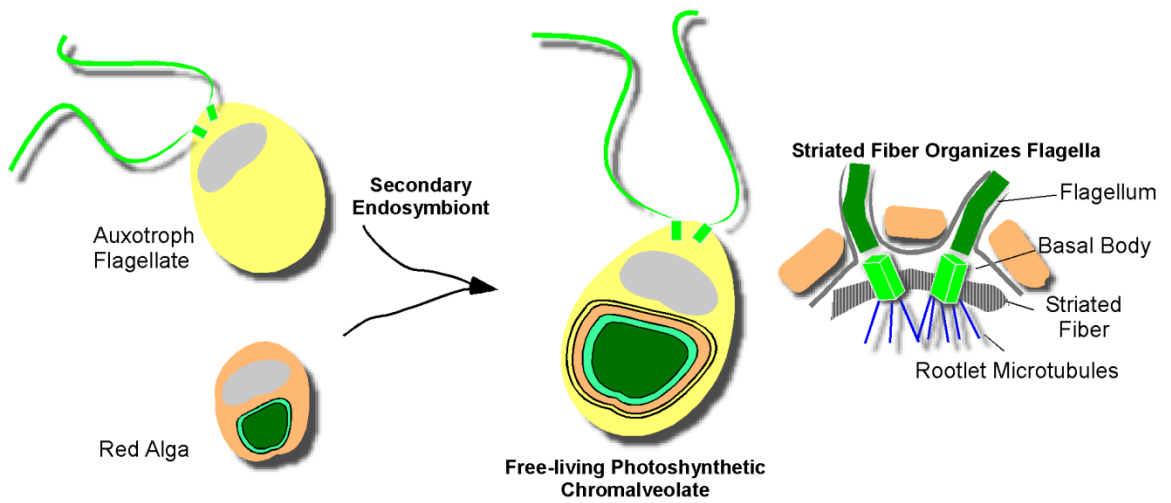
**Adaptation of Algal Structures
to Parasitism**

Striated Fiber Coordinates
Budding by placing the MTOC

Apical MTOC places
invasion machinery

IMC

MT

Pellicle Anchors
Gliding Motor

Symbiosis + Parasitism

Secretion + Gliding
Intracellular Parasitism

131
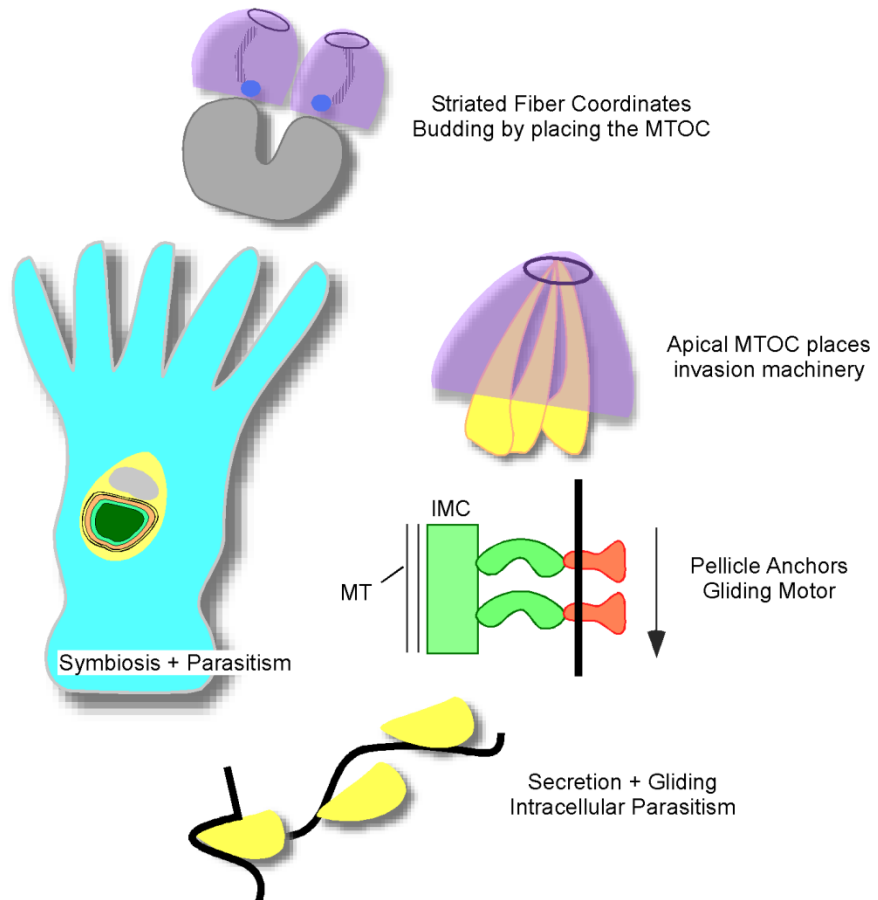
**Figure 4.7. Apicomplexa adapted the principles of flagellum organization of the algal ancestor to organize the assembly of invasive stages.** Apicomplexans belong to the super phylum Chromalveolata, a very large and diverse branch of the eukaryotic tree of life. This group of organisms arose from an endosymbiosis event between an auxotrophic flagellate and a red alga. In flagellated free-living algae, such as Chlamydomonas, the basal bodies of the flagella are coordinated with each other and the remainder of the cell by the flagellar rootlet, an assembly of microtubules and associated structures including the striated fiber. The striated fiber also plays a role in algal mitosis, flagella are resorbed during division and the basal bodies act as centrosomes. Apicomplexa developed an early and intimate parasitic relationship with animals, which probably pre-dates the main diversification of animals. Apicomplexa retooled the striated fiber to organize and place the apical MTOC of the invasive stage. This MTOC places apical secretory organelles and organizes a polarized pellicle which anchors the myosin motor of the gliding apparatus (note that glideosome is shown highly simplified here). Both the gliding machinery and the secretory organelles cooperate in motility and host cell invasion.

REFERENCES

1.  Burke-Gaffney, H.J., *Malaria.* Trop Dis Bull, 1964. **61**: p. 329-53.
2.  Dubey, J.P., et al., *A review of Sarcocystis neurona and equine protozoal myeloencephalitis (EPM).* Vet Parasitol, 2001. **95**(2-4): p. 89-131.
3.  Levine, N.D., *Coccidiosis.* Annu Rev Microbiol, 1963. **17**: p. 179-98.
4.  Dobbelaere, D. and V. Heussler, *Transformation of leukocytes by Theileria parva and T. annulata.* Annu Rev Microbiol, 1999. **53**: p. 1-42.
5.  Chaussepied, M. and G. Langsley, *Theileria transformation of bovine leukocytes: a parasite model for the study of lymphoproliferation.* Res Immunol, 1996. **147**(3): p. 127-38.
6.  Montoya, J.G. and O. Liesenfeld, *Toxoplasmosis.* Lancet, 2004. **363**(9425): p. 1965-76.
7.  Miller, C.M., et al., *The immunobiology of the innate response to Toxoplasma gondii.* Int J Parasitol, 2009. **39**(1): p. 23-39.
8.  Kasper, L.H. and D. Buzoni-Gatel, *Some Opportunistic Parasitic Infections in AIDS: Candidiasis, Pneumocystosis, Cryptosporidiosis, Toxoplasmosis.* Parasitol Today, 1998. **14**(4): p. 150-6.
9.  Jones, J.L., et al., *Congenital toxoplasmosis: a review.* Obstet Gynecol Surv, 2001. **56**(5): p. 296-305.
10. Striepen, B., *The apicoplast: a red alga in human parasites.* Essays Biochem, 2011. **51**: p. 111-25.
11. Van Dooren, G.G. and B. Striepen, *The Algal Past and Parasite Present of the Apicoplast.* Annu Rev Microbiol, 2013. **67**.
12. Cavalier-Smith, T., *Archamoebae: the ancestral eukaryotes?* Biosystems, 1991. **25**(1-2): p. 25-38.
13. Levine, N.D., *Some corrections of coccidian (Apicomplexa: Protozoa) nomenclature.* J Parasitol, 1980. **66**(5): p. 830-4.
14. Levine, N.D., *Dorisa n. gen. (Protozoa, Apicomplexa, Eimeriidae).* J Parasitol, 1980. **66**(1): p. 11.
15. Levine, N.D., et al., *A newly revised classification of the protozoa.* J Protozool, 1980. **27**(1): p. 37-58.
16. Escalante, A.A., E. Barrio, and F.J. Ayala, *Evolutionary origin of human and primate malarias: evidence from the circumsporozoite protein gene.* Mol Biol Evol, 1995. **12**(4): p. 616-26.
17. Escalante, A.A. and F.J. Ayala, *Evolutionary origin of Plasmodium and other Apicomplexa based on rRNA genes.* Proc Natl Acad Sci U S A, 1995. **92**(13): p. 5793-7.
18. Gubbels, M.J. and M.T. Duraisingh, *Evolution of apicomplexan secretory organelles.* Int J Parasitol, 2012. **42**(12): p. 1071-81.
19. Hunter, C.A. and L.D. Sibley, *Modulation of innate immunity by Toxoplasma gondii virulence effectors.* Nat Rev Microbiol, 2012. **10**(11): p. 766-78.
20. Soldati, D., B.J. Foth, and A.F. Cowman, *Molecular and functional aspects of parasite invasion.* Trends Parasitol, 2004. **20**(12): p. 567-74.
21. Sibley, L.D., *Invasion and intracellular survival by protozoan parasites.* Immunol Rev, 2011. **240**(1): p. 72-91.

22. Black, M.W. and J.C. Boothroyd, *Lytic cycle of Toxoplasma gondii.* Microbiol Mol Biol Rev, 2000. **64**(3): p. 607-23.

23. Saeij, J.P., J.P. Boyle, and J.C. Boothroyd, *Differences among the three major strains of Toxoplasma gondii and their specific interactions with the infected host.* Trends Parasitol, 2005. **21**(10): p. 476-81.

24. Howe, D.K. and L.D. Sibley, *Toxoplasma gondii comprises three clonal lineages: correlation of parasite genotype with human disease.* J Infect Dis, 1995. **172**(6): p. 1561-6.

25. Striepen, B., et al., *Building the perfect parasite: cell division in apicomplexa.* PLoS Pathog, 2007. **3**(6): p. e78.

26. Russell, D.G. and R.G. Burns, *The polar ring of coccidian sporozoites: a unique microtubule-organizing centre.* J Cell Sci, 1984. **65**: p. 193-207.

27. D'Haese, J., H. Mehlhorn, and W. Peters, *Comparative electron microscope study of pellicular structures in coccidia (Sarcocystis, Besnoitia and Eimeria).* Int J Parasitol, 1977. **7**(6): p. 505-18.

28. Ogino, N. and C. Yoneda, *The fine structure and mode of division of Toxoplasma gondii.* Arch Ophthalmol, 1966. **75**(2): p. 218-27.

29. Tran, J.Q., et al., *RNG1 is a late marker of the apical polar ring in Toxoplasma gondii.* Cytoskeleton (Hoboken), 2010. **67**(9): p. 586-98.

30. Francia, M.E., et al., *Cell division in apicomplexan parasites is organized by a homolog of the striated rootlet fiber of algal flagella.* PLoS Biol, 2012. **10**(12): p. e1001444.

31. Hu, K., D.S. Roos, and J.M. Murray, *A novel polymer of tubulin forms the conoid of Toxoplasma gondii.* J Cell Biol, 2002. **156**(6): p. 1039-50.

32. Hu, K., et al., *Cytoskeletal components of an invasion machine--the apical complex of Toxoplasma gondii.* PLoS Pathog, 2006. **2**(2): p. e13.

33. Kremer, K., et al., *An overexpression screen of Toxoplasma gondii Rab-GTPases reveals distinct transport routes to the micronemes.* PLoS Pathog, 2013. **9**(3): p. e1003213.

34. Beck, J.R., et al., *A Toxoplasma Palmitoyl Acyl Transferase and the Palmitoylated Armadillo Repeat Protein TgARO Govern Apical Rhoptry Tethering and Reveal a Critical Role for the Rhoptries in Host Cell Invasion but Not Egress.* PLoS Pathog, 2013. **9**(2): p. e1003162.

35. Dubremetz, J.F., *L'ultrastructure du centriole et du centrocone chez la coccidie Eimeria necatrix. Étude au cours de la schizogonie.* Journal de Microscopie, 1971. **12**(3): p. 453-458.

36. Dubremetz, J.F., *[Ultrastructural study of schizogonic mitosis in the coccidian, Eimeria necatrix (Johnson 1930)].* J Ultrastruct Res, 1973. **42**(3): p. 354-76.

37. Gubbels, M.J., et al., *A MORN-repeat protein is a dynamic component of the Toxoplasma gondii cell division apparatus.* J Cell Sci, 2006. **119**(Pt 11): p. 2236-45.

38. Mann, T. and C. Beckers, *Characterization of the subpellicular network, a filamentous membrane skeletal component in the parasite Toxoplasma gondii.* Mol Biochem Parasitol, 2001. **115**(2): p. 257-68.

39. Gaskins, E., et al., *Identification of the membrane receptor of a class XIV myosin in Toxoplasma gondii.* J Cell Biol, 2004. **165**(3): p. 383-93.

40. Keeley, A. and D. Soldati, *The glideosome: a molecular machine powering motility and host-cell invasion by Apicomplexa.* Trends Cell Biol, 2004. **14**(10): p. 528-32.

41. Kudryashev, M., et al., *Positioning of large organelles by a membrane- associated cytoskeleton in Plasmodium sporozoites.* Cell Microbiol, 2010. **12**(3): p. 362-71.

42. Morrissette, N.S., J.M. Murray, and D.S. Roos, *Subpellicular microtubules associate with an intramembranous particle lattice in the protozoan parasite Toxoplasma gondii.* J Cell Sci, 1997. **110 ( Pt 1)**: p. 35-42.

43. Beck, J.R., et al., *A novel family of Toxoplasma IMC proteins displays a hierarchical organization and functions in coordinating parasite division.* PLoS Pathog, 2010. **6**(9): p. e1001094.

44. Fung, C., et al., *Toxoplasma ISP4 is a central IMC sub-compartment protein whose localization depends on palmitoylation but not myristoylation.* Mol Biochem Parasitol, 2012. **184**(2): p. 99-108.

45. Frenal, K., et al., *Global analysis of apicomplexan protein S-acyl transferases reveals an enzyme essential for invasion.* Traffic, 2013.

46. Anderson-White, B., et al., *Cytoskeleton assembly in Toxoplasma gondii cell division.* Int Rev Cell Mol Biol, 2012. **298**: p. 1-31.

47. Morrissette, N.S. and L.D. Sibley, *Cytoskeleton of apicomplexan parasites.* Microbiol Mol Biol Rev, 2002. **66**(1): p. 21-38; table of contents.

48. Anderson-White, B.R., et al., *A family of intermediate filament-like proteins is sequentially assembled into the cytoskeleton of Toxoplasma gondii.* Cell Microbiol, 2011. **13**(1): p. 18-31.

49. Dubey, J.P. and J.K. Frenkel, *Feline toxoplasmosis from acutely infected mice and the development of Toxoplasma cysts.* J Protozool, 1976. **23**(4): p. 537-46.

50. Aramini, J.J., C. Stephen, and J.P. Dubey, *Toxoplasma gondii in Vancouver Island cougars (Felis concolor vancouverensis): serology and oocyst shedding.* J Parasitol, 1998. **84**(2): p. 438-40.

51. Frenkel, J.K., A. Ruiz, and M. Chinchilla, *Soil survival of toxoplasma oocysts in Kansas and Costa Rica.* Am J Trop Med Hyg, 1975. **24**(3): p. 439-43.

52. Dubey, J.P., *Toxoplasma gondii oocyst survival under defined temperatures.* J Parasitol, 1998. **84**(4): p. 862-5.

53. Bohne, W., J. Heesemann, and U. Gross, *Induction of bradyzoite-specific Toxoplasma gondii antigens in gamma interferon-treated mouse macrophages.* Infect Immun, 1993. **61**(3): p. 1141-5.

54. Goldman, M., R.K. Carver, and A.J. Sulzer, *Reproduction of Toxoplasma gondii by internal budding.* J Parasitol, 1958. **44**(2): p. 161-71.

55. Sheffield, H.G. and M.L. Melton, *The fine structure and reproduction of Toxoplasma gondii.* J Parasitol, 1968. **54**(2): p. 209-26.

56. Vaishnava, S., et al., *Plastid segregation and cell division in the apicomplexan parasite Sarcocystis neurona.* J Cell Sci, 2005. **118**(Pt 15): p. 3397-407.

57. Radke, J.R., et al., *Defining the cell cycle for the tachyzoite stage of Toxoplasma gondii.* Mol Biochem Parasitol, 2001. **115**(2): p. 165-75.

58. Radke, J.R. and M.W. White, *A cell cycle model for the tachyzoite of Toxoplasma gondii using the Herpes simplex virus thymidine kinase.* Mol Biochem Parasitol, 1998. **94**(2): p. 237-47.

59. Gubbels, M.J., M. Wieffer, and B. Striepen, *Fluorescent protein tagging in Toxoplasma gondii: identification of a novel inner membrane complex component conserved among Apicomplexa.* Mol Biochem Parasitol, 2004. **137**(1): p. 99-110.

60. Brooks, C.F., et al., *Toxoplasma gondii sequesters centromeres to a specific nuclear region throughout the cell cycle.* Proc Natl Acad Sci U S A, 2011. **108**(9): p. 3767-72.

61. Harper, J.D., et al., *Proteins related to green algal striated fiber assemblin are present in stramenopiles and alveolates.* Protoplasma, 2009. **236**(1-4): p. 97-101.

62. Lechtreck, K.F., *Striated fiber assemblin in apicomplexan parasites.* Mol Biochem Parasitol, 2003. **128**(1): p. 95-9.

63. Morrissette, N.S. and L.D. Sibley, *Disruption of microtubules uncouples budding and nuclear division in Toxoplasma gondii.* J Cell Sci, 2002. **115**(Pt 5): p. 1017-25.

64. Hoeijmakers, W.A., et al., *Plasmodium falciparum centromeres display a unique epigenetic makeup and cluster prior to and during schizogony.* Cell Microbiol, 2012.

65. Morrissette, N.S., et al., *Dinitroanilines bind alpha-tubulin to disrupt microtubules.* Mol Biol Cell, 2004. **15**(4): p. 1960-8.

66. Zhang, Q., et al., *A critical role of perinuclear filamentous actin in spatial repositioning and mutually exclusive expression of virulence genes in malaria parasites.* Cell Host Microbe, 2011. **10**(5): p. 451-63.

67. Suvorova, E.S., et al., *Nuclear actin-related protein is required for chromosome segregation in Toxoplasma gondii.* Mol Biochem Parasitol, 2012. **181**(1): p. 7-16.

68. Nasmyth, K. and C.H. Haering, *Cohesin: its roles and mechanisms.* Annu Rev Genet, 2009. **43**: p. 525-58.

69. Wong, R.W., *An update on cohesin function as a 'molecular glue' on chromosomes and spindles.* Cell Cycle, 2010. **9**(9): p. 1754-8.

70. Hu, K., *Organizational changes of the daughter basal complex during the parasite replication of Toxoplasma gondii.* PLoS Pathog, 2008. **4**(1): p. e10.

71. Kudo, N., et al., *Leptomycin B inactivates CRM1/exportin 1 by covalent modification at a cysteine residue in the central conserved region.* Proc Natl Acad Sci U S A, 1999. **96**(16): p. 9112-7.

72. Yoshida, M., N. Kudo, and S. Horinouchi, *[Leptomycin: a specific inhibitor of protein nuclear export].* Tanpakushitsu Kakusan Koso, 1999. **44**(9): p. 1379-88.

73. Gissot, M., et al., *Toxoplasma gondii chromodomain protein 1 binds to heterochromatin and colocalises with centromeres and telomeres at the nuclear periphery.* PLoS One, 2012. **7**(3): p. e32671.

74. Losada, A. and T. Hirano, *Dynamic molecular linkers of the genome: the first decade of SMC proteins.* Genes Dev, 2005. **19**(11): p. 1269-87.

75. Hirano, T., *SMC proteins and chromosome mechanics: from bacteria to humans.* Philos Trans R Soc Lond B Biol Sci, 2005. **360**(1455): p. 507-14.

76. Tanaka, T., et al., *Identification of cohesin association sites at centromeres and along chromosome arms.* Cell, 1999. **98**(6): p. 847-58.

77. Losada, A. and T. Hirano, *Biology in pictures. New light on sticky sisters.* Curr Biol, 2000. **10**(17): p. R615.

78. Onn, I., et al., *Sister chromatid cohesion: a simple concept with a complex reality.* Annu Rev Cell Dev Biol, 2008. **24**: p. 105-29.

79. Peters, J.M., A. Tedeschi, and J. Schmitz, *The cohesin complex and its roles in chromosome biology.* Genes Dev, 2008. **22**(22): p. 3089-114.

80. Gruber, S., C.H. Haering, and K. Nasmyth, *Chromosomal cohesin forms a ring.* Cell, 2003. **112**(6): p. 765-77.

81. Huang, C.E., M. Milutinovich, and D. Koshland, *Rings, bracelet or snaps: fashionable alternatives for Smc complexes.* Philos Trans R Soc Lond B Biol Sci, 2005. **360**(1455): p. 537-42.

82. Losada, A., M. Hirano, and T. Hirano, *Identification of Xenopus SMC protein complexes required for sister chromatid cohesion.* Genes Dev, 1998. **12**(13): p. 1986-97.

83. Wendt, K.S., et al., *Cohesin mediates transcriptional insulation by CCCTC-binding factor.* Nature, 2008. **451**(7180): p. 796-801.

84. Parelho, V., et al., *Cohesins functionally associate with CTCF on mammalian chromosome arms.* Cell, 2008. **132**(3): p. 422-33.

85. Peric-Hupkes, D. and B. van Steensel, *Linking cohesin to gene regulation.* Cell, 2008. **132**(6): p. 925-8.

86. del Cacho, E., et al., *Meiotic chromosome pairing and bouquet formation during Eimeria tenella sporulation.* International Journal for Parasitology, 2010. **40**(4): p. 453-62.

87. Kahms, M., et al., *Lighting up the nuclear pore complex.* Eur J Cell Biol, 2011. **90**(9): p. 751-8.

88. Gorlich, D. and U. Kutay, *Transport between the cell nucleus and the cytoplasm.* Annu Rev Cell Dev Biol, 1999. **15**: p. 607-60.

89. Ishii, K., et al., *Chromatin boundaries in budding yeast: the nuclear pore connection.* Cell, 2002. **109**(5): p. 551-62.

90. Shinkura, N. and W.C. Forrester, *Pushing the envelope: chromatin boundaries at the nuclear pore.* Mol Cell, 2002. **9**(6): p. 1156-8.

91. Wong, R.W. and G. Blobel, *Cohesin subunit SMC1 associates with mitotic microtubules at the spindle pole.* Proc Natl Acad Sci U S A, 2008. **105**(40): p. 15441-5.

92. Brown, C.R., et al., *Global histone acetylation induces functional genomic reorganization at mammalian nuclear pore complexes.* Genes Dev, 2008. **22**(5): p. 627-39.

93. Weiner, A., et al., *3D nuclear architecture reveals coupled cell cycle dynamics of chromatin and nuclear pores in the malaria parasite Plasmodium falciparum.* Cell Microbiol, 2011. **13**(7): p. 967-77.

94. Brooks, C.F., et al., *The toxoplasma apicoplast phosphate translocator links cytosolic and apicoplast metabolism and is essential for parasite survival.* Cell Host Microbe, 2010. **7**(1): p. 62-73.

95. Funabiki, H., et al., *Cell cycle-dependent specific positioning and clustering of centromeres and telomeres in fission yeast.* J Cell Biol, 1993. **121**(5): p. 961-76.

96. Adachi, Y. and M. Yanagida, *Higher order chromosome structure is affected by cold-sensitive mutations in a Schizosaccharomyces pombe gene crm1+ which encodes a 115-kD protein preferentially localized in the nucleus and its periphery.* J Cell Biol, 1989. **108**(4): p. 1195-207.

97. Stavenhagen, J.B. and V.A. Zakian, *Internal tracts of telomeric DNA act as silencers in Saccharomyces cerevisiae.* Genes Dev, 1994. **8**(12): p. 1411-22.

98. Feuerbach, F., et al., *Nuclear architecture and spatial positioning help establish transcriptional states of telomeres in yeast.* Nat Cell Biol, 2002. **4**(3): p. 214-21.

99. Galy, V., et al., *Nuclear pore complexes in the organization of silent telomeric chromatin.* Nature, 2000. **403**(6765): p. 108-12.

100. Wells, J. and P.J. Farnham, *Characterizing transcription factor binding sites using formaldehyde crosslinking and immunoprecipitation.* Methods, 2002. **26**(1): p. 48-56.

101. Gissot, M., et al., *Epigenomic modifications predict active promoters and gene structure in Toxoplasma gondii.* PLoS Pathog, 2007. **3**(6): p. e77.

102. Striepen, B. and D. Soldati, *Genetic manipulation of Toxoplasma gondii*, in *Toxoplasma gondii. The Model Apicomplexan—Perspectives and Methods*, L.M. Weiss and K. Kim, Editors. 2007, Elsevier: London. p. 391-415.

103. Aslanidis, C. and P.J. de Jong, *Ligation-independent cloning of PCR products (LIC-PCR).* Nucleic Acids Res, 1990. **18**(20): p. 6069-74.

104. Huynh, M.H. and V.B. Carruthers, *Tagging of endogenous genes in a Toxoplasma gondii strain lacking Ku80.* Eukaryot Cell, 2009. **8**(4): p. 530-9.

105. Cremer, M., et al., *Cell Preparation and Multicolor FISH in 3D Preserved Cultured Mammalian Cells.* CSH Protoc, 2007. **2007**: p. pdb prot4723.

106. Alexandrov, A., et al., *A facile method for high-throughput co-expression of protein pairs.* Mol Cell Proteomics, 2004. **3**(9): p. 934-8.

107. Agrawal, S., et al., *Genetic evidence that an endosymbiont-derived endoplasmic reticulum-associated protein degradation (ERAD) system functions in import of apicoplast proteins.* J Biol Chem, 2009. **284**(48): p. 33683-91.

108. Francia, M.E., et al., *A Toxoplasma gondii protein with homology to intracellular type Na(+)/H(+) exchangers is important for osmoregulation and invasion.* Exp Cell Res, 2011. **317**(10): p. 1382-96.

109. Wichroski, M.J., et al., *Clostridium septicum alpha-toxin is active against the parasitic protozoan Toxoplasma gondii and targets members of the SAG family of glycosylphosphatidylinositol-anchored surface proteins.* Infect Immun, 2002. **70**(8): p. 4353-61.

110. van Dooren, G.G., et al., *Toxoplasma gondii Tic20 is essential for apicoplast protein import.* Proc Natl Acad Sci U S A, 2008. **105**(36): p. 13574-9.

111. Sibley, L.D., *Intracellular parasite invasion strategies.* Science, 2004. **304**(5668): p. 248-53.

112. Frenal, K., et al., *Functional dissection of the apicomplexan glideosome molecular architecture.* Cell Host Microbe, 2010. **8**(4): p. 343-57.

113. Santos, J.M., et al., *Apicomplexan cytoskeleton and motors: key regulators in morphogenesis, cell division, transport and motility.* Int J Parasitol, 2009. **39**(2): p. 153-62.

114. Riglar, D.T., et al., *Super-resolution dissection of coordinated events during malaria parasite invasion of the human erythrocyte.* Cell Host Microbe, 2011. **9**(1): p. 9-20.

115. Hartmann, J., et al., *Golgi and centrosome cycles in Toxoplasma gondii.* Mol Biochem Parasitol, 2006. **145**(1): p. 125-7.

116. Striepen, B., et al., *The plastid of Toxoplasma gondii is divided by association with the centrosomes.* J Cell Biol, 2000. **151**(7): p. 1423-34.

117. Lechtreck, K.F. and M. Melkonian, *Striated microtubule-associated fibers: identification of assemblin, a novel 34-kD protein that forms paracrystals of 2-nm filaments in vitro.* J Cell Biol, 1991. **115**(3): p. 705-16.

118. Melkonian, M., *Ultrastructural aspects of basal body associated fibrous structures in green algae: a critical review.* Biosystems, 1980. **12**(1-2): p. 85-104.

119. Lechtreck, K.F. and C.D. Silflow, *SF-assemblin in Chlamydomonas: sequence conservation and localization during the cell cycle.* Cell Motil Cytoskeleton, 1997. **36**(2): p. 190-201.

120. Behnke, M.S., et al., *Coordinated progression through two subtranscriptomes underlies the tachyzoite cycle of Toxoplasma gondii.* PLoS One, 2010. **5**(8): p. e12354.

121. Gajria, B., et al., *ToxoDB: an integrated Toxoplasma gondii database resource.* Nucleic Acids Res, 2008. **36**(Database issue): p. D553-6.

122. Hu, K., et al., *Daughter cell assembly in the protozoan parasite Toxoplasma gondii.* Mol Biol Cell, 2002. **13**(2): p. 593-606.

123. Sheiner, L., et al., *A systematic screen to discover and analyze apicoplast proteins identifies a conserved and essential protein import factor.* PLoS Pathog, 2011. **7**(12): p. e1002392.

124. Meissner, M., et al., *Modulation of myosin A expression by a newly established tetracycline repressor-based inducible system in Toxoplasma gondii.* Nucleic Acids Res, 2001. **29**(22): p. E115.

125. Dutcher, S.K., *Elucidation of basal body and centriole functions in Chlamydomonas reinhardtii.* Traffic, 2003. **4**(7): p. 443-51.

126. Plessmann, U., I. Reiter-Owona, and K.F. Lechtreck, *Posttranslational modifications of alpha-tubulin of Toxoplasma gondii.* Parasitol Res, 2004. **94**(5): p. 386-9.

127. Marshall, W.F., *Basal bodies platforms for building cilia.* Curr Top Dev Biol, 2008. **85**: p. 1-22.

128. Mittelmeier, T.M., et al., *Asymmetric properties of the Chlamydomonas reinhardtii cytoskeleton direct rhodopsin photoreceptor localization.* J Cell Biol, 2011. **193**(4): p. 741-53.

129. Ehler, L.L. and S.K. Dutcher, *Pharmacological and genetic evidence for a role of rootlet and phycoplast microtubules in the positioning and assembly of cleavage furrows in Chlamydomonas reinhardtii.* Cell Motil Cytoskeleton, 1998. **40**(2): p. 193-207.

130. Salisbury, J.L., *Centrin, centrosomes, and mitotic spindle poles.* Curr Opin Cell Biol, 1995. **7**(1): p. 39-45.

131. Geimer, S., et al., *A novel 95-kD protein is located in a linker between cytoplasmic microtubules and basal bodies in a green flagellate and forms striated filaments in vitro.* J Cell Biol, 1998. **140**(5): p. 1149-58.

132. Yang, J., et al., *Rootletin, a novel coiled-coil protein, is a structural component of the ciliary rootlet.* J Cell Biol, 2002. **159**(3): p. 431-40.

133. Stearns, M.E., J.A. Connolly, and D.L. Brown, *Cytoplasmic microtubule organizing centers isolated from Polytomella agilis.* Science, 1976. **191**(4223): p. 188-91.

134. Brown, D.L., A. Massalski, and R. Patenaude, *Organization of the flagellar apparatus and associate cytoplasmic microtubules in the quadriflagellate alga Polytomella agilis.* J Cell Biol, 1976. **69**(1): p. 106-25.

135. Lechtreck, K.F., *Analysis of striated fiber formation by recombinant SF-assemblin in vitro.* J Mol Biol, 1998. **279**(2): p. 423-38.

136. Keeling, P.J., *Chromalveolates and the evolution of plastids by secondary endosymbiosis.* J Eukaryot Microbiol, 2009. **56**(1): p. 1-8.

137. Brugerolle, G., *Colpodella vorax : ultrastructure, predation, life-cycle, mitosis, and phylogenetic relationships.* Europ. J. Protistol., 2002. **38**: p. 113-125


138. Moore, R.B., et al., *A photosynthetic alveolate closely related to apicomplexan parasites.* Nature, 2008. **451**(7181): p. 959-63.

139. Obornik, M., et al., *Morphology and ultrastructure of multiple life cycle stages of the photosynthetic relative of apicomplexa, Chromera velia.* Protist, 2011. **162**(1): p. 115-30.

140. Schrevel, J., et al., *Vesicle trafficking during sporozoite development in Plasmodium berghei: ultrastructural evidence for a novel trafficking mechanism.* Parasitology, 2008. **135**(Pt 1): p. 1-12.

141. Dubremetz, J.F., *[Genesis of merozoites in the coccidia, Eimeria necatrix. Ultrastructural study].* J Protozool, 1975. **22**(1): p. 71-84.

142. Donald, R.G., et al., *Insertional tagging, cloning, and expression of the Toxoplasma gondii hypoxanthine-xanthine-guanine phosphoribosyltransferase gene. Use as a selectable marker for stable transformation.* J Biol Chem, 1996. **271**(24): p. 14010-9.

143. DeRocher, A.E., et al., *A thioredoxin family protein of the apicoplast periphery identifies abundant candidate transport vesicles in Toxoplasma gondii.* Eukaryot Cell, 2008. **7**(9): p. 1518-29.

144. Cowman, A.F., D. Berry, and J. Baum, *The cellular and molecular basis for malaria parasite invasion of the human red blood cell.* J Cell Biol, 2012. **198**(6): p. 961-71.

145. Sinden, R.E. and M.E. Smalley, *Gametocytogenesis of Plasmodium falciparum in vitro: the cell-cycle.* Parasitology, 1979. **79**(2): p. 277-96.

146. Schrevel, J., G. Asfaux-Foucher, and J.M. Bafort, *[Ultrastructural study of multiple mitoses during sporogony of Plasmodium b. berghei].* J Ultrastruct Res, 1977. **59**(3): p. 332-50.

147. Gupta, A., P. Mehra, and S.K. Dhar, *Plasmodium falciparum origin recognition complex subunit 5: functional characterization and role in DNA replication foci formation.* Mol Microbiol, 2008. **69**(3): p. 646-65.

148. Arnot, D.E., E. Ronander, and D.C. Bengtsson, *The progression of the intra-erythrocytic cell cycle of Plasmodium falciparum and the role of the centriolar plaques in asynchronous mitotic division during schizogony.* Int J Parasitol, 2011. **41**(1): p. 71-80.

149. Gerald, N., B. Mahajan, and S. Kumar, *Mitosis in the human malaria parasite Plasmodium falciparum.* Eukaryot Cell, 2011. **10**(4): p. 474-82.

150. Nishi, M., et al., *Organellar dynamics during the cell cycle of Toxoplasma gondii.* J Cell Sci, 2008. **121**(Pt 9): p. 1559-68.

151. Bornens, M., *The centrosome in cells and organisms.* Science, 2012. **335**(6067): p. 422-6.

152. Bornens, M., et al., *Structural and chemical characterization of isolated centrosomes.* Cell Motil Cytoskeleton, 1987. **8**(3): p. 238-49.

153. Mardin, B.R. and E. Schiebel, *Breaking the ties that bind: new advances in centrosome biology.* J Cell Biol, 2012. **197**(1): p. 11-8.

154. Mahajan, B., et al., *Centrins, cell cycle regulation proteins in human malaria parasite Plasmodium falciparum.* J Biol Chem, 2008. **283**(46): p. 31871-83.

155. Sinden, R.E., *Gametocytogenesis of Plasmodium falciparum in vitro: an electron microscopic study.* Parasitology, 1982. **84**(1): p. 1-11.

156. Read, M., et al., *Microtubular organization visualized by immunofluorescence microscopy during erythrocytic schizogony in Plasmodium falciparum and investigation of post-translational modifications of parasite tubulin.* Parasitology, 1993. **106 ( Pt 3)**: p. 223-32.

157. Speer, C.A. and J.P. Dubey, *Ultrastructure of shizonts and merozoites of Sarcocystis falcatula in the lungs of budgerigars (Melopsittacus undulatus).* J Parasitol, 1999. **85**(4): p. 630-7.

158. Ferguson, D.J., et al., *Ultrastructural study of early stages of asexual multiplication and microgametogony of Toxoplasma gondii in the small intestine of the cat.* Acta Pathol Microbiol Scand B Microbiol Immunol, 1974. **82**(2): p. 167-81.

159. Heussler, V.T., et al., *Hijacking of host cell IKK signalosomes by the transforming parasite Theileria.* Science, 2002. **298**(5595): p. 1033-6.

160. von Schubert, C., et al., *The transforming parasite Theileria co-opts host cell mitotic and central spindles to persist in continuously dividing cells.* PLoS Biol, 2010. **8**(9).

161. Romano, J.D., N. Bano, and I. Coppens, *New host nuclear functions are not required for the modifications of the parasitophorous vacuole of Toxoplasma.* Cell Microbiol, 2008. **10**(2): p. 465-76.

162. Walker, M.E., et al., *Toxoplasma gondii actively remodels the microtubule network in host cells.* Microbes Infect, 2008. **10**(14-15): p. 1440-9.

163. Malumbres, M., et al., *Cyclin-dependent kinases: a family portrait.* Nat Cell Biol, 2009. **11**(11): p. 1275-6.

164. Morgan, D.O., et al., *Control of eukaryotic cell cycle progression by phosphorylation of cyclin-dependent kinases.* Cancer J Sci Am, 1998. **4 Suppl 1**: p. S77-83.

165. Morgan, D.O., *Cyclin-dependent kinases: engines, clocks, and microprocessors.* Annu Rev Cell Dev Biol, 1997. **13**: p. 261-91.

166. Mocciaro, A. and M. Rape, *Emerging regulatory mechanisms in ubiquitin-dependent cell cycle control.* J Cell Sci, 2012. **125**(Pt 2): p. 255-63.

167. Loyer, P., et al., *Role of CDK/cyclin complexes in transcription and RNA splicing.* Cell Signal, 2005. **17**(9): p. 1033-51.

168. Doerig, C., J. Endicott, and D. Chakrabarti, *Cyclin-dependent kinase homologues of Plasmodium falciparum.* Int J Parasitol, 2002. **32**(13): p. 1575-85.

169. Halbert, J., et al., *A Plasmodium falciparum transcriptional cyclin-dependent kinase-related kinase with a crucial role in parasite proliferation associates with histone deacetylase activity.* Eukaryot Cell, 2010. **9**(6): p. 952-9.

170. Gubbels, M.J., M. White, and T. Szatanek, *The cell cycle and Toxoplasma gondii cell division: tightly knit or loosely stitched?* Int J Parasitol, 2008. **38**(12): p. 1343-58.

171. Kvaal, C.A., et al., *Isolation of a Toxoplasma gondii cyclin by yeast two-hybrid interactive screen.* Mol Biochem Parasitol, 2002. **120**(2): p. 187-94.

172. Dorin-Semblat, D., et al., *Plasmodium falciparum NIMA-related kinase Pfnek-1: sex specificity and assessment of essentiality for the erythrocytic asexual cycle.* Microbiology, 2011. **157**(Pt 10): p. 2785-94.

173. Le Roch, K.G., et al., *Discovery of gene function by expression profiling of the malaria parasite life cycle.* Science, 2003. **301**(5639): p. 1503-8.

174. Bozdech, Z., et al., *The transcriptome of the intraerythrocytic developmental cycle of Plasmodium falciparum.* PLoS Biol, 2003. **1**(1): p. E5.

175. Gaji, R.Y., et al., *Cell cycle-dependent, intercellular transmission of Toxoplasma gondii is accompanied by marked changes in parasite gene expression.* Mol Microbiol, 2011. **79**(1): p. 192-204.

176. Riechmann, J.L. and E.M. Meyerowitz, *The AP2/EREBP family of plant transcription factors.* Biol Chem, 1998. **379**(6): p. 633-46.

177. Radke, J.B., et al., *ApiAP2 transcription factor restricts development of the Toxoplasma tissue cyst.* Proc Natl Acad Sci U S A, 2013.

178. Painter, H.J., T.L. Campbell, and M. Llinas, *The Apicomplexan AP2 family: integral factors regulating Plasmodium development.* Mol Biochem Parasitol, 2011. **176**(1): p. 1-7.

179. De Silva, E.K., et al., *Specific DNA-binding by apicomplexan AP2 transcription factors.* Proc Natl Acad Sci U S A, 2008. **105**(24): p. 8393-8.

180. Suvorova, E.S., et al., *Discovery of a splicing regulator required for cell cycle progression.* PLoS Genet, 2013. **9**(2): p. e1003305.

181. Doerig, C., et al., *Signalling in malaria parasites. The MALSIG consortium.* Parasite, 2009. **16**(3): p. 169-82.

182. Ferguson, D.J., et al., *MORN1 has a conserved role in asexual and sexual development across the apicomplexa.* Eukaryot Cell, 2008. **7**(4): p. 698-711.

183. Chen, C.T.a.G., M.J. , *The Toxoplasma gondii centrosome is the platform for internal daughter budding as revealed by a Nek1 kinase mutant.* J Cell Sci, 2013. **In Press**.

184. Reininger, L., et al., *An essential Aurora-related kinase transiently associates with spindle pole bodies during Plasmodium falciparum erythrocytic schizogony.* Mol Microbiol, 2011. **79**(1): p. 205-21.

185. Aikawa, M., C.G. Huff, and H. Sprinz, *Fine structure of the asexual stages of Plasmodium elongatum.* J Cell Biol, 1967. **34**(1): p. 229-49.

186. Aikawa, M. and R.L. Beaudoin, *Studies on nuclear division of a malarial parasite under pyrimethamine treatment.* J Cell Biol, 1968. **39**(3): p. 749-54.

187. Arnot, D.E. and K. Gull, *The Plasmodium cell-cycle: facts and questions.* Ann Trop Med Parasitol, 1998. **92**(4): p. 361-5.

188. Kelly, J.M., L. McRobert, and D.A. Baker, *Evidence on the chromosomal location of centromeric DNA in Plasmodium falciparum from etoposide-mediated topoisomerase-II cleavage.* Proc Natl Acad Sci U S A, 2006. **103**(17): p. 6706-11.

189. Iwanaga, S., et al., *Functional identification of the Plasmodium centromere and generation of a Plasmodium artificial chromosome.* Cell Host Microbe, 2010. **7**(3): p. 245-55.

190. Barale, J.C. and R. Menard, *Centromeric plasmids and artificial chromosomes: new kids on the Plasmodium transfection block.* Cell Host Microbe, 2010. **7**(3): p. 181-3.

191. Petter, M., et al., *H2A.Z and H2B.Z double-variant nucleosomes define intergenic regions and dynamically occupy var gene promoters in the malaria parasite Plasmodium falciparum.* Mol Microbiol, 2013. **87**(6): p. 1167-82.

192. Bartfai, R., et al., *H2A.Z demarcates intergenic regions of the plasmodium falciparum epigenome that are dynamically marked by H3K9ac and H3K4me3.* PLoS Pathog, 2010. **6**(12): p. e1001223.

193. Dalmasso, M.C., et al., *Toxoplasma H2A variants reveal novel insights into nucleosome composition and functions for this histone family.* J Mol Biol, 2009. **392**(1): p. 33-47.

194. Lopez-Rubio, J.J., L. Mancio-Silva, and A. Scherf, *Genome-wide analysis of heterochromatin associates clonally variant gene regulation with perinuclear repressive centers in malaria parasites.* Cell Host Microbe, 2009. **5**(2): p. 179-90.

195. Choi, S.W., M.K. Keyes, and P. Horrocks, *LC/ESI-MS demonstrates the absence of 5-methyl-2'-deoxycytosine in Plasmodium falciparum genomic DNA.* Mol Biochem Parasitol, 2006. **150**(2): p. 350-2.

196. Baum, J., et al., *Molecular genetics and comparative genomics reveal RNAi is not functional in malaria parasites.* Nucleic Acids Res, 2009. **37**(11): p. 3788-98.

197. Dalmasso, M.C., W.J. Sullivan, Jr., and S.O. Angel, *Canonical and variant histones of protozoan parasites.* Front Biosci, 2011. **16**: p. 2086-105.

198. Flueck, C., et al., *Plasmodium falciparum heterochromatin protein 1 marks genomic loci linked to phenotypic variation of exported virulence factors.* PLoS Pathog, 2009. **5**(9): p. e1000569.

199. Duraisingh, M.T., et al., *Heterochromatin silencing and locus repositioning linked to regulation of virulence genes in Plasmodium falciparum.* Cell, 2005. **121**(1): p. 13-24.

200. del Cacho, E., et al., *Meiotic chromosome pairing and bouquet formation during Eimeria tenella sporulation.* Int J Parasitol, 2010. **40**(4): p. 453-62.

201. Hinterberg, K., et al., *Interchromosomal exchange of a large subtelomeric segment in a Plasmodium falciparum cross.* EMBO J, 1994. **13**(17): p. 4174-80.

202. Freitas-Junior, L.H., et al., *Frequent ectopic recombination of virulence factor genes in telomeric chromosome clusters of P. falciparum.* Nature, 2000. **407**(6807): p. 1018-22.

203. Volz, J., et al., *Potential epigenetic regulatory proteins localise to distinct nuclear sub-compartments in Plasmodium falciparum.* Int J Parasitol, 2010. **40**(1): p. 109-21.

204. Oehring, S.C., et al., *Organellar proteomics reveals hundreds of novel nuclear proteins in the malaria parasite Plasmodium falciparum.* Genome Biol, 2012. **13**(11): p. R108.

205. Aikawa, M., *The fine structure of the erythrocytic stages of three avian malarial parasites, Plasmodium fallax, P. lophurae, and P. cathemerium.* Am J Trop Med Hyg, 1966. **15**(4): p. 449-71.

206. Dubremetz, J.F. and G. Torpier, *Freeze fracture study of the pellicle of an eimerian sporozoite (Protozoa, Coccidia).* J Ultrastruct Res, 1978. **62**(2): p. 94-109.

207. Gould, S.B., et al., *Ciliate pellicular proteome identifies novel protein families with characteristic repeat motifs that are common to alveolates.* Mol Biol Evol, 2011. **28**(3): p. 1319-31.

208. Gould, S.B., et al., *Alveolins, a new family of cortical proteins that define the protist infrakingdom Alveolata.* Mol Biol Evol, 2008. **25**(6): p. 1219-30.

209. Leander, B.S., et al., *Molecular phylogeny and surface morphology of Colpodella edax (Alveolata): insights into the phagotrophic ancestry of apicomplexans.* J Eukaryot Microbiol, 2003. **50**(5): p. 334-40.

210. Khater, E.I., R.E. Sinden, and J.T. Dessens, *A malaria membrane skeletal protein is essential for normal morphogenesis, motility, and infectivity of sporozoites.* J Cell Biol, 2004. **167**(3): p. 425-32.

211. Tremp, A.Z., E.I. Khater, and J.T. Dessens, *IMC1b is a putative membrane skeleton protein involved in cell shape, mechanical strength, motility, and infectivity of malaria ookinetes.* J Biol Chem, 2008. **283**(41): p. 27604-11.

212. Tremp, A.Z. and J.T. Dessens, *Malaria IMC1 membrane skeleton proteins operate autonomously and participate in motility independently of cell shape.* J Biol Chem, 2011. **286**(7): p. 5383-91.

213. Mann, T., E. Gaskins, and C. Beckers, *Proteolytic processing of TgIMC1 during maturation of the membrane skeleton of Toxoplasma gondii.* J Biol Chem, 2002. **277**(43): p. 41240-6.

214. De Napoli, M.G., et al., *N-terminal palmitoylation is required for Toxoplasma gondii HSP20 inner membrane complex localization.* Biochim Biophys Acta, 2013. **1833**(6): p. 1329-1337.

215. Lorestani, A., et al., *A Toxoplasma MORN1 null mutant undergoes repeated divisions but is defective in basal assembly, apicoplast division and cytokinesis.* PLoS One, 2010. **5**(8): p. e12302.

216. Heaslip, A.T., et al., *TgMORN1 is a key organizer for the basal complex of Toxoplasma gondii.* PLoS Pathog, 2010. **6**(2): p. e1000754.

217. Carruthers, V. and J.C. Boothroyd, *Pulling together: an integrated model of Toxoplasma cell invasion.* Curr Opin Microbiol, 2007. **10**(1): p. 83-9.

218. Bannister, L.H., et al., *Ultrastructure of rhoptry development in Plasmodium falciparum erythrocytic schizonts.* Parasitology, 2000. **121 ( Pt 3)**: p. 273-87.

219. Shaw, M.K., D.S. Roos, and L.G. Tilney, *Acidic compartments and rhoptry formation in Toxoplasma gondii.* Parasitology, 1998. **117 ( Pt 5)**: p. 435-43.

220. Soldati, D., J.F. Dubremetz, and M. Lebrun, *Microneme proteins: structural and functional requirements to promote adhesion and invasion by the apicomplexan parasite Toxoplasma gondii.* Int J Parasitol, 2001. **31**(12): p. 1293-302.

221. Hager, K.M., et al., *The nuclear envelope serves as an intermediary between the ER and Golgi complex in the intracellular parasite Toxoplasma gondii.* J Cell Sci, 1999. **112 ( Pt 16)**: p. 2631-8.

222. Agop-Nersesian, C., et al., *Biogenesis of the inner membrane complex is dependent on vesicular transport by the alveolate specific GTPase Rab11B.* PLoS Pathog, 2010. **6**(7): p. e1001029.

223. Heaslip, A.T., S.C. Ems-McClung, and K. Hu, *TgICMAP1 is a novel microtubule binding protein in Toxoplasma gondii.* PLoS One, 2009. **4**(10): p. e7406.

224.    Mueller, C., et al., *The Toxoplasma Protein ARO Mediates the Apical Positioning of Rhoptry Organelles, a Prerequisite for Host Cell Invasion.* Cell Host Microbe, 2013. **13**(3): p. 289-301.

225.    Reiff, S.B., S. Vaishnava, and B. Striepen, *The HU Protein Is Important for Apicoplast Genome Maintenance and Inheritance in Toxoplasma gondii.* Eukaryot Cell, 2012. **11**(7): p. 905-15.

226.    Seow, F., et al., *The plastidic DNA replication enzyme complex of Plasmodium falciparum.* Mol Biochem Parasitol, 2005. **141**(2): p. 145-153.

227.    Dar, M.A., et al., *Molecular cloning of apicoplast-targeted Plasmodium falciparum DNA gyrase genes: unique intrinsic ATPase activity and ATP-independent dimerization of PfGyrB subunit.* Eukaryot Cell, 2007. **6**(3): p. 398-412.

228.    van Dooren, G.G., et al., *Development of the endoplasmic reticulum, mitochondrion and apicoplast during the asexual life cycle of Plasmodium falciparum.* Mol Microbiol, 2005. **57**(2): p. 405-19.

229.    Stanway, R.R., et al., *Organelle segregation into Plasmodium liver stage merozoites.* Cell Microbiol, 2011. **13**(11): p. 1768-82.

230.    van Dooren, G.G., et al., *A novel dynamin-related protein has been recruited for apicoplast fission in Toxoplasma gondii.* Curr Biol, 2009. **19**(4): p. 267-76.